Pharmacokinetic Factors in the Neurotoxicities of *p*-Bromophenylacetylurea and *m*-Dinitrobenzene.

Thesis

PHARMACOKINETIC FACTORS IN THE NEUROTOXICITIES OF *p*-BROMOPHENYLACETYLUREA AND *m*-DINITROBENZENE

Jinsheng Xu

DOCTOR OF PHILOSOPHY

March 1998

UNRESTRICTED

PHARMACOKINETIC FACTORS IN THE NEUROTOXICITIES OF *p*-BROMOPHENYLACETYLUREA AND *m*-DINITROBENZENE

Jinsheng Xu

A THESIS PRESENTED FOR THE DEGREE OF DOCTOR OF PHILOSOPHY IN THE OPEN UNIVERSITY

Medical Research Council Toxicology Unit
Hodgkin Building
University of Leicester
P. O. Box 138
Leicester LE1 9HN
England

Date of award: 10th August 1998

March 1998

The candidate confirms that the work submitted is his own original work.

ACKNOWLEDGEMENTS

I wish to thank Dr D. E. Ray, my supervisor, for his support, encouragement and constructive instructions during my PhD study, Dr P. Glynn, my second supervisor, and Mr C. C. Nolan for there helpful discussions and co-operation, Professor L. L. Smith and Dr M. K. Johnson for their encouragement and helpful discussions, Mr T. Lister for his general assistance, Dr P. B. Farmer, Dr C-K Lim, Mr J. H. Lamb and Ms R. Jukes for their help and discussions on the characterisation of BPAU metabolites, and Dr R. M. Ellam (Division of Chemistry, Faculty of Natural Sciences, University of Hertfordshire) for his help in the nomenclature of BPAU metabolites. My study was supported by MRC Toxicology Unit, Leicester, UK.

ABSTRACT

Pharmacokinetic Factors in the Neurotoxicities of p-Bromophenylacetylurea and *m*-Dinitrobenzene

Jinsheng Xu, MRC Toxicology Unit, University of Leicester, Leicester

Conventional approaches to the study of neurotoxicants focus exclusively on the direct action of neurotoxicants on the nervous system. In fact, pharmacokinetic and metabolic factors can greatly modify the effect of neurotoxicants. This thesis presents the investigations of the pharmacokinetic and metabolic factors in chemical-induced neurotoxicities. *p*-Bromophenylacetylurea (BPAU) and *m*-dinitrobenzene (*m*-DNB) were selected as model neurotoxicants. Wistar (LACP) and F344 rats, and the analytical techniques of HPLC, MS and NMR were used in the present studies.

This study has demonstrated that metabolism and pharmacokinetic behaviour of BPAU and *m*-DNB significantly modified their neurotoxicity. Three metabolites of BPAU, 3-hydroxy-5-(4-bromophenyl)-1,3-diazapentane-2,4-dione (M1), 4-(4-bromo-phenyl)-3-oxapyrrolidine-2,5-dione (M2) and 3-methyl-5-(4-bromophenyl)-1,3-diaza- pentane-2,4-dione (M3), were identified and charaterised in this study. Phenylmethanesulfonyl fluoride (PMSF) which can intensify BPAU-induced neuropathy significantly delayed BPAU elimination, increased M1 levels in tissues and decreased M2 concentration in serum. This metabolic interaction and neurotoxic synergy between the two compounds represent a distinct model in the mechanistic studies of the promotion of delayed neuropathy. The present study also showed that 1-year old rats which are more susceptible to BPAU-induced neuropathy produced more M1 and less M2 than 6-week old rats.

In vivo and *in vitro* studies in this thesis also demonstrated that *m*-DNB can be metabolised in brain. The major metabolite was 3-nitroaniline (3-NA). An activated intermediate, 3-nitrosonitrobenzene (3-NNB) was detected in the cultured astrocytes and endothelial cells. This suggests that metabolic activation may play an important role in *m*-DNB-induced neurotoxicity. The infusion-lesion model revealed that once a concentration threshold for *m*-DNB is exceeded, the time which *m*-DNB is maintained above that threshold is a more important factor in producing brain lesions than a higher transient concentration.

This study has demonstrated that pharmacokinetic approaches have a great potential in understanding chemical-induced neurotoxicity.

Key words: *p*-bromophenylacetylurea (BPAU), *m*-dinitrobenzene (*m*-DNB), phenylmethanesulfonyl fluoride (PMSF), neurotoxicity, pharmacokinetics, metabolism, rat

CONTENTS

ABBREVIATIONS

3-AA: 3-Aminoacetanilide.

4-A-2-NP: 4-Amino-2-nitrophenol.

2-A-4-NP: 2-Amino-4-nitrophenol.

AUC: Area under concentration-time curve.

BPAU: p-Bromophenylacetylurea.

CNS: Central nervous system.

C_0: Concentration of test agent at time t = 0.

C_t: Concentration of test agent at time t.

2,4-DAP: 2,4-Diacetaminophenol.

DMEM: Dulbecco's Modified Eagle's Medium.

m-DNB: *m*-Dinitrobenzene.

HPLC: High-pressure liquid chromatography.

ip: Intraperitoneal injection.

iv; Intravenous injection.

Min; Minute(s).

M1: 3-Hydroxy-5-(4-bromophenyl)-1,3-diazapentane-2,4-dione;common name: N'-hydroxy-p-bromophenylacetylurea, HBPAU.

M2: 4-(4-Bromophenyl)-3-oxapyrrolidine-2,5-dione.

M3: 3-Methyl-5-(4-bromophenyl)-1,3-diazapentane-2,4-dione; common name: N'-methyl-p-bromophenylacetylurea, MBPAU.

h: Hour(s).

k: Rate constant.

3-NA: 3-Nitroaniline.

3-NAA: 3-Nitroacetaniline.

3-NNB: 3-Nitrosonitrobenzene.

PMSF: Phenylmethanesulfonyl fluoride.

p.o.: Per oral.

T_d: The time from the end of infusion to decline to a certain concentration.

T_i: Infusion time.

T_m: The time maintaining a test agent above a certain concentration.

$t_{1/2}$: Half life.

t: Time.

V: Apparent distribution volume.

INDEX OF FIGURES

Section 1.

Section 2.

Appendix

INDEX OF TABLES

Section 2

Section 3

Appendix

SECTION 1 INTRODUCTION

1.1 Pharmacokinetics in toxicology

Humans and other animals are exposed to many potentially toxic drugs or other chemicals either from industry, the environment or from food contamination. These compounds are generally called xenobiotics which are defined as the compounds that are foreign to the normal metabolism of the body (Caldwell, 1995). Not all xenobiotics are toxic, but those which are may exhibit their toxic effect on target tissues in several ways, see FIG 1-1. Any

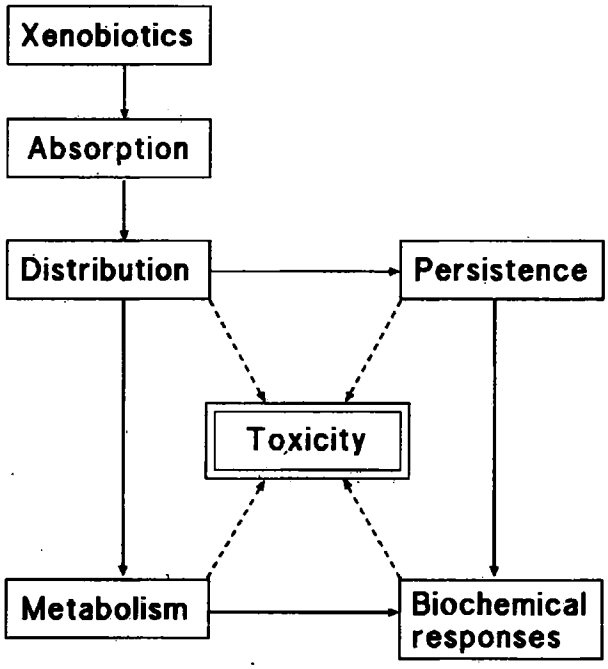

FIG 1-1. Factors influencing toxicities of xenobiotics.

adverse effects produced by xenobiotics are ultimately the results of the interactions between target tissues and the agents. The study of toxicity has historically been

associated with the toxic effects of toxicants on target tissues and molecules. In fact, other, non-target processes, in one way or another, markedly modify the toxic effects of xenobiotics. For example, different species, ages, sexes as well as different individual tissues in an animal can have different responses to a given toxicant. To understand these susceptible differences we need to know what animals do to the xenobiotics as well as what xenobiotics do to animals. Pharmacokinetics may be defined as what the body does to foreign compounds (Benet, 1995) as it deals with the absorption, distribution and elimination of xenobiotics. So, pharmacokinetics plays an important role in understanding how body factors modify susceptibilities to toxicants.

Pharmacokinetics is the mathematical description of the rates of absorption, distribution, metabolism and excretion (ADME) of a drug. It was originally established to describe drug behaviour in the body. From the toxicology point of view, most drugs are also toxicants; this distinction merely depending on their dosage. On the other hand, most toxicants are not drugs. So when the principles of pharmacokinetics are used in toxicology, they are also termed *toxicokinetics*. Both pharmacokinetics and toxicokinetics were based on the same mathematical principles. In the present context, the terms pharmacokinetics and toxicokinetics will be used interchangeably.

Toxicokinetics has emerged as an invaluable tool in the conduct and interpretation of drug safety data (Chasseaud, 1993, Clark and Smith, 1984, Dayan, 1994 and 1995, and Kato, *et al.*, 1993, Takacs, 1995). The discipline of its scope has been defined by the Second International Conference on Harmonization (ICH-2) (1993): "Toxicokinetics is defined as the generation of pharmacokinetic data, either

as an integral of component in the conduct of non-clinical toxicity studies or in specially designed supportive studies, in order to assess systemic exposure. These data may be used in the interpretation of toxicology findings and their relevance to clinical safety issues." The other useful definition was given by Chasseaud, "The primary purpose of toxicokinetics is to provide information on the rate, extent, and duration of exposure of test animal species to the test compound during the course of a toxicity study." (Chasseaud, 1993).

Plasma is a more easily accessible matrix than other tissues in both animals and humans and is, therefore, convenient to use in monitoring body exposure to xenobiotics. However, plasma concentrations of a xenobiotic or its metabolite(s) may not reflect the concentrations at the target sites. Also, a toxic response may not be directly associated with plasma kinetics because of the differences in receptor binding, distribution and metabolic capacity (Igarashi, 1994; Cayen, 1995). Therefore, the toxic effect directly depends on the concentration of the toxicant or its metabolite(s) at the target site and on the sensitivity of the target tissues (Monro, 1994; Caldwell, 1995; Cayen, 1995). Thus pharmacokinetic information about xenobiotics in individual target tissues is important in understanding the interactions between targets and xenobiotics.

1.2 Basic concepts in pharmacokinetics

1.2.1 Absorption and bioavailability

Absorption is the process which leads to the entry of a xenobiotic into the systemic circulation of the body (Caldwell, 1995). Thus absorption is the beginning of the kinetic process of xenobiotics in the body. The dosing routes and regimen

significantly influence the kinetics of xenobiotics (Gibaldi and Perrier, 1982). Therefore, the dosing route and regimen must be carefully considered in pharmacokinetic studies. There are several routes by which drugs are commonly administered. These may be classified as either intravascular or extravascular (Rowland and Tozer, 1980). Intravascular administration refers to the placement of a drug directly into the blood, either intravenously or intra-arterially. The xenobiotics given through extravascular administration have to undergo an absorption process. The percentage of an absorbed xenobiotic is between 0%-100%. In fact, few xenobiotics can be absorbed either 100 % or 0 % through extravascular routes (Gibaldi and Perrier, 1982). The real absorbed amount is usually expressed as bioavailability (F).

Bioavailability is defined as the fraction of the dose reaching the systemic circulation in an unchanged form following administration by any route (Benet, 1995). When a xenobiotic is administered orally, the bioavailability may be less than unity for several reasons: incomplete absorption, liver clearance prior to entry into the systemic circulation, and enterohepatic cycling with incomplete re-absorption following elimination into the bile.

1.2.2 Disposition

Once absorbed, a xenobiotic is delivered to all tissues at a rate determined by local blood flow or vascular permeability. Distinction between distribution and elimination is often difficult. Disposition is the term used when this distinction is not desired or is difficult to obtain. Disposition may be defined as all the processes that

occur subsequent to the absorption. By definition, the components of disposition include distribution and elimination (Rowland and Tozer, 1980).

1.2.2.1 Distribution

Distribution is the process of reversible transfer of a xenobiotic to and from the site of measurement. Any xenobiotic that leaves the site of measurement and does not return has undergone elimination, not distribution (Rowland and Tozer, 1980).

The factors modifying the distribution of xenobiotics include the physiochemical properties of the xenobiotics, the physiological and biochemical constitutions of organs or tissues, blood supply and lipid content of tissues. Fat and central nervous system (CNS) are rich in lipid. So lipophilic compounds readily distribute and accumulate in these tissues. Liver, brain, heart and kidney have high regional blood flows. A toxicant can quickly reach equilibration between blood and these tissues.

1.2.2.2 Apparent volume of distribution

The volume of distribution is the measure of the apparent space in the body available to contain the xenobiotics. It relates the amount of xenobiotic in the fluid measured. This volume does not necessarily refer to an identifiable physiological compartment but merely to the fluid volume which would be required to account for all the compound in the body (Gibaldi and Perrier 1982).

If the drug is given by iv injection, the apparent volume of distribution (V) can theoretically be estimated by the following equation:

V = amount of drug in body / C (1)

where C is the concentration of a xenobiotic in blood.

The volume of distribution depends on many factors such as pKa of the compound, the degree of plasma protein binding, the partition coefficient of the xenobiotic in the fatty tissues, differences in regional blood flow, as well as the degree of binding to other tissues within the body (Caldwell, *et al.*, 1995; Rowland and Tozer, 1980).

1.2.2.3 Elimination

Elimination is the irreversible loss of xenobiotic from the site of measurement. The conversion of one chemical species to another and the excretion of the chemically unchanged drug are the irreversible loss (Rowland and Tozer, 1980).

1.2.2.4 Systemic clearance

Systemic clearance (CL_s) is a measure of the body's ability to eliminate xenobiotics. It is the rate of elimination by all routes relative to the concentration of xenobiotics in any biological fluid. It refers to the volume of blood or plasma which would be completely cleared of xenobiotics, and can be expressed as a volume per unit of time.

CL = rate of elimination / C (2)

C: the concentration of xenobiotic in any biological fluid.

Clearance is usually further defined as blood clearance (CL_b), plasma clearance (CL_p), or clearance based on unbound or free compound concentration (Cl_u). These concepts will not be described here.

1.2.2.5 AUC

Area under the concentration-time curve (AUC) is an important parameter in relation to clearance (CL) and distribution volume (V). Their relationships are expressed as following

$$AUC = \text{amount eliminated}/CL = k.dose/C \qquad (3)$$

or

$$AUC = dose/V.k \qquad (4)$$

where k is elimination rate constant and C is drug concentration.

1.2.2.6 Half-life ($T_{1/2}$)

In the single compartment model, half-life ($t_{1/2}$) is the time it takes for the concentration to be reduced by 50 %. However, when the xenobiotic concentration in the body is described by two or more compartments, each disposition phase has a characteristic half-life. The estimation of $t_{1/2}$ will be described in 1.2.3.1.

1.2.3 Models and compartments

The distribution of a drug in the body is so complex that one cannot expect to achieve anything approaching a complete mathematical description. It is therefore necessary to make various simplifying assumptions and to replace the actual system with a model system which is rigidly defined and simple enough to be described mathematically. Many aspects of pharmacokinetics are based on model systems (Gibaldi and Perrier 1982).

1.2.3.1 One compartment model

This is the simplest model and regards the body water as one well-stirred volume with no subdivision, i.e. as one compartment of uniform xenobiotic concentration throughout. This model has many limitations, but there is a terminal phase in the elimination of most drugs when the plasma concentration declines according to a single compartment model.

In the case of intravascular injection, suppose that the elimination of a xenobiotic follow first order kinetics, the following relationship is established:

$$- dD/d_t = kD \qquad (5)$$

D: the amount of a xenobiotic in the body at time t; dD: the small amount of the xenobiotic eliminated over an instant of time d_t; dD/d_t: the elimination rate; k: elimination rate constant that defines the overall rate of elimination of the xenobiotic by all routes. The negative sign indicates that the amount of drug decreases with time.

Equation (5) can be integrated to give the equation (6) so as to show how the amount of a xenobiotic changes with time,

$$D_t = D_0 e^{-kt} \qquad (6)$$

D_0: the amount of the xenobiotic in the body at time t = 0, or, in units of concentration,

$$C_t = C_0 e^{-kt} \qquad (7)$$

where C_0 is the concentration of the xenobiotic in plasma at time t= 0 and C_t is the concentration at time t.

In natural logarithms,

$$\ln C_t = \ln C_0 e^{-kt} \qquad (8)$$

converting (8) into common logarithms ($\ln C = 2.303 \log C$):

$$\log C_t = \log C_0 - kt/2.303 \qquad (9)$$

This is the equation of a straight line, being of the form y = Bx + A, and a plot of the logarithm of plasma concentration against time after a dosage can often exhibit a terminal linear section of slope equal to -k/2.303 from which k can be calculated.

Generally, the half-life is determined from plasma or tissue concentration measurements during the terminal or elimination phase. The relationship of the elimination rate constant k to the half-life ($t_{1/2}$) of a xenobiotic can be derived from rearranging Equation (9) and giving

$$t = 2.303/k.\log(C_0/C_t) \qquad (10)$$

When C_t decreases to the half of the original concentration within the time $t_{1/2}$, the following relationship can be established:

$$t_{1/2} = 2.303/k.\log 2 = 0.693/k \qquad (11)$$

In the case of a xenobiotic given through extravascular routes, an absorption phase exists. Thus the description of the concentration change of a xenobiotic in the body can be modified by the absorption phase. The concentration C_t at any time t can be estimated by

$$C_t = C_0 (e^{-kt} - e^{-kat}) \qquad (13)$$

C_0 can be obtained by $(k_a F X_0) / [V(k_a - k)]$. Where k_a is the rate constant of absorption phase; X_0 is the dosage; F is the bioavailability; and V is the apparent distribution volume. Therefore, Equation 13 can be transformed to the following form

$$C_t = (k_a F X_0)/[V(k_a - k) (e^{-kt} - e^{-kat})] \qquad (14)$$

The parameters and constants of the absorption phase can be estimated by using the residual technique given by Gibaldi and Perrier (1975) which will not be described here.

1.2.3.2 Two compartment models

In two compartment models, the body consists of two separate volumes and xenobiotics undergo reversible distribution between the two compartment which are most simply regarded as the plasma and the tissues. Behaviour of this type is seen immediately following the rapid intravenous injection of most drugs. The drug in the two compartments can ultimately attain a state in which the concentration of a xenobiotic declines at the same fractional rate. Under these conditions, the plasma concentration of a xenobiotic finally declines according to a single compartment model.

There are three patterns in the two-compartment models which are shown in FIG 1-2 (Gibaldi and Perrier, 1975). As shown in FIG 1-2, FIG 1-2A assumes that the xenobiotic is strictly eliminated from the central compartment, FIG 1-2B assumes that the xenobiotic is strictly eliminated from the peripheral compartment and FIG 1-2C is assumed that the xenobiotic is eliminated from both the central and peripheral compartments.

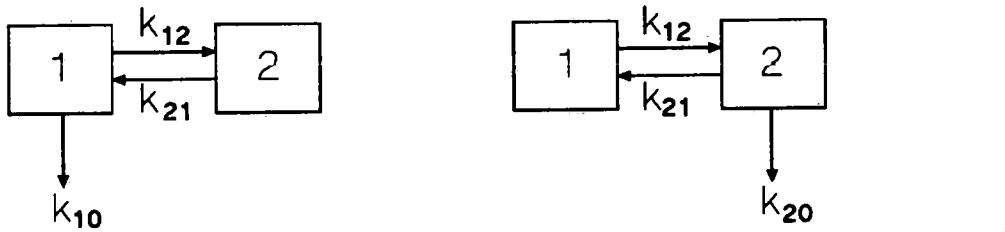

A. Elimination from central compartment. B. Elimination from peripheral compartment.

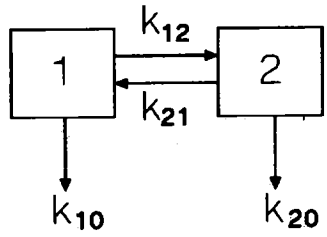

C. Elimination from both compartments.

1: Represents central compartment.

2: Represents peripheral compartment.

0: Represents elimination.

k: Represents rate constant.

FIG 1-2 Three patterns of two-compartment models.

In the two compartment model, the concentration (C_t) of a xenobiotic at any time t can be estimated by

$$C_t = Ae^{-\alpha t} + Be^{-\beta t}$$

where A ($=C_1$) is the concentration of the xenobiotic in central compartment at time t=0, α is the elimination rate constant of the xenobiotic from central compartment, B ($=C_2$) is the concentration of the xenobiotic in peripheral compartment at time t=0, β is the elimination rate constant of the xenobiotic from peripheral compartment.

In pattern FIG 1-2A, the rate constants can be estimated by

$$k_{21} = (\beta A + \alpha B)/(A + B)$$

$k_{10} = \alpha\beta /(k_{21})$

$k_{12} = \alpha + \beta - k_{21} - k_{10}$

In patter FIG 1-2B, the rate constants can be obtained by

$k_{12} = (\beta A + \alpha B)/(A + B)$

$k_{20} = \alpha\beta/(k_{12})$

$k_{21} = \alpha + \beta - k_{12} - k_{20}$

In the pattern of FIG 1-2C, the rate constants can not be calculated in the above ways. The reason has been described by Gibaldi and Perrier (1975). It will not be discussed here.

1.2.3.3 Three compartment and other models

Models based on three or more compartments are often necessary to provide a more accurate interpretation of the experimental observations. Physiological models have also been introduced and these relate to the known blood flow to various organs and seek to describe the drug concentration profile in different tissues (Bischoff and Dedrick, 1968; Martin, 1986). These models are not described here.

1.3 Metabolism:

The absorbed xenobiotics may undergo elimination unchanged, retention unchanged, spontaneous chemical transformation and enzymatic metabolism. Highly polar or volatile substance are likely to be eliminated unchanged. In contrast, non-polar, highly lipophilic compounds may be retained for longer periods in tissue lipids (Caldwell, *et al.*, 1995). Some compounds may undergo spontaneous chemical changes: this may include hydrolysis at the appropriate pH and reaction

with nucleophilic or electrophilic centres in tissue macromolecules (Testa, 1983). But for most compounds, enzymatic metabolism is the major way for them to be eliminated from body tissues. This enzymatic metabolism includes Phase I (oxidation, reduction, hydrolysis) and Phase II (conjugation) reactions. Phase I reaction introduces or uncovers a functional group suitable for subsequent conjugation or for excretion.

1.3.1 Phase I metabolism

Oxidative metabolism: The most important enzyme system involved in Phase I oxidative metabolism is cytochrome P450, the terminal oxidase component of the microsomal electron transfer system. The electrons required are supplied by the closely associated enzyme NADPH-cytochrome P450 reductase, a flavoprotein that transfers 2 electrons to cytochrome P450 from NAD(P)H (Caldwell, *et al.*, 1995). The cytochromes P450 which are responsible for the oxidation of many xenobiotics are an enzyme superfamily consisting of a number of related isoenzymes, all of which possess an iron protoporphyrin IX as prosthetic group. There are 10 mammalian gene families comprised of 18 subfamilies (Nebert, *et al.*, 1991). The most important enzymes involved in xenobiotic metabolism belong to the 1A, 2B, 2C, 2D, and 3A subfamilies. The individual enzymes are thought to metabolise substrates via the same catalytic mechanism (Guengerich and Macdonald, 1990). But they tend to show selectivity toward substrates (Caldwell, 1995).

The another major enzyme involved in xenobiotic metabolism is flavin-containing monooxygenase (FMO) which is a oxygen- and NADPH-dependent microsomal flavoprotein. It catalizes the N-oxidation of secondary and tertiary

amines and the S-oxidation of thiols and thiourea as well as hydrazine derivatives (Paulsen, *et al.*, 1974; Ziegler, 1988, 1990; Parkinson, 1996)

Reductive metabolism: Even though microsomal cytochrome P-450 is classified as oxygenase, it also catalyses the reductive biotranformation of certain xenobiotics, for example, azo reduction, aromatic nitro reduction and reductive dehalogenation as well as the reduction of arene oxides, N-oxides, and alkyl halides. Both the flavoprotein enzyme, NADPH-cytochrome P-450 reductase, and the terminal oxidase, cytochrome P-450, are involved in these reductions (Sipes and Gandolfi, 1991). The very low redox potential, broad substrate specificity, and strong ligand binding of these systems allow the donation of electrons to electron-accepting xenobiotics, which results in a reduction rather than the predominant oxidative biotransformation (Sipes and Gandolfi, 1991).

Reductive metabolism may detoxify a xenobiotic, but it often results in more toxic products or reactive intermediates. For example, numerous nitro compounds undergo reduction to amino derivatives, which can then be oxidized to toxic N-hydroxyl metabolites (Parkinson, 1996). Carbon tetrachloride and halothane are two classic examples of cytochrome P-450-catalyzed reductive bioactivation to free radical intermediates (Sipes and Gandolfi, 1991).

The other oxidation-reduction enzymatic systems include aldehyde/ketone reductase and alcohol dehydrogenase. Aldehydes, ketones, and alcohols are functional groups that produced from the oxidation of carbon or the hydrolysis of ester linkages. In addition, they are frequent functional groups that appear in drugs and other xenobiotics. These functional groups are often further biotransformed in the body by oxidation or reduction (Sipes and Gandolfi, 1991; Parkinson, 1996).

1.3.2 Phase II metabolism

Metabolites or intermediates of xenobiotics may further react with endogenous components to form conjugates. Conjugation reactions may be divided into 2 distinct groups according to the source of energy for the reactions (Caldwell, 1980): the energy derived from the activated endogenous conjugating agent and the energy derived by prior metabolic activation of the xenobiotics. For example, the energy of the reaction of glucuronic acid, sulphate, methylation, and acetylation is derived from the endogenous conjugating agents, and the energy of glutathione and amino acid conjugations is derived from the metabolic activation of xenobiotics (Caldwell, *et al.*, 1995; Parkinson, 1996).

The important enzymes involved in phase II reaction include glucuronyl transferase, glutathione-S-transferases, N-acetyltransferase, epoxide hydrolase, methyltransferase (O-, N- and S- forms) and sulfotransferase (Commandeur, 1995; Caldwell, 1995; Parkinson, 1996). They all have their own specific substrates.

1.3.3 Metabolism of xenobiotics in brain

Liver is the main site of metabolism of xenobiotics. Many extrahepatic tissues are also capable of metabolising foreign compounds. It has been demonstrated that brain has major Phase I and Phase II enzymes and is actively involved in metabolising xenobiotics (Haglund, 1984; Lowndes, 1994; Ravindranath, *et al.*, 1995; Bhagwat, *et al.*, 1995). Whole brain microsomal P450 levels are approximately 2.5-4 % of the liver (Warner, 1988). However, mitochondrial P450 content in brain is significantly higher than the microsomal P450 content, in contrast to the liver (Walther, *et al.*, 1986; Bhagwar, *et al.*, 1995). Brain exhibits regional

differences in the distribution of P450. Maximal P450 levels have been detected in olfactory lobes, cerebellum and brain stem (Anandatheerthavarada, *et al.*, 1993). The other major metabolising enzyme in brain is FMO. It has been demonstrated that FMO exists in neuronal cell bodies and localises in microsomes (Bhamre, 1993).

Glutathione S-transferases (GSTs), a Phase II enzyme family, also exist in brain. The cell-specific distribution of the GSTs varies according to isoforms of GSTs. For example, μ-GST was mainly detected in astroglial cells (Abramovitz *et al.*, 1988; Cammer, *et al.*, 1989), π-GST was observed in myelin and myelinating cells (Tansey and Cammer, 1991) and α-GST was found in neurons (Carder, *et al.*, 1990; Johnson, *et al.*, 1993). All these isoforms also exist in other cell types in the nervous system but their activities greatly vary from cell type to cell type or from region to region.

1.4 Features of the central nervous system

1.4.1 Interrelationships between neurons and neuroglia

The mammalian nervous system is an extensively organised tissue. Nervous tissue consists of two cell-types: nerve cells, or neurons, and several types of glial cells, or neuroglia (including astrocytes, oligodendrocytes, microglia, and ependymal cells). Neurons are excitable cells which process internal and external information and directly or indirectly control or co-ordinate physical and biochemical activities. Whereas neuroglia play an important role in supporting and protecting neurons and participating in the neural activity, development, nutrition, defence and repair processes of the central nervous system. Due to the physiological and biochemical differences between neurons and neuroglia, they may interact in

the neurotoxicities induced by neurotoxicants in different ways. For example, neuroglia may be the first target of some neurotoxicants and the neuronal damage may be a secondary event due to the functional failure or loss of support cells. On the other hand, neurotoxicants may be biotransformed into either detoxified or activated forms in neuroglia before they reach neurons. As a result, neuroglia may reduce or increase toxic potentials of neurotoxicant to neurons. Therefore the interactions between the two classes of cells in physiological functions and metabolism of xenobiotics ultimately determine the balance between resistance and susceptability to functional or morphological damage in the brain.

1.4.2 Blood-brain barrier

In the central nervous system, the tight junctions between the endothelial cells form a integrated membrane barrier known as the blood-brain barrier which prevents the entry of proteins and other water-soluble substances of low molecular weight (Risau and Wolburg, 1990). The blood-brain barrier plays an important role in protecting the brain from exposure to some toxic substances. However, some areas in the CNS have no blood-brain barrier, namely the choroid plexus, neurohypophysis, media eminance, pineal gland, area postrema, and subfornical organ. The tight junctions in these areas are formed between the ependymal cells. In addition, sensory and autonomic ganglia are not protected by blood-tissue barriers, their neurons thus being particularly exposed to neurotoxins. However, peripheral nerve has a somewhat less effective barrier : the perineurium forming a connective tissue sheath. The inner layers of perineurial cells are connected by tight junctions (Rechthand and Rapoport, 1987).

However, certain lipophilic compounds can simply diffuse through endothelial cells of brain capillaries by a trans-cellular route and penetrate into the brain (Ravindranath, 1995). The permeability is proportional to the lipid/water partition coefficient. Brain, spinal cord and peripheral nerves are the organs with the highest lipid concentration after adipose tissue. It is evident that lipid solubility of toxicants plays a fundamental role in their neurotoxicities (Lefauconnier and Bouchaud, 1994). Therefore, the physical characteristics of the blood-brain barrier cannot provide sufficient protection for the CNS from lipophilic toxicants, for these the xenobiotic metabolic systems in the barrier provide the major defence (Ghersi-Egea, *et al.*, 1994).

1.4.3 Regeneration ability

As is well known, unlike other cells, neurons can not be replaced once they are lost from the adult nervous system. Although some glia cells can repair the injury, they can not functionally replace neurons. Therefore any damage to neurons in the central nervous system will cause irreversible functional loss. This feature makes the nervous system particularly vulnerable to neurotoxicant-induced damage.

1.4.4 Regional heterogeneity and selective vulnerability in brain

Over 100 years ago, the German pathologist Franz Nissl did a series of experiments in order to identify cellular changes specific to each of a variety of toxicants. He observed that the administration of particular agents consistently resulted in characteristic injury to neurons of defined area of the brain. These studies stimulated later pathologists to propose the hypothesis that the cells in particular

regions of the brain, by virtue of unique biochemical or anatomic features, are vulnerable to intoxication by certain classes of xenobiotics and not by others. This theory became known as *pathoclisis* (Vogt, *et. al.*, 1922).

During the past two decades, the basis of pathoclisis has become clearer. Brain exhibits tremendous regional heterogeneity and each region displays specialised and selective functions. Its heterogeneity may present in different levels. The differences in lipid content and metabolic capacity and specificity of different regions or cell types are all responsible for the selective susceptibility to neurotoxicants. For example, myelin is rich in lipids which comprise 75 to 80 percent of the dry weight of CNS myelin. The major lipid molecules in myelin are cholesterol, cerebroside sulphate, sphingomyelin, ethanolamine glycero-phosphatides (EGP), serine glycerophosphatides (SGP) and choline glycerophosphatides (CGP). Small amounts of lipids such as phosphatidyl glycerol, polyglycerol phosphatides, phosphatidic acid, galactosyl-diglyceride, ceramide, and cholesterol esters also present (Finean, 1960). Therefore myelin is particularly important in the distribution of lipophilic substances in the central nervous system. For example, the distribution of toluene, a lipophilic compound, in brain correlates well with the lipid contents in different regions of brain (Gospe, 1988).

The heterogeneity in metabolic ability and specificity may be due to the differences in the presence of metabolising enzyme systems, or the efficiency of these systems (Lowndes, *et al.*, 1994). The level of glutathione in the brainstem is lower than that in other regions (Ravindranath, *et al.*,1989). The presence of high amounts of P450 in brainstem coupled with the low levels of glutathione may render the brainstem particularly vulnerable to damage through P450-mediated

bioactivation of xenobiotics to reactive electrophilic metabolites (Ravindranath, 1989; 1995).

It has been demonstrated that the distribution of certain cytochromes P450 are highly dependent on the isoform of the enzyme, brain region and cell type. For instance, CYP2E1, an isoenzyme of cytochromes P450, is mainly found in neurons but not in glia (Hansson, *et al.*, 1990; Anandatheerthavarada, *et al.*, 1993). However, there are important exceptions, it being present in cerebellar Bergman glia, but not in Purking's cells for example (Lowndes, *et al.*, 1994). In certain brain regions, CYP2B1 appears restricted to glia cells while in other regions neurons also contain appreciable amounts of this enzyme (Volk, *et al.*, 1991). The other major drug metabolising enzyme FMO mainly locates in neuronal cells (Bhamre, *et al.*, 1993). The difference in the distribution of metabolising enzymes is perhaps the most important factor in regional vulnerability to specific neurotoxicants, but is at present very incompletely understood.

There is no doubt that the heterogeneity of brain is the basis of selective neurotoxicities of neurotoxicants.

1.5 Approaches of this study

Conventional studies in neurotoxicology focus on what neurotoxicants do to the nervous system. In fact, systemic factors and the nervous system itself can greatly modify the toxicities of neurotoxic agents. Their interaction causes particular damages in the nervous system. The purpose of this thesis is to investigate the significance of these modifying factors in the case of two model agents, *p*-Bromophenylacetylurea (BPAU) and *m*-dinitrobenzene (*m*-DNB). Pharmacokinetics

plays an important role in describing how body factors influence neurotoxicant behaviour. The concentration, persistence and metabolism of neurotoxicants as well as the primary biochemical events at target sites are responsible for neurotoxicant-induced injury. BPAU and *m*-DNB were selected as model neurotoxicants for this study. BPAU is widely used as a model compound in studying delayed neuropathy (details see the **Introduction** of **Section 2**). *m*-Dinitrobenzene (*m*-DNB) can selectively cause brain stem damage (details see the **Introduction** of **Section 3**). Both were suspected to be subject to significant metabolic transformation and, therefore, they were chosen as model neurotoxicants to investigate the metabolic and pharmacokinetic factors in their neurotoxicities.

SECTION 2. METABOLISM AND PHARMACOKINETIC FACTORS IN *p*-BROMOPHENYLACETYLUREA-INDUCED NEUROPATHY

2.1. INTRODUCTION

p-Bromophenylacetylurea (BPAU) was originally synthesised as one of a series of halogenated congeners of phenylacetylurea (Phenurone, Abbott chemicals), see FIG 2-1, an antiepileptic agent, to search for a more effective anticonvulsive drug (Diezel and Quadbeck, 1960).

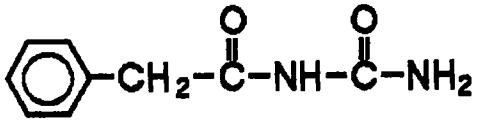

a. Phenylacetylurea

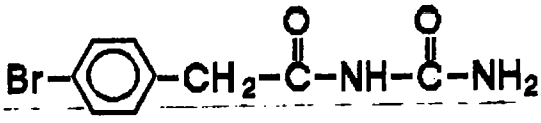

b. Bromophenylacetylurea (BPAU)

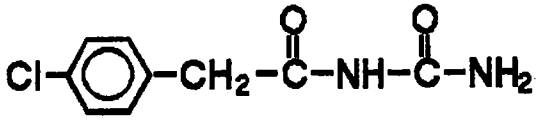

c. Chlorophenylacetylurea (CPAU)

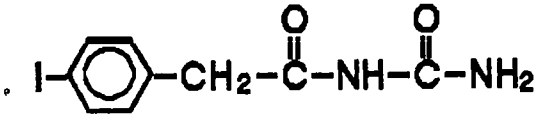

d. Iodophenylacetylurea

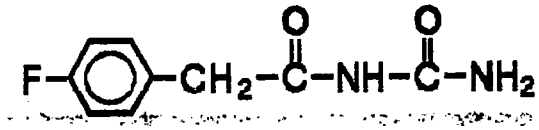

e. Flourophenylacetylurea

FIG 2-1. Phenylacetylurea and its derivatives

Although its anticonvulsive effect was better than other derivatives of phenylacetylurea, it produced serious delayed ataxia and paralysis in rats (Diezel and Quadbeck, 1960). A further study which was done by Cavanagh (1968) showed that BPAU-induced delayed neuropathy in rats was clinically similar to organic phosphorous compounds induced delayed neuropathy (OPIDN) in chicken. Rats were more susceptible to BPAU neurotoxicity than other species. Therefore, BPAU has widely been used as a model compound in mechanistic studies of delayed neuropathy in rats by many researchers though it is not commercially available (Canavagh, 1968; Fossom, 1985; and Nagata,1986).

2.1.1 Physiochemical properties of BPAU

BPAU is a white crystalline solid. The molecular structure of BPAU is shown in FIG 2-1b. Its chemical formula is $C_9H_9O_2N_2Br$ and molecular weight is 257. The melting point of BPAU is at 230-231 °C (Jakobsen, 1981). BPAU is very poorly soluble in water and common organic solvents such as ethanol, methanol, acetone, chloroform and glycerinformal. It dissolves well in dimethylsulphoxide (DMSO), which is the commonly used vehicle for administration.

2.1 2 p-Bromophenylacetylurea-induced neurotoxicity

BPAU can induce a typical delayed ataxia in rats. The animals developed paralysis in hindlimbs after a 'silent' period of 7-10 days after dosing (Diezel and Quadbeck,1960; Canavagh, 1968). The clinical feature of delayed ataxia was not observed on rabbit, guinea-pig, and chicken, which suggests that there are species differences in susceptibility to BPAU neurotoxicity (Canavagh, 1968). The clinical

severity of delayed ataxia and the silent period before its development depends on dosage. Either double or single doses of 400, 200, or 100 mg/kg BPAU can induce different degree of clinical ataxia and/or paralysis in rats (Diezel & Quadbeck, 1960; Canavagh, 1968; Fossom, 1985; Nagata,1986). In addition, similar clinical changes were also produced when rats were given daily oral doses of 10 or 40 mg/kg BPAU for two or six months (Fossom, 1985). Therefore, either a higher bolus dose (100-400 mg/kg) or long-term repeated lower doses (10-40 mg/kg/day for 2-6 moths) induced the same target damage. This suggests that BPAU may show some accumulation in target tissues. Pharmacokinetically, a single large dose can produce a instant high level in target tissues but long-term repeated lower doses allow the toxicant to accumulate in target tissues until it exceeds a certain threshold and trigger toxic damage. In addition, age differences of sensitivity to BPAU have also been documented. Adult rats are more sensitive to BPAU than young ones (Canavagh, *et al.*, 1968; Chen, *et al.*, 1971).

Axonal degeneration, particularly of distal axons, is the distinctive character of BPAU axonopathy. It shows the Wallerian-like degeneration (Canavagh, *et al.*, 1968). The earliest pathologic changes were detectable 7 days after BPAU dosing. Distal myelinated axons showed mild swelling, enlargement of mitochondria, and irregularly arranged membranous trabeculae made up vesicles and tubules. The severity of these changes increased with time. By 3 weeks, rats showed 18 to 50 per cent loss of axons in the distal phrenic nerve (Troncoso, 1982). Anatomically, long fibres are more sensitive than short fibres (Canavagh, *et al.*, 1968). A decreased number of nerve fibres, and myelinated axons containing osmiophilic accumulations were also observed after chronic intoxication with lower daily doses of 10 or 40

mg/kg BPAU for 2 or 6 months. BPAU can also cause degeneration in ganglionic cells in the anterior horns of the lumbar and lower thoracic spinal cord in rats (Potkonjak, 1965). The dorsal columns showed loss of axons and gliosis; cervical, thoracic, and lumbar levels of spinal cord showed greater amounts of degeneration in the rostral regions of ascending tracts, and in caudal regions of decending tracts 14-17 days after dosing (Cavanagh, *et al.*,1968).

BPAU can cause a reduction in the amount of protein transported retrogradely. This suggests that retrograde axonal transport was affected (Nagata, 1986). Fast axonal transport were affected in both sensory and motor nerves (Nagata, 1986; Oka, 1990). Electrophysiological studies showed that the decrease in amplitude of muscle action potential induced by BPAU agreed well with the severity of ataxia (Jakobsen, 1981). This also provides an index of peripheral nerve damage.

The mechanism of BPAU-induced delayed neuropathy is not known. A reduction in amino acid incorporation into proteins during the period before the onset of paralysis due to BPAU was found in spinal ganglia (Cavanagh, 1971). The toxic effects of BPAU can be reduced or even prevented by the co-administration of 1,1,3-tricyano-2-amino-1-propene (TAP), which is now used for the treatment of hypothyroidism (Potkonjak, 1965). TPA can increase the quantity of ribonucleic acid in nerve cells (Egyhazi, 1961) and induce the regeneration of cut nerve in dogs and rabbits (Davanzo, 1963). BPAU did not cause changes in glucose-dependent lactate production (LoPachin, 1984) nor alter energy utilization (Brimijoin and Mintz, 1984). These observations suggest that the biochemical lesion caused by BPAU does not impair energy metabolism.

Of the derivatives of halogenated phenylacetylurea, see FIG 2-1 , only *p*-chloro- and *p*-brominated forms exhibited serious neurotoxicity (Diezel and Quadbeck, 1960; Brimijoin and Nagata, 1986). This implies that the chemical properties of the halogenated phenylacetylureas may play an important role in their neurotoxicities because it may significantly modify the absorption, distribution and metabolism of these compounds as well as the specificity and susceptibility of target sites.

2.1.3 Phenylmethanesulphonyl fluoride and 'promotion'

A non-neurotoxicant can exaggerate the neurotoxicity induced by neurotoxicants. This phenomenon was originally observed in organophosphorous compound induced neuropathy (OPIDN) and has been termed 'promotion' (Veronesi and Padilla, 1985; Pope and Padilla, 1990; Lotti, *et al*, 1991). Phenylmethanesulfonyl fluoride (PMSF) is a commonly used potentiator. PMSF is widely used as a protease inhibitor in protein purification to protect proteins from degradation. It can inhibit serine proteases, including chymotrypsin, trypsin, thrombin, thiol protease such as papain (Keesey, 1987). It can also inhibit some non-protease enzymes such as human erythrocyte acetylcholinesterase, human liver arylsulfatase A (Keesey, 1987). The inhibition mechanism of PMSF on enzymes lies on its sulfonating the active serine residue in the active site of a protease (Keesey, 1987).

The mechanism of OPIDN is believed to relate to irreversible inhibition or 'ageing' of neuropathy target esterase (NTE). Similar to organophosphates, PMSF can also inhibit NTE, but itself does not induce delayed neuropathy. The LD_{50} of

PMSF is 200 mg/kg in mice by ip dose and 500 mg/kg in rat by oral dose (Keesey, 1987). When PMSF was given before exposure to an organophosphate, it protected animals from OPIDN. The protective effect of PMSF was thought to be due to its reversible occupation of NTE, thereby preventing subsequent binding with the organophosphate. However, when PMSF was given after the organophosphate, it enhanced OPIDN. These data suggested that PMSF can act at a site other than NTE to promote OPIDN (Fioroni *et al*, 1995). This promotion site(s) is still unknown. BPAU does not inhibit NTE (Johnson, 1969) but can induce clinically delayed ataxia similar to OPIDN and its neuropathy can also be intensified by PMSF (Ray & Johnson, 1992). The mechanism of promotion is not known yet.

2.1.4 Approaches of this study

As reviewed above, BPAU represents a distinct category of neurotoxicant and has widely been used as a model compound in studying delayed neuropathy. Several factors, for example, age, dosing regimen as well as a non-neurotoxicant PMSF, can significantly modify its neurotoxicity. The mechanism of its neurotoxicity is not yet known. So far, the clinical features, histopathology and electrophysiology of BPAU-induced neuropathy have been well described but its metabolism and pharmacokinetics have not been studied. The studies of metabolism and pharmacokinetics may provide important information for a better understanding to its neurotoxicity. Therefore, this part of the thesis investigated the roles of metabolic and pharmacokinetic factors in BPAU-induced delayed neuropathy and its modification by the both age and PMSF.

2.2. EXPERIMENTS

2.2.1 Chemicals

p-Bromophenylacetylurea (BPAU) was synthesised by Dr A. R. Mattocks (MRC Toxicology Unit); phenylmethanesulphonyl fluoride (PMSF) was purchased from Koch-Light Laboratories LTD; acetonitrile (HPLC grade) and diethyl ether were obtained from Sigma; dimethyl sulphoxide (DMSO) was purchased from BDH; glycerinformal, methanol, trichloroacetic acid and ammonium acetate were obtained from Fisons.

2.2 2 Pharmacokinetics of BPAU

2.2.2.1 Animals and procedures

Groups of 4 female F344 rats, weight 170-210 g, were given a single i.p. dose of 150 mg/kg BPAU in DMSO. All the animals were kept in plastic cages with stainless steel grill tops and free access food and water. The room temperature in animal house was 22 ± 1 °C. The animals were killed at either 1, 2, 4, 6, 12, 18, 24, 48, or 72 hour(s) after dosing. Two rats were used as control and given the same volume of DMSO as test groups. They were killed at either 6 or 18 hours after administration.

2.2.2.2 Sample preparation for the determination of BPAU and its metabolites

Animals were killed by the inhalation of carbon dioxide. Blood samples were collected from the heart immediately after death of animals. Brain, spinal cord,

liver, and muscle were dissected, weighed, and stored at -20 °C. Before analysis, they were thawed and homogenised in a mixture of methanol and DMSO (95 : 5 by volume) at 100 mg tissue per ml solution. Blood was centrifuged at 3000g for 10 min. 1 ml serum was taken and then mixed with 4 ml methanol/DMSO solution. In addition, five samples of fresh serum were spiked with 5 mg BPAU per ml to study the recovery of this analytical system. These samples were also mixed with methanol/DMSO solution (1:4) as stated above. All samples were centrifuged with an Eppendorf centrifuge at 9000 g for 5 min and the supernatant kept for HPLC analysis at -20 °C for up to 4 weeks. The supernatant of brain or spinal cord was filtered with a syringe filter (0.2 μm) before injection into HPLC, see 2.2.2.3.

2.2.3 HPLC analytical conditions

2.2.3.1 Gradient

HPLC system: Waters HPLC system with a Controller 600, a tunable absorbance detector 486, and an autosampler plus 717. The column was a S5 ODS2 – 250 × 4.6 mm (Spherisorb); and the detector wavelength: 240 nm. The mobile phase (A= 0.1 M ammonium acetate, pH = 6.5, B = acetonitrile) used a gradient: 25 % B linear to 50 % B within 10 min and then maintaining 50 % B from 10 to 20 min; and a flow rate at 1ml/min. The injected volume of each sample was 25-50 μl. The HPLC profiles of BPAU and its metabolites are shown in FIG 2-2.

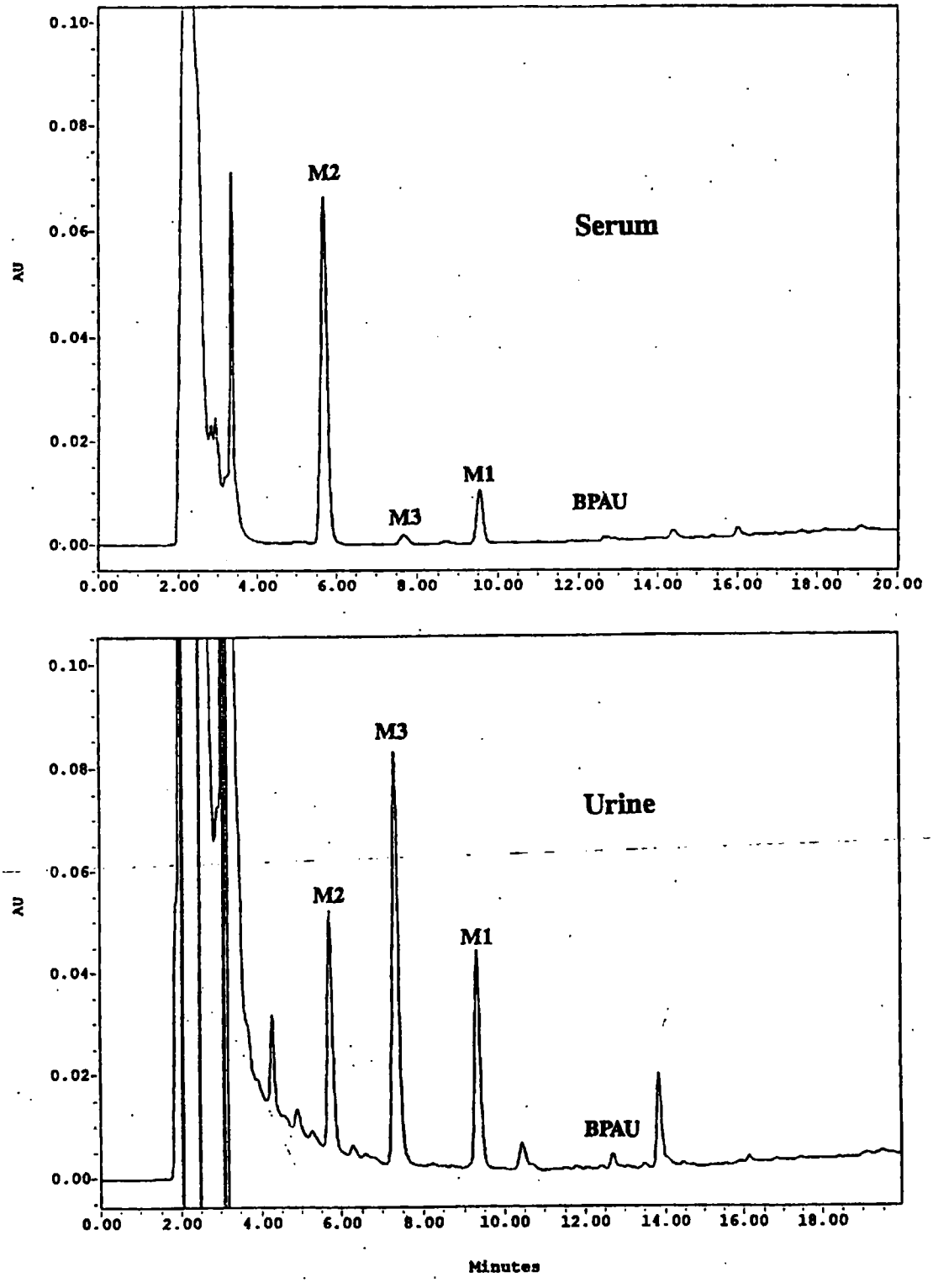

FIG 2-2, HPLC profiles of BPAU and its metabolites - gradient condition

2.2.3.2 Isocratic

HPLC system: Philips, Pye Unicam with a PU4010 pump (LDC/Milton) and a Roy Spectromonitor III. Column: S5 ODS2 250 × 4.6 mm (Spherisorb); Wavelength: 240 nm; Mobile phase: 32% acetonitrile in 0.1 M ammonium acetate for BPAU and its metabolite M1 analysis, 23 % acetonitrile in 0.1 M ammonium acetate for the determination of metabolites M1, M2, and M3; Velocity: 1ml/min; The injected volume of each sample: was 25-50 μl. HPLC profiles of BPAU and its metabolites are shown in FIG 2-3.

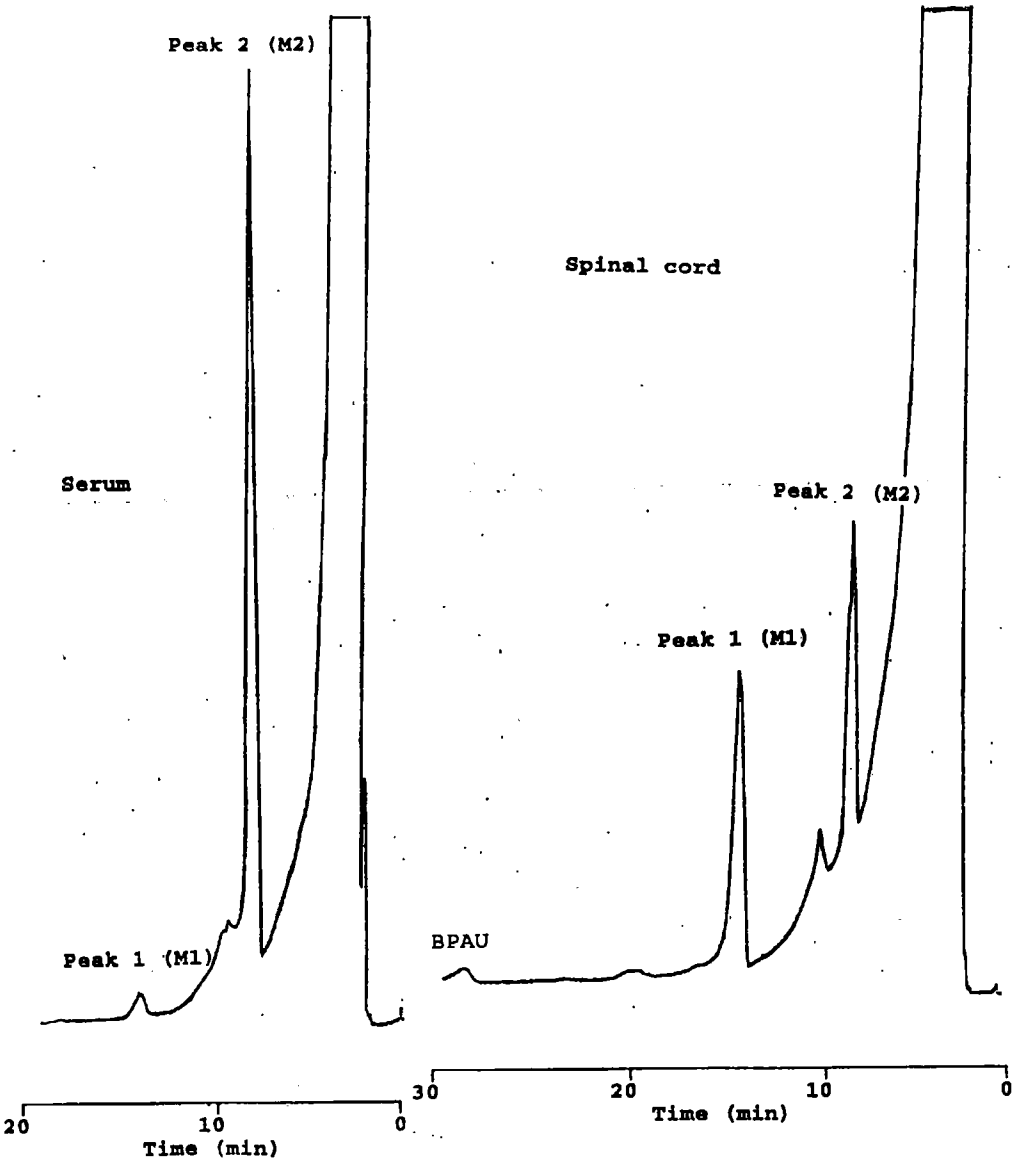

FIG 2-3. HPLC profiles of BPAU and its metabolites - isocratic condition

2.2.4 BPAU metabolism *in vivo*

2.2.4.1 Sample preparation

Three metabolites were detected in tissues, serum and urine by HPLC, see FIG 2-2. They were temporarily designated M1, M2 and M3 respectively. In order to do further study, they were purified. Liver and blood were collected from rats killed at either 18 or 24 hr after dosing for M1 and M2 purification. The procedures are as stated in 2.2.2.2. Urine was obtained from rats kept in metabolic cages from 12 to 48 hr after dosing for metabolite purification, especially for M3 purification.

2.2.4.2 Pre-extraction

M1: Liver was thawed and homogenised in a mixture of methanol and DMSO (95:5) at 100 mg tissue per ml solution. The homogenate was centrifuged at 6000 g for 20 min. The supernatant was concentrated under reduced pressure with a Rotovaper-R in 37 °C water bath for about 40 min to allow methanol evaperated and then stored at 4 °C overnight. Then it was centrifuged with an Eppendorf centrifuge at 9000 g for 5 min to get rid of insoluble residue. The supernatant was kept and diluted with an equal volume of distilled water for extraction by diethyl ether. Then it was extracted with equal volume of diethyl ether 3 times. The extraction was concentrated again by evaporating diethyl ether with a Rotovaper-R for 30 min. The residue of the extraction was diluted with an equal volume of 21 % acetonitrile. The solution was kept at 4 °C overnight, then centrifuged with an Eppendorf centrifuge at 9000 g for 5 min. The supernatant was kept for the isolation of M1 by HPLC.

M2: Serum was mixed with methanol/DMSO (95 : 5) at 0.2 ml serum per ml solvent and centrifuged at 6000 g for 20 min. Further procedures as for M1.

M3: All the collected urine was pooled and centrifuged at 6000 g for 20 min. The supernatant was kept and extracted with an equal volume of diethyl ether three times. Further procedures were as for M1.

2.2.4.3 Purification of BPAU metabolites

HPLC analytical conditions were as stated in 2.2.2.3. A 500 µl loop was used for metabolite isolation. The mobile phase for metabolite analysis was 23 % acetonitrile for M1 purification and 21 % acetonitrile in 0.1 M ammonium acetate for metabolite M2 and M3 purification. The injection volume for purification was 250-350 µl.

M1 or M3: The peak fractions containing M1 or M3 were collected and pooled into a glass bottle. The bottle was placed in a 25 °C water bath and blown with nitrogen for 40 min to allow acetonitrile to evaporate. After that, the rest of the solution was extracted with an equal volume of diethyl ether three times. Then the extraction was concentrated by evaporating diethyl ether with a Rotovaper-R at room temperature for 30-40 min. The residue was dissolved in 5-10 ml of 23 % acetonitrile and purified for the second time by HPLC and the peak fractions were collected and extracted again as above. Then ether residue from this second purification was placed in a glass test tube and dried with nitrogen.

M2: The peak fraction was collected and pooled in a glass bottle. Then it was blown with nitrogen in 37 °C water bath for 40 min, diluted with 0.1 M ammonium acetate (1:1) and filtered through a cartridge (Bond Elut C18, Varian). When all of

the diluted solution had been filtered, the cartridge was washed with 2 ml water and M2 was then washed off with 5 ml methanol. The methanol eluate was then dried with nitrogen.

2.2.4.4 Mass spectrum analysis of metabolites

BPAU and purified M1, M2 and M3 were analysed by mass spectrometry (MS). Mass spectra were obtained on a V.G.70-SEQ instrument (Fisons Instruments, VG Analytical, Manchester, UK.) of EBqQ geometry. All samples were ionised by negative ion fast atom bombardment (FAB) using xenon as the source of fast atoms. The primary beam impacted on the sample at 8.5 keV with a beam flux equivalent to 1 A. The secondary ions produced were accelerated to 8 keV from the source region and analysed in the first mass spectrometer (EB) using a scan speed of 5s.decade^{-1} at a resolution of 1500. Samples, in chloroform, were analysed by dissolving 2 μl of sample in 2 μl of 3-amino-1,2-propanediol (Aldrich Chemical Co.Inc.), which served as the FAB-MS matrix.

2.2.4.5 Nuclear magnetic resonance (NMR)

BPAU and its purified metabolites M1, M2 or M3 were dissolved in DMSO. Scanning was carried out on a BRUKER ARX 250 instrument. The scanning times varied with the sample quantity.

2.2.5 Animal model of BPAU-induced delayed neuropathy and its time-dependent promotion by PMSF

2.2.5.1 Animals and procedures

Groups of 6 female Wistar rats (LACP), weight 170-210 g, were given two daily oral doses of 150 mg/kg BPAU in DMSO. Time-dependent promotion was studied by giving a single dose of 100 mg/kg PMSF in glycerinformal at either 1 day before the first BPAU dose (PMSF-1d-BPAU) or 4 hours (BPAU-4hr-PMSF), 1 day (BPAU-1d-PMSF) or 4 days (BPAU-4d-PMSF) after the second BPAU dose. A BPAU only control group were given two daily oral doses of 150 mg/kg BPAU and the same volume of glycerinformal (solvent) as the above groups 4 hours after the second BPAU dose. A PMSF only control group was given two daily oral doses of an equal volume DMSO (solvent) and a single ip dose of 100 mg/kg PMSF in glycerinformal 4 hours after the second DMSO dose. The rats were kept in stainless steel cages with free access to food and water. Glass dishes with food were placed on the floor of cages for disabled rats from day 7 after BPAU dosing. Room temperature was maintained at 22 ± 1 °C. Natural light and dark cycles were adopted for the whole duration of the experiment. Animals were examined and weighed every day.

2.2.5.2 Evaluation of ataxia, slope test, and body weight

2.2.5.2.1 Ataxia scores:

The evaluation of ataxia was based on a 0 - 10 point system (Johnson & Ray, 1993): 0: Normal; 1: Body sways when walking; 2: Legs extended or splayed when walking; 3: Slow to pick up hind legs when walking; 4: Clear signs of hind limb weakness; 5: Occasionally drags a leg when walking; 6: Hind legs splayed out behind body; 7: Some additional forelimb weakness; 8: Rats cannot lift 350 g with forelimbs; 9: Difficulty in righting body; and 10: Full ataxia, unable to right body.

2.2.5.2.2 Slope test:

A wooden board (82 × 40 cm) was placed horizontally. Each rat was placed on the centre of the board and one end of the board was elevated slowly until the rat began to slip down. Then the height which the end reached was recorded. The height was converted into the angle of the slope. The test was repeated three times and the mean value recorded. If the rat attempted to move off the board during the test, the result was discarded and a new test made.

2.2.5.2.3 Body weight:

Each rat was weighed and recorded every day or every other day.

These three measures were made for every day or every two days from 1 day before intoxication to 80 days after intoxication. All animals were terminated by inhalation of carbon dioxide at the end of the experiment.

2.2.6 Effects of PMSF on the metabolism and pharmacokinetics of BPAU

2.2.6.1 On metabolism

2.2.6.1.1 Animal and procedures

Four groups of 5 female F344 rats were given two daily po dose of 150 mg/kg BPAU. Two test groups were given 100 mg/kg PMSF at either 1 day before the first BPAU dose or 4 hours after the second BPAU dose. Two control groups were given the same volume of glycerinformal (solvent) as test groups at 4 hours after the second BPAU dose. One of the two control groups was killed at 6 hours after the second BPAU dose, which was used as peak control because BPAU

reached its peak value in tissues at 6 hours after dosing. Other groups were killed at 24 hours after the second BPAU dose.

2.2.6.1.2 Sample preparation

Animals were killed by carbon dioxide. Blood of each animal was collected immediately after death. Brain, spinal cord, liver, and muscle were removed, weighed, and stored at -20 °C. For sample preparation and analysis see 2.2.2.2 and 2.2.2.3.

2.2.6.2 On pharmacokinetics

2.2.6.2.1 Animal and procedures

Two groups of 5 female F344 rats, weight 250-280 g, were dosed with 150 mg/kg BPAU. One group of them was given 100 mg/kg PMSF 4 hours after BPAU. All the animals were kept in metabolic cages with free access to food and water. Blood samples of 30-50 μl were taken by pricking the tail tips of rats at 6, 12, 24, 48, 72, 96 and 122 hours after BPAU dosing.

2.2.6.2.2 Sample preparation and analysis

Whole blood of 30-50 μl was mixed with 0.2 ml methanol/DMSO. All samples were centrifuged with an Ependof centrifuge at 9000 g for 5 min and the supernatant was kept for HPLC analysis. For analytical conditions see 2.2.2.2 and 2.2.2.3.

2.2.7 Age differences in BPAU metabolism

Four 6-week old female F344 rats and four 1 year old rats were given a single oral dose of 150 mg/kg BPAU by gavage. They were killed by carbon dioxide at 18 hours after dosing. Blood, brain, spinal cord and liver of each rat were taken for the measurement of BPAU.

For sample preparation and analysis refer to 2.2.2.2 and 2.2.2.3.

2.2.8 Statistics and pharmacokinetics

2.2.8.1 Statistics

ANOVA was used for the comparisons of the concentration of BPAU or its metabolites in different tissues and the blood/tissue ratios. Student's t-test was employed for two sample comparison. The standard errors of elimination rate constants were calculated according to the method given by Mead and Curnow (1987).The Z test was used for half life comparison. Wilcoxon's test was used for the comparison of ataxia scores.

2.2.8.2 Pharmacokinetics

Pharmacokinetic data were analysed according to the methods and equations given by Gibaldi & Perrier (10). BPAU follows apparent first order absorption and elimination kinetics and a one-compartment model was employed. The area under curve (AUC) was estimated using the trapezoidal rule (Martin, 1986).

2.3. RESULTS

2.3 1 Pharmacokinetics of BPAU

2.3.1.1 Absorption and bioavailability of BPAU

Following a single ip dose of 150 mg/kg BPAU, BPAU reached its peak value in blood at 4 hours and in tissues at 6 hours after dosing. A relatively quick absorption phase took place within first 6 hours after ip injection. After the first 6 hours, the absorption of BPAU was still continuing but much slower than over the first 6 hours. Some residue of BPAU was seen in the peritoneal cavity even at 72 hours after dosing. It was difficult to estimate the amount of residue left. The absorption processes of BPAU from blood to brain, spinal cord and liver were similar to that from peritoneum to blood but different from that in muscles. The recovery of BPAU in the overall tissue extraction was 94.2 ± 3.7% (n=5). The concentration-time curves of BPAU in serum and tissues are shown in FIG 2-4.

2.3.1.2 Distribution and tissue/serum ratio of BPAU

BPAU distributes in liver, muscle, brain, and spinal cord. The order of their peak concentrations was spinal cord > liver > brain > muscle. Spinal cord reached the highest level in all tissues observed. In addition, it was also detected in fat and kidney at 18 hours after dosing and their value levels were similar to that in liver. Thus BPAU seems to distribute all over the body.

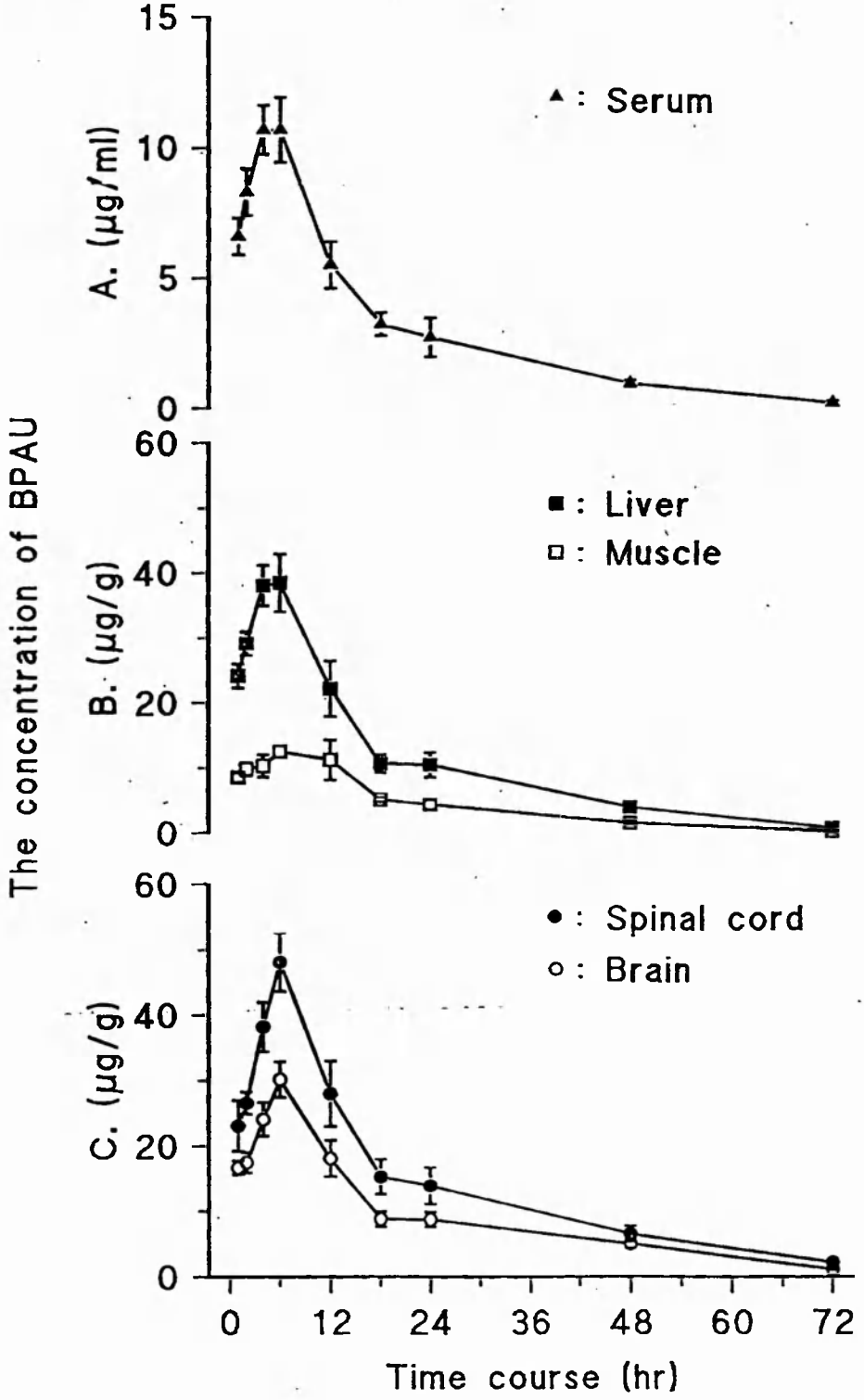

FIG 2-4 Concentration-time curves of BPAU in serum and tissues. Rats were given a single bolus ip dose of 150 mg/kg BPAU. They were killed at 1, 2, 4, 6, 12, 18, 24, 48, and 72 hours after dosing. The values are presented as mean ± SE, n = 4.

To reflect the partition of BPAU between serum and tissues, each value of BPAU in tissues (mg/g) and in serum (mg/ml) was converted into their ratios (tissue/serum). The results show that the tissue/serum ratio of BPAU for each tissue was roughly constant during the period of 6-18 hours after dosing. The order of the tissue/serum ratio at 6 hours (peak point) was spinal cord (4. 6 ± 0.2) > liver (3.7 ± 0.1) > brain (2.9 ± 0.1) > muscle (1.2 ± 0.1). The ratio in spinal cord was significantly higher than in other tissues.

2.3.1.3 Pharmacokinetic parameters of BPAU

The pharmacokinetic behaviour of BPAU is described based on individual tissues observed. As shown in FIG 2-4, BPAU given intraperitoneally followed apparent first order absorption and elimination kinetics both in serum and in tissues of the rats. The concentration-time data were transformed into the logarithm of concentration versus time data and the pharmacokinetic models were identified. All the data from serum and tissues were best fitted with a one-compartment model, see A-I-B, Appendix. Fitting these data using exponential regression yielded straight lines and the kinetic parameters were determined according to the equations given by Gibaldi & Perrier (1982). The area under concentration-time curve (AUC) in each individual tissue is estimated using the method of trapezoidal rule (Martin, 1986). The parameters are presented in Table 2-1. Table 2-1 shows that the elimination rate of BPAU in the nervous system is different from non-nervous tissues. The half lives of BPAU in brain and spinal cord were significantly longer than in serum or in liver or in muscle. The value of AUC in spinal cord is the biggest as well, see Table 2-1.

Table 2-1. The pharmacokinetic parameters of BPAU in serum after ip administration

Tissue	Absorption phase		Elimination phase			
	k_a	$T_{a1/2}$ (h)	C_0 (μg/g)	k	$T_{1/2}$ (h)	AUC ($\mu g. g^{-1}. h^{-1}$)
Serum	0.617	1.1	12.3#	0.059	11.8 ± 1.7	204.5
Brain	0.410	1.7	30.4	0.045	15.5 ± 1.1*	643.1
Spinal cord	0.302	2.3	45.3	0.044	15.6 ± 1.3*	982.5
Liver	0.474	1.5	46.0	0.062	11.2 ± 1.1	769.6
Muscle	0.226	3.1	17.6	0.059	11.6 ± 1.4	294.5

C_0 is the concentration estimated from the extrapolated line of -k/2.303 when time t is zero. #: The unit of BPAU in serum is μg/ml. k_a: the apparent first-order absorption rate constant, and k: the apparent first-order elimination rate constant. $Ta_{1/2}$ and $T_{1/2}$ are the half lives of absorption and elimination phases respectively. AUC is the area under concentration-time curve. *: $p<0.05$ (Z test, n=6) comparing with that in liver or muscle.

2.3.2 BPAU metabolism *in vivo*

Three metabolites of BPAU in tissue, serum and urine were primarily detected by HPLC in this study, see FIG 2-2 and FIG 2-3. They were further purified and characterised by HPLC, MS and NMR.

2.3.2.1 Purification of BPAU metabolites

As shown in FIG 2-2, BPAU and its metabolites were well separated under the analytical condition established in this study. The retention times of metabolites and parent compound, BPAU, were 5.5 min (M2), 7.5 min (M3), 9.4 min (M1), and 12.6 min (BPAU). Ammonium acetate significantly influenced the chromatographic

performance of M2. Under the condition of the absence of ammonium acetate in the mobile phase, the peak of M2 significantly delayed, broadened and even disappeared, whereas M1, M3 and BPAU were not affected by ammonium acetate. Therefore, ammonium acetate in mobile phase is necessary for M2 analysis. For this reason, the purification procedure for M2 was different from M1 and M3 to avoid the ammonium acetate in the final product, see 2.2.4.3.

M1 can be purified from either liver or urine but M3 was solely purified from urine. M2 can be purified from either serum or urine but serum was the main source because it reached a very high concentration between 18-24 hours after BPAU dosing. The level of M2 in serum was higher than that in whole blood.

2.3.2.2 Identification of BPAU and its metabolites

2.3.2.2.1 Mass and NMR spectra of BPAU

The mass spectrum of starting material, BPAU, is shown in FIG 2-5. The molecular ion of BPAU is at m/z 255/257. The double peak results from isotopes of bromine (Br) which also serves as a natural MS marker for its metabolites, see M1, M2 and M3 below. Two major fragment ions at m/z 79/81 (which is not shown in FIG 2-5) and m/z 176 were observed. They represent the ions of Br and phenylacetylurea respectively and indicate the cleavage took place at the bond of Br-C during ionisation.

To understand the NMR spectra of BPAU and its metabolites, the molecular structure of BPAU and its possible transient states caused by the chemical shifts of protons are shown in FIG 2-6. Proton *d* can momentarily shift either to *f* or to *g* and

proton *e* can also move to *g* as well. These tautoric movements can be detected by NMR.

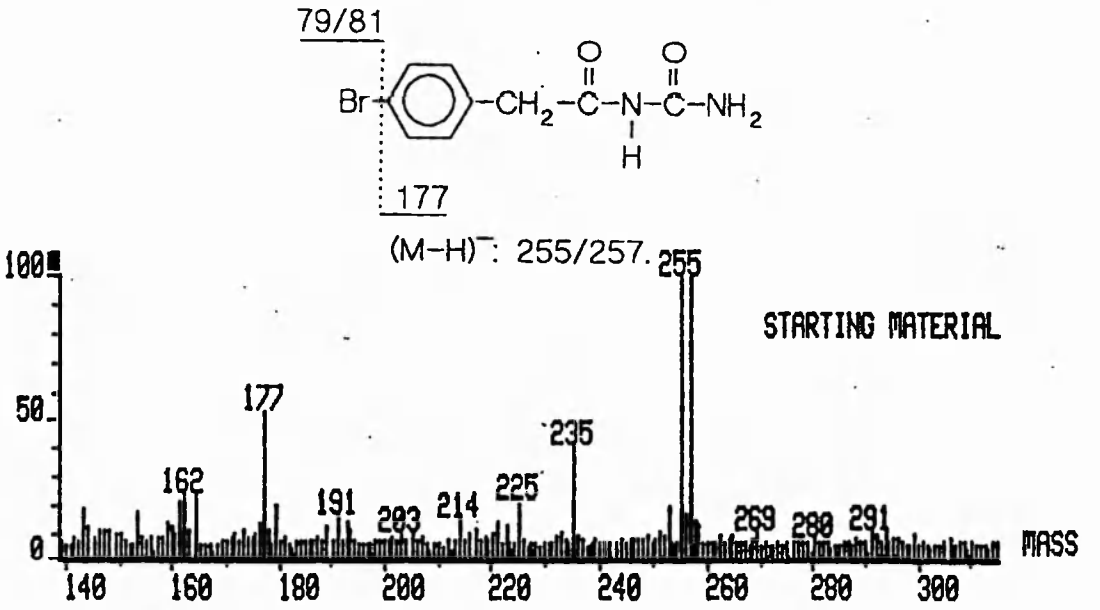

FIG 2-5. Mass spectrum of BPAU.

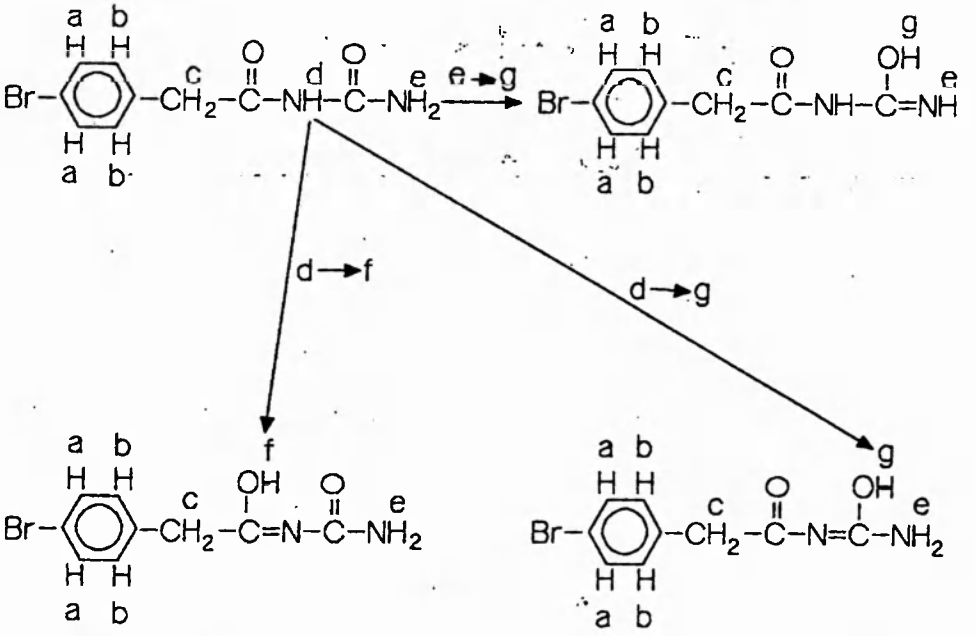

FIG 2-6 A illustration of the tautomerism of proton *d* and e on BPAU molecule. Proton *d* may transiently move to form either proton f or *g* and *e* proton may also move to form proton *g*.

The NMR spectrum of BPAU is shown in FIG 2-7. Proton *a* and *b* on benzene ring are clearly displayed between δ 7.2 and δ 7.7 ppm. The proton *c* is seen at δ 2.5 ppm and *d* is seen at around δ 10.4 ppm. Proton *e* is not seen in this graph because the peak of protons on $-NH_2$ is often broadened or invisible (11). Two shifting proton resonance peaks, *f* and *g*, appeared at δ 7.8 and δ 6.9 ppm respectively, see FIG 2-6 and FIG 2-7.

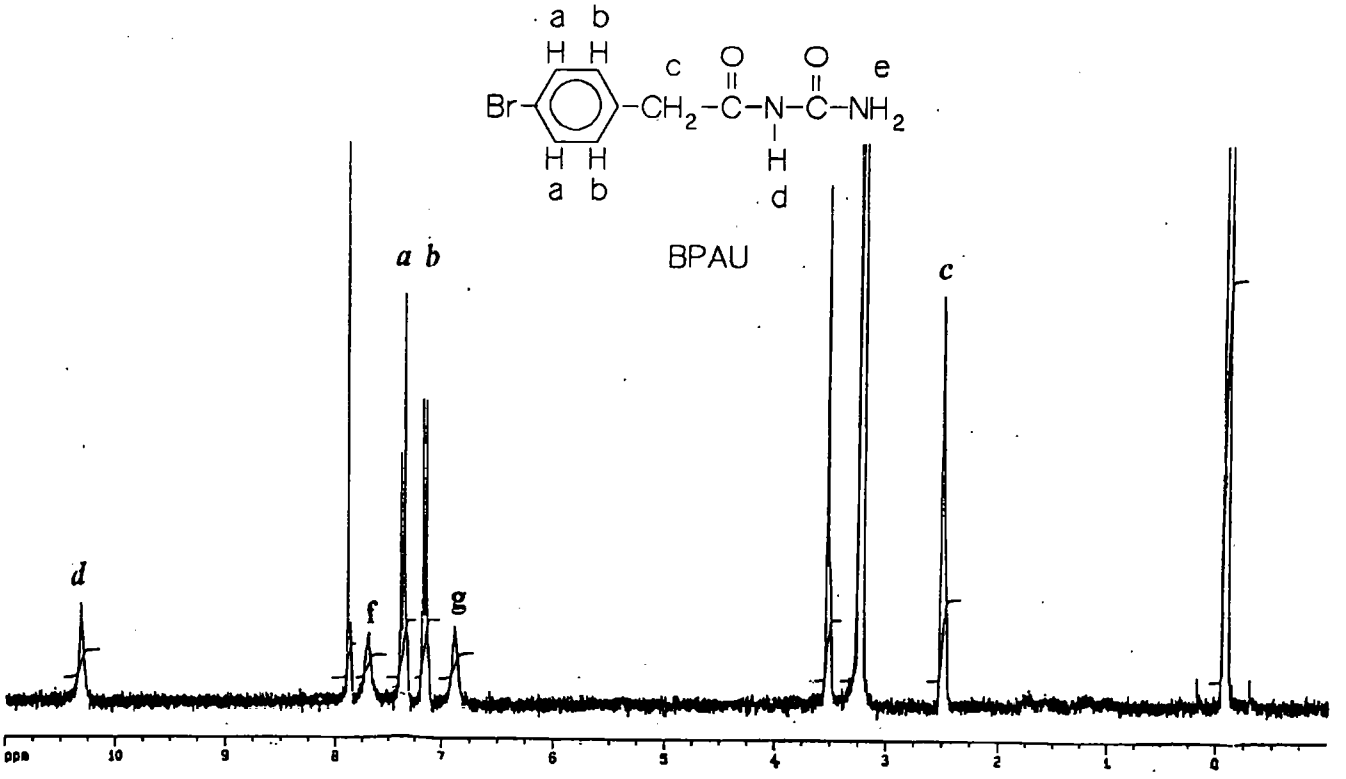

FIG 2-7. NMR spectrum of BPAU.

2.3.2.2.2 Mass and NMR spectra of M1

The mass spectrum of M1 displays a molecular ion at m/z 271/273 and three major fragment ions at m/z 79/81, 192 and 228/230 respectively, see FIG 2-8. The molecular ion is 16 mass units more than its parent compound, BPAU, see FIG 2-5 and FIG 2-8. This suggests that a oxygen, [O], was added to BPAU to form M1. The fragment ion peaks at m/z 79/81 and m/z 192 indicate the cleavage between Br and rest part of M1. The ion peak at m/z 228/230 results from the cleavage between the secondary N and the carbon of urea, N-C(O). This indicates the [O] was not added to the primary N.

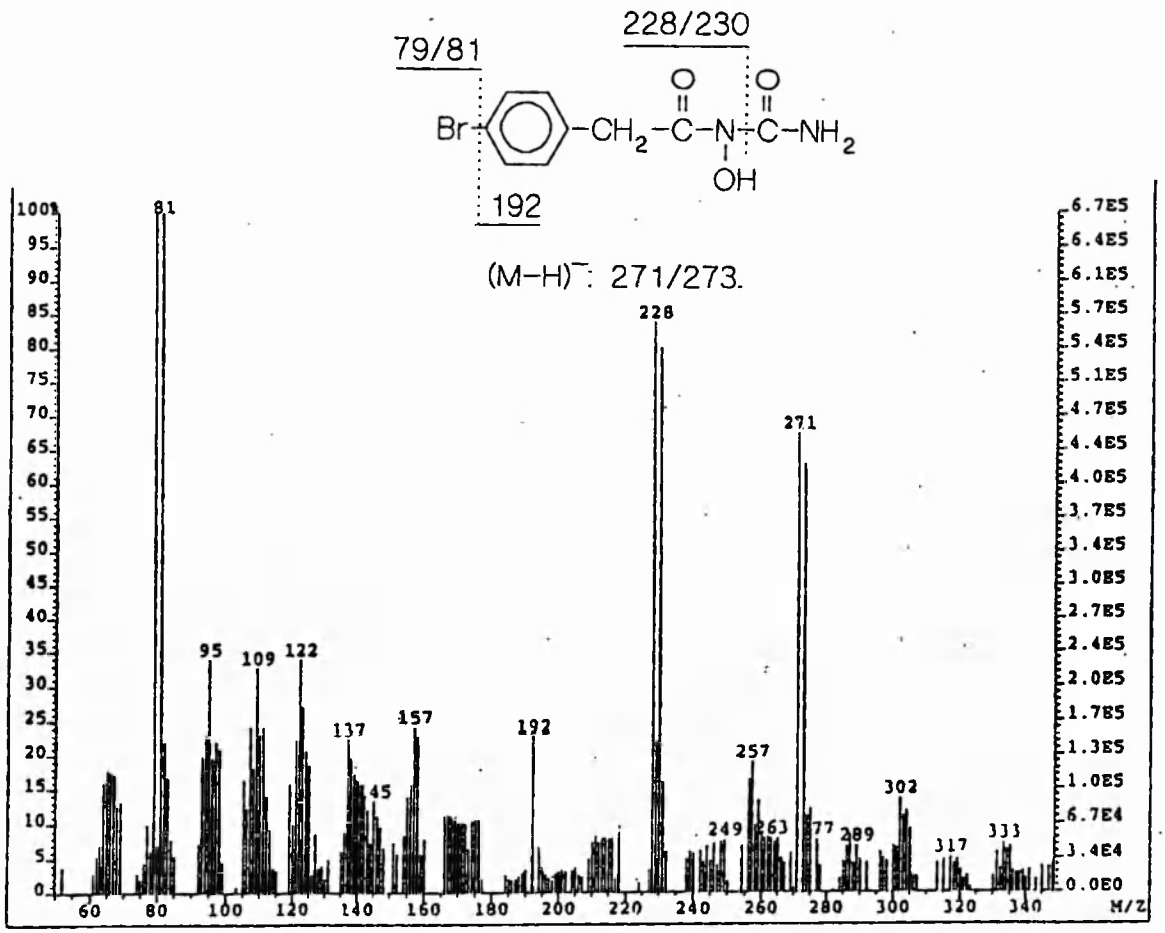

FIG 2-8. Mass spectrum of M1.

NMR spectrum of M1 is shown in FIG 2-9. Two doublet proton peaks were observed between δ 7.3 ppm and δ 7.8 ppm which represent 2 *a* and 2 *b* protons on benzene ring. This clearly indicates that no substitution took place on the benzene ring of M1. A single proton peak of *c* which represents -CH_2- was seen at δ 2.6 ppm, but this peak is bigger than it should be. Some unrelated peaks were seen at 5.1-5.3 and 5.9 ppm. These peaks may be from impurity of the smple. A single broadened proton peak was observed at 11.8 ppm which represents the proton *h* on =N-O-H. This directly indicates hydroxylation took place on the secondary N of BPAU to form M1. Its molecular structure is shown in FIG 2-8 and FIG 2-9.

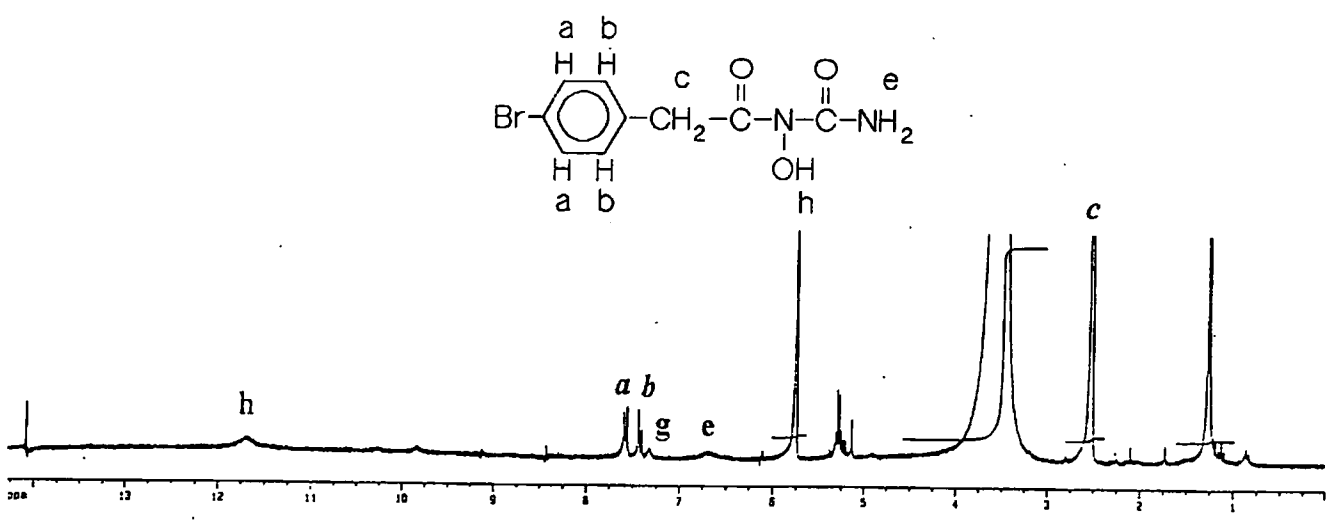

FIG 2-9. NMR spectrum of M1

Two indirect pieces of evidence for this structure were revealed by MS and NMR spectra. One was that the fragment ion peak at m/z 228/230 indicated the cleavage took place at the bond between the secondary N and C(O)-. This was probably due to the replacement of the proton *d* on secondary N by -OH weakening the bond N-C and therefore, facilitating the cleavage during ionisation of M1. This fragment ion peak is not seen in BPAU MS, see FIG 2-5 and FIG 2-8. The another evidence is that the proton peak *f* disappeared. This was due to the replacement of proton *d*, which made the tautomerism between *d* and *f* impossible, see FIG 2-6, FIG 2-7 and FIG 2-9. Based on the above evidence, the molecular formula of M1 is proposed as following: $Br(C_6H_4)CH_2CON(OH)CONH_2$.

According to the IUPAC nomenclature system of chemicals, M1 is named as 3-hydroxy-5-(4-bromophenyl)-1,3-diazapentane-2,4-dione. Its common name is called N'-hydroxy-*p*-bromophenylacetylurea (HBPAU). The molecular structure is as shown in FIG 2-8 and FIG 2-9.

2.3.2.2.3 Mass and NMR spectra of M2

The molecular ion peak of M2 is seen at m/z 254/256 which is 1 mass unit less than its parent compound, BPAU, see FIG 2-10. Its fragment ions are seen at m/z 79/81 and at m/z 176 which indicate that the cleavage took place between Br and the rest part of M2 during ionisation. The double ion peak indicates that the atom Br is still on the molecule of the metabolite.

The accurate MS indicates that M2 is composed of 9C, 6H, 3O, 1N and 1Br. This shows that M2 is one [O] more and 1 N and 3 H less than BPAU (9C, 9H, 2O, 2N and 1 Br), see FIG 2-11.

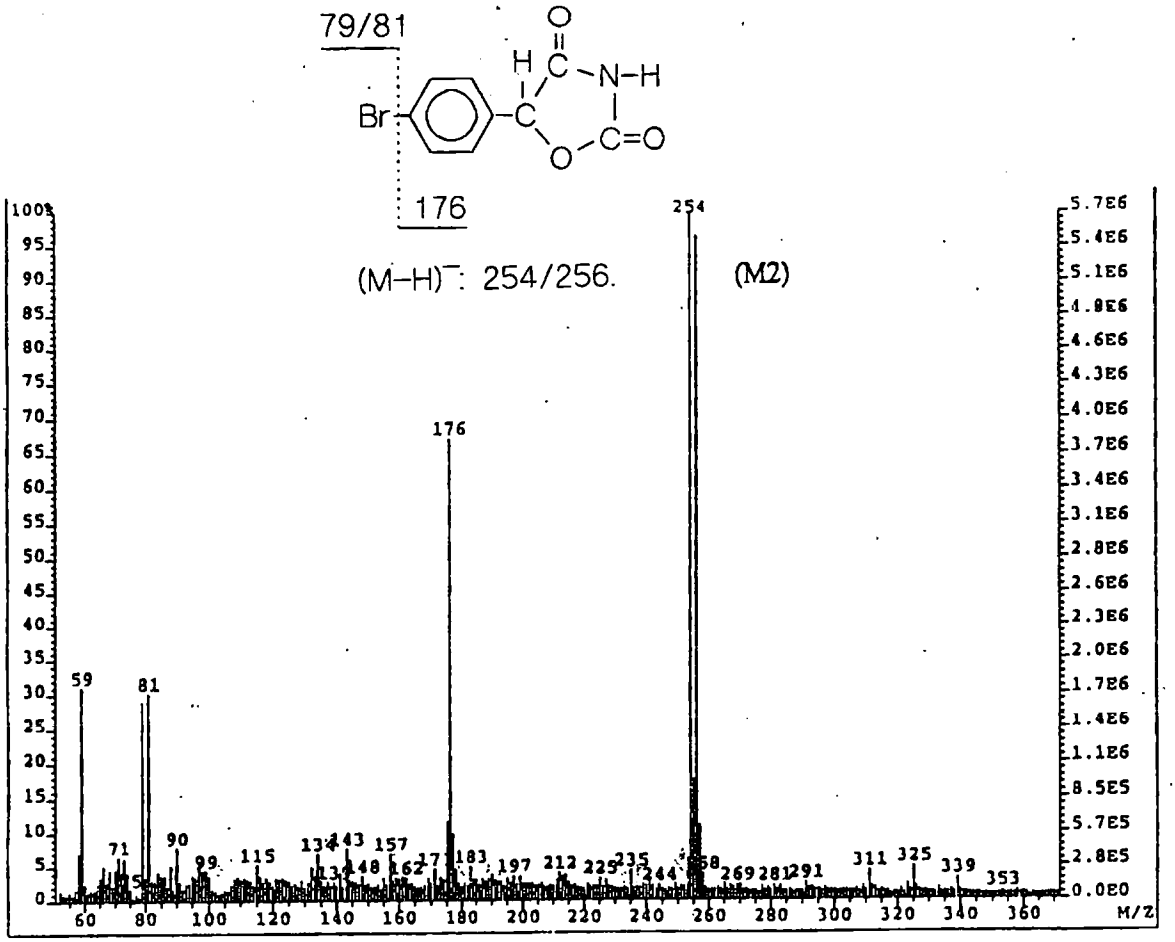

FIG 2-10. Mass spectrum of M2.

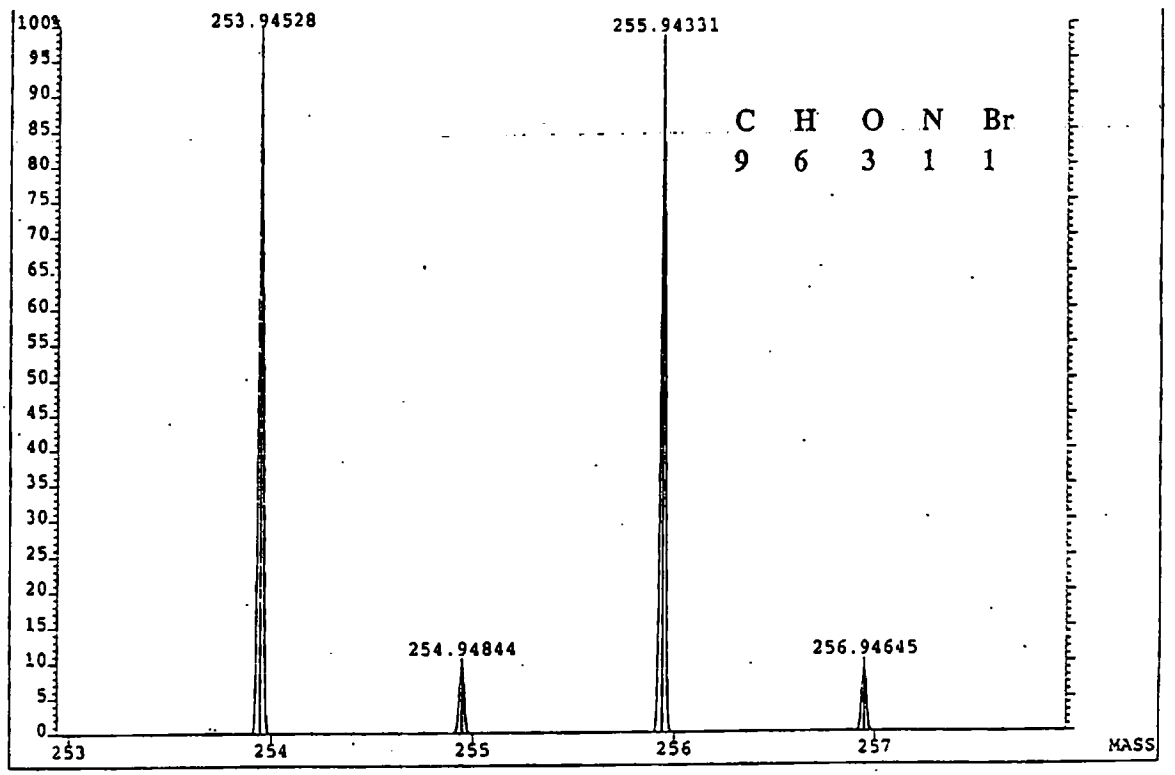

FIG 2-11. Accurate mass spectrum of M2

NMR spectrum shows that two doublet proton peaks were observed between δ 7.3 ppm and δ 7.8 ppm which indicate that the proton *a* and *b* on the benzene ring were not replaced, see FIG 2-12. A single proton peak was observed at δ 6.0 ppm which is likely to result from the resonance of proton *c*, see FIG 2-6 and FIG 2-12. The shifting proton peaks, *f* and *g* disappeared, comparing FIG 7 and FIG 12. The resonance peak of the proton *d* on =N-H is not observed in FIG 12 because the resonance peak of =N-H is often broadened or invisible (11).

All above evidences suggest that a ring structure was formed as shown in FIG 9 and FIG 11. According to IUPAC nomenclature system, M2 is named 4-(4-bromophenyl)-3-oxapyrrolidine-2,5-dione.

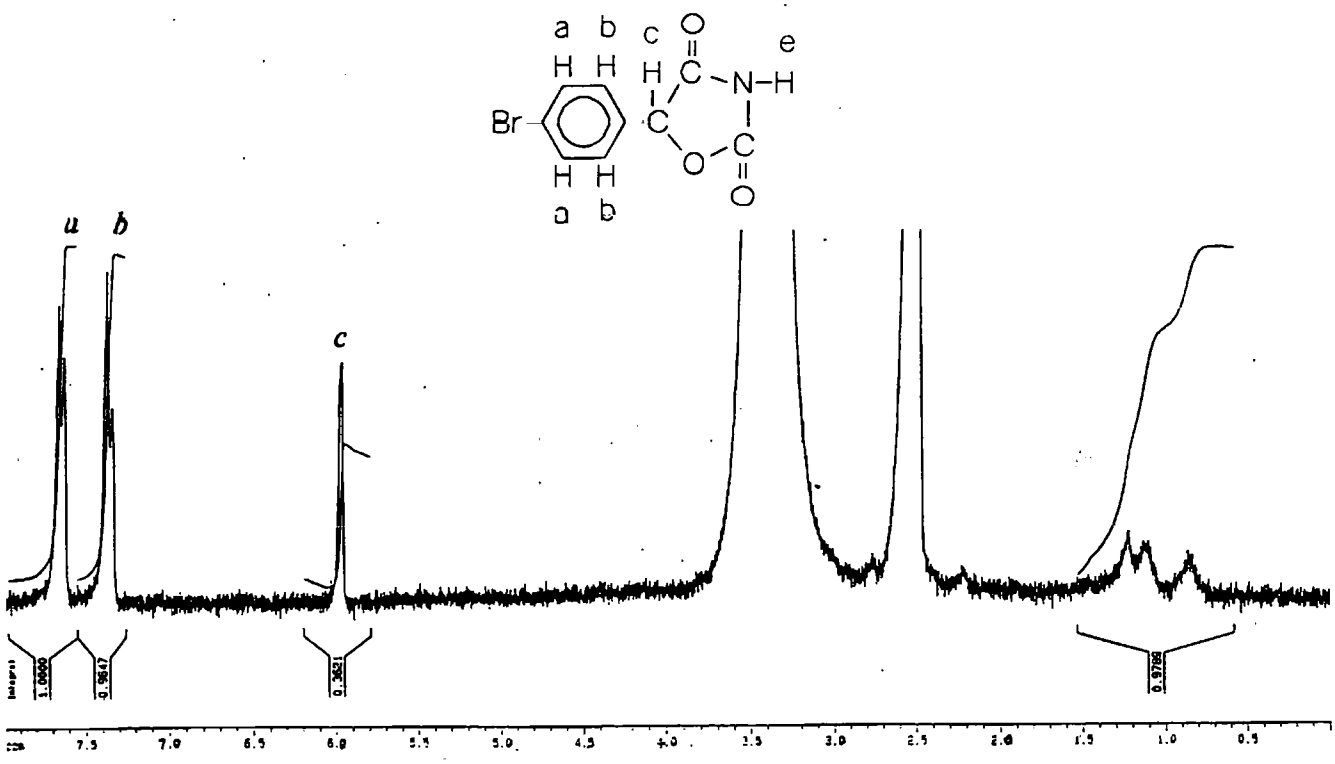

FIG 2-12. NMR spectrum of M2

2.3.2.2.4 Mass and NMR spectra of M3

M3 has a molecular ion peak at m/z 269/271, see FIG 2-13. It is two mass units less than M1 and 14 mass units more than BPAU. Two fragment ion peaks are seen at m/z 79/81 and 191. They resulted from the cleavage between Br and the rest part of M3.

NMR spectrum of M3 indicates that proton *a*, *b* and *c* remain unchanged, see FIG 2-14. The singlet proton peak of *g* is still seen at around 7.2 ppm and again the shifting proton peak *f* disappeared, which indicates that the substitution took place on the secondary N, which made the tautomeric shift from *d* to *f* impossible, see FIG 2-6 and FIG 2-14. The resonant peak of proton *i* was overlapped by the resonant peak of the protons on DMSO which was used as the solvent. Chemically, therefore, it is suggested that methylation took place on the secondary N of BPAU.

According to IUPAC nomenclature system, it is named as 3-methyl-5-(4-bromophenyl)-1,3-diazapentane-2,4-dione. Its common name is N'-methyl-p-bromophenylacetylurea (MBPAU).

M3 is probably formed in the kidney and directly excreted through urine because its concentration in serum is just detectable but in urine is very high. It, therefore, has less toxic potential than M1 because of its direct elimination. Its bioformation needs further confirming.

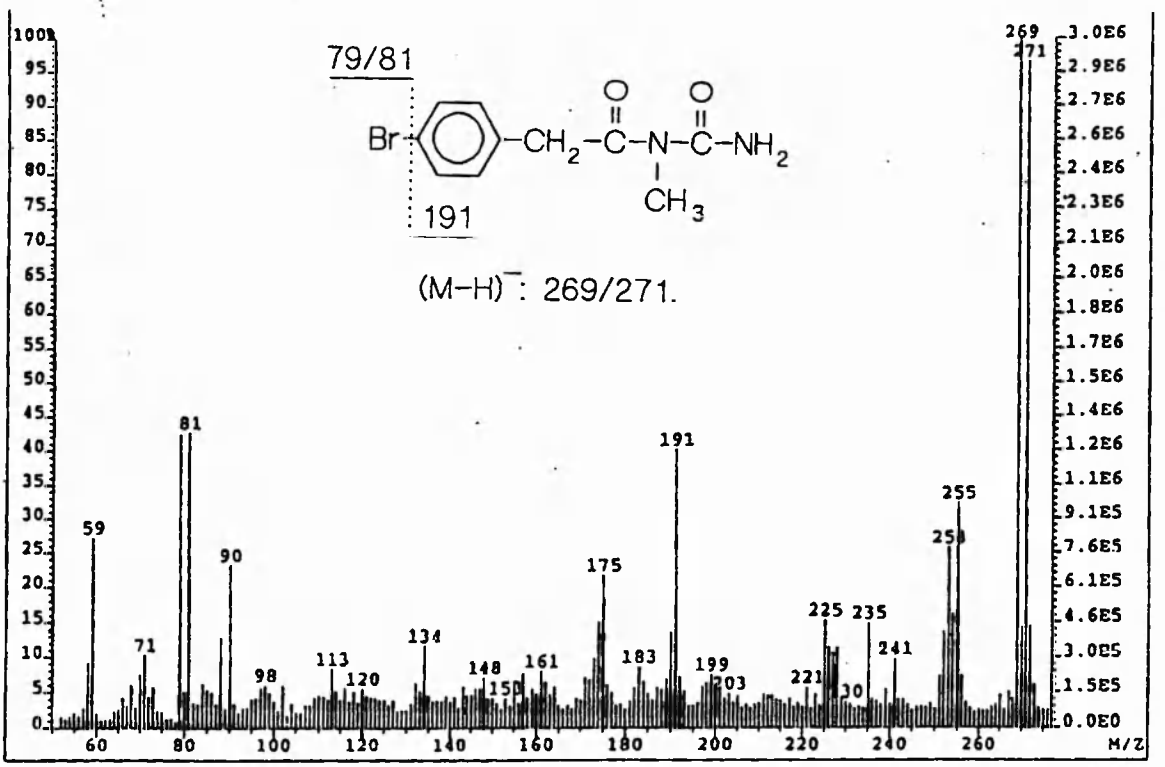

FIG 2-13. Mass spectrum of M3

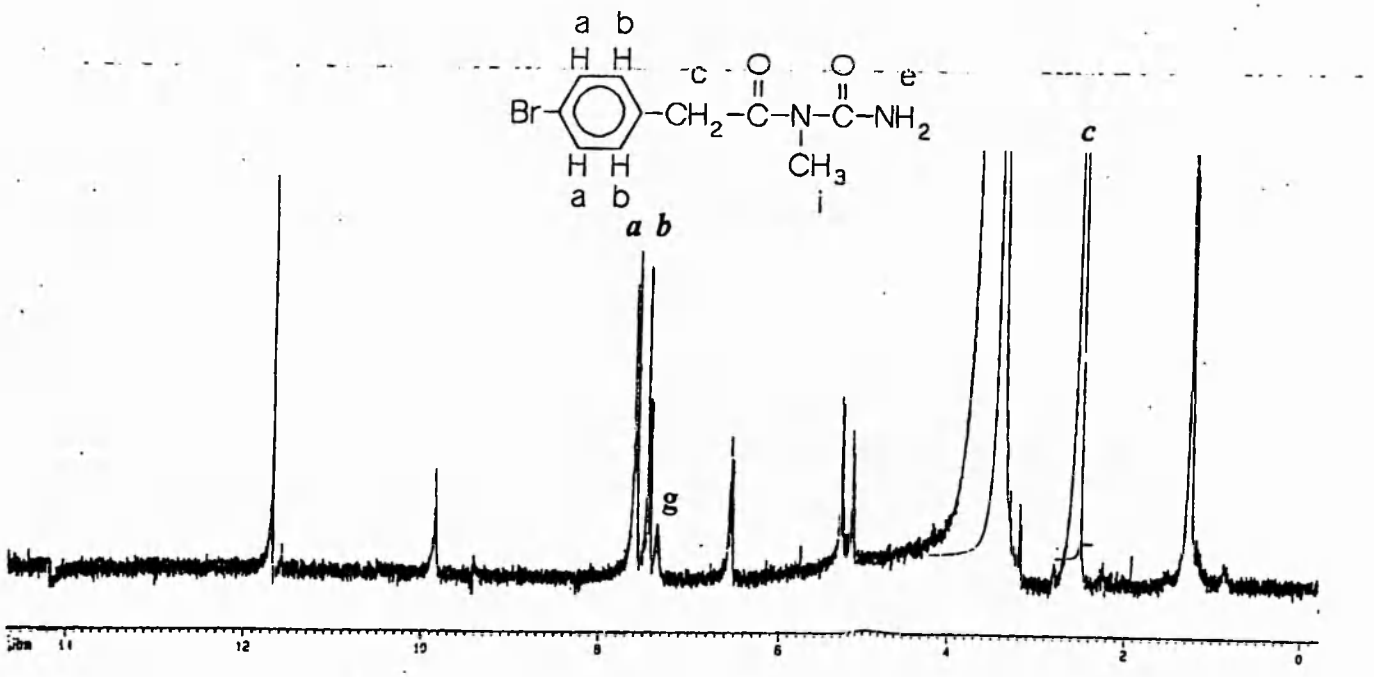

FIG 2-14. NMR spectrum of M3

The proposed metabolic pathways of BPAU is shown in FIG 2-15.

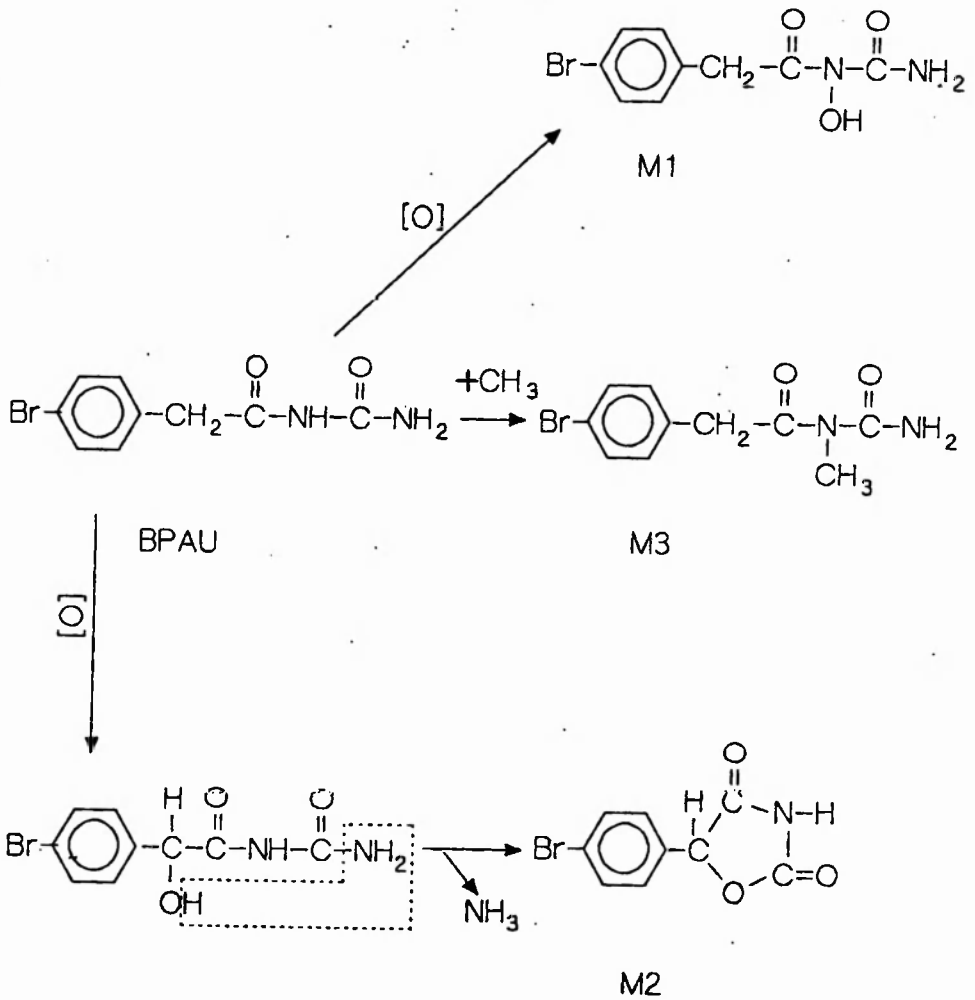

FIG 2-15. Metabolic pathways of *p*-bromophenylacetylurea *in vivo*.

BPAU: *p*-bromophenylacetylurea

M1: 3-hydroxy-5-(4-bromophenyl)-1,3-diazapentane-2,4-dione

M2: 4-(4-bromophenyl)-3-oxapyrrolidine-2,5-dione.

2.3.2.3 The distribution and kinetics of metabolites

M1 is the dominant metabolite of BPAU detected in tissues but a low concentration in serum. Its distribution pattern is similar to its parent compound BPAU but it stayed in tissues much longer than BPAU itself. The peak value of M1 was observed at 18 hours which was 12 hours later than BPAU. M2 reached a high concentration in serum but very low levels in tissues. M3 was mainly found in urine. The kinetics of M1 and M2 are presented in FIG.2-16.

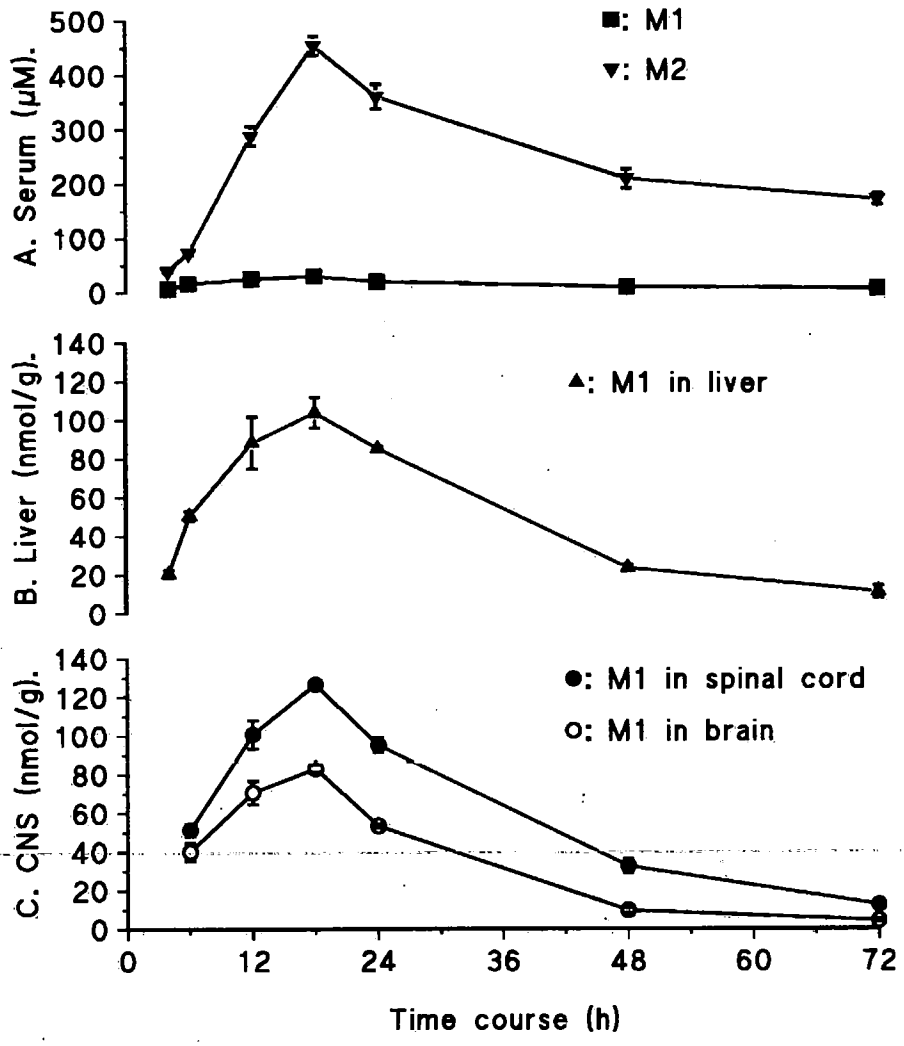

FIG 2-16. The concentration-time curves of M1 and M2 in serum and tissues.

2.3.2.4 Excretion of BPAU metabolites

All three metabolites, M1, M2 and M3 were eliminated through the kidney. The relative amount of each metabolite excreted from urine are shown in table 2-2. Table 2-2 shows that about half of absorbed BPAU was excreted in the form of M2.

Table 2-2 Excretion of M1, M2 and M3 from rats' urine after a single oral dose of 150 mg/kg (586 μmol/kg) BPAU.

Absorbed BPAU (μmol./rat*)	M1 (μmol./rat)	M2 (μmol./rat)	M3 (μmol./rat)	% of absorbed BPAU
71.76 ± 2.74	8.69 ± 1.29	35.8 ± 5.25	17.65 ± 4.52	86.6

n = 6. *: rat body weight 186 ± 5 g.

2.3.3 Animal model of time-dependent promotion of BPAU neuropathy by PMSF

2.3.3.1 Ataxia score

Rats were given two daily oral doses of 150 mg/kg BPAU. The model of time-dependent promotion was established by co-administrating 100 mg/kg PMSF at either 1 day before the first BPAU dose or 4 hours, 1 day or 4 days after the second BPAU dose. After a week's delay, all the animals including the BPAU controls developed different degrees of ataxia. The ataxia scores are shown in FIG. 2-17. BPAU alone caused minor to medium degree of ataxia. PMSF significantly increased BPAU-induced ataxia scores ($p<0.01$) when it was given either 1 day before or 4 hours or 1 day after BPAU doses. The strongest effect was seen in both the PMSF-1d-BPAU and the BPAU-4h-PMSF groups ($p<0.01$). The effect of PMSF

given 1 day before BPAU was significantly stronger than that given 1 day after BPAU ($p<0.01$). No effect was observed when PMSF was given 4 days after BPAU dosing. PMSF alone did not induce any recognisable ataxia signs.

The development and severity of ataxia in BPAU-4h-PMSF and PMSF-1d-BPAU groups before day 20 were nearly the same. However, their recovery time courses were different. The recovery of rats in BPAU-4h-PMSF group delayed comparing with other groups. The more affected rats, the later the recovery, see FIG 2-17.

2.3.3.2 Weight loss

Following the administration of either BPAU or PMSF, body weight losses were observed in all animals. It took 3-4 days to recovery to the original weight and then increased again. At the appearance of ataxia signs in the BPAU-4h-PMSF or PMSF-1d-BPAU or BPAU-1d-PMSF groups, the weight decreased again, see FIG 2-18. The weight loss coincided with the severity of ataxia. The order of weight loss is BPAU-4h-PMSF > PMSF-1d-BPAU > BPAU-1d-PMSF. There was no second weight loss in the BPAU-4d-PMSF group or in the BPAU or PMSF control groups after their recovery from intoxication.

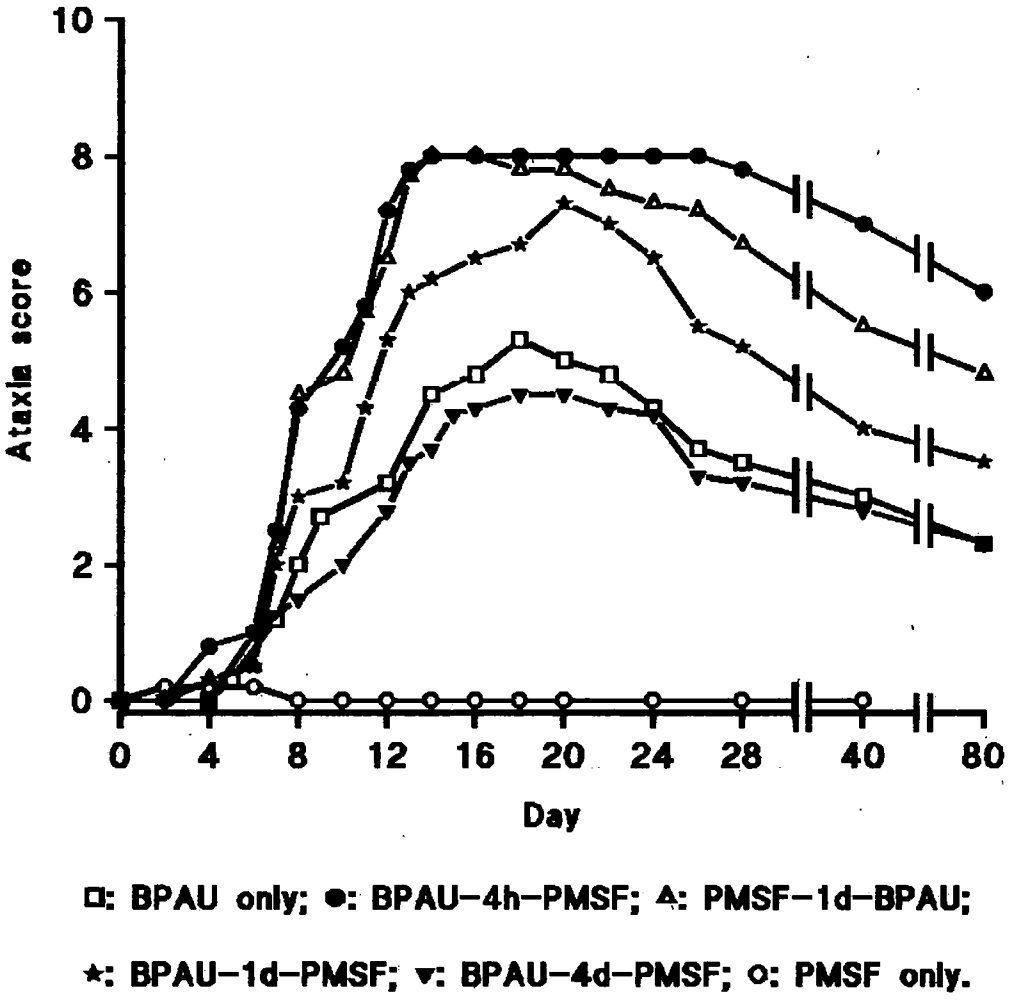

FIG 2-17. Development of ataxia after BPAU and/or PMSF dosing. Rats were given two daily doses of 150 mg/kg BPAU. The time dependent promotion of BPAU-induced neuropathy by PMSF was studied by co-administration of 100 mg/kg PMSF at either 1 day before the first BPAU dose (PMSF-1d-BPAU), or 4 hours (BPAU-4h-PMSF), 1 day (BPAU-1d-PMSF) or 4 days (BPAU-4d-PMSF) after the second BPAU dose. Two control groups were given either two daily doses of BPAU (BPAU only) or a single dose of PMSF (PMSF control).

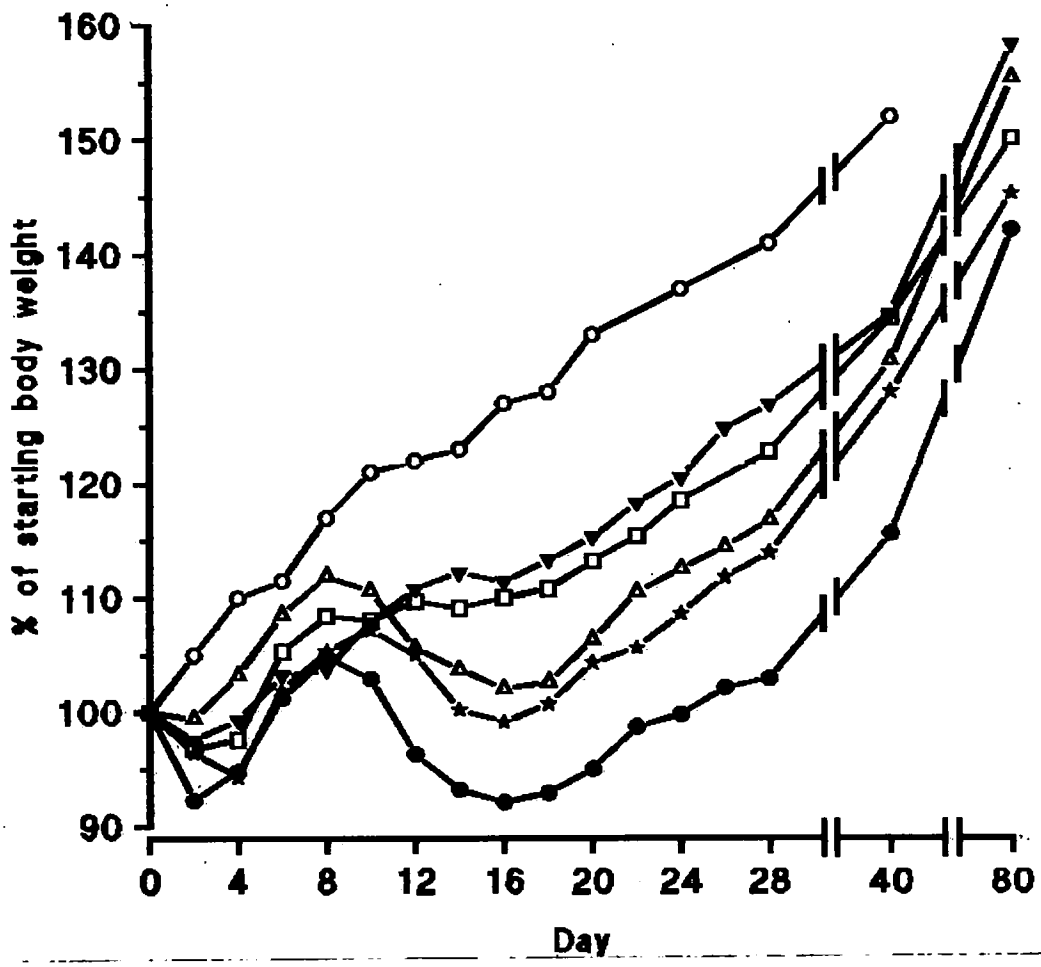

□: BPAU only; ●: BPAU–4h–PMSF; △: PMSF–1d–BPAU;

★: BPAU–1d–PMSF; ▼: BPAU–4d–PMSF; ○: PMSF only.

FIG 2-18. Body weight changes after BPAU and PMSF dosing and during the development of ataxia. PMSF was given at either 1 day before the first BPAU dose (PMSF-1d-BPAU), or 4 hours (BPAU-4h-PMSF), 1 day (BPAU-1d-PMSF) or 4 days (BPAU-4d-PMSF) after the second BPAU dose. Two control groups were given either two daily doses of BPAU (BPAU only) or a single dose of PMSF (PMSF only).

2.3.3.3 Slope test

The value of the slope test in the BPAU-4h-PMSF, PMSF-1d-BPAU, and BPAU-1d-PMSF groups were significantly lower than that in the BPAU control during the period of 7-17 days after dosing ($P<0.05$). After that period, they were only occasionally significantly lower than that in BPAU control groups. There was no significant difference between BPAU control and BPAU-4d-PMSF groups. No significant decrease of slope test was observed in PMSF controls. The decrease of slope test appeared 1-2 days earlier than that ataxia signs did, see FIG 2-19. Data from BPAU-1d-PMSF, and BPAU-4d-PMSF groups come between the curves of BPAU control and BPAU-4h-PMSF groups (They were not plotted in FIG 2-19 because they were too close to each other to be recognised easily).

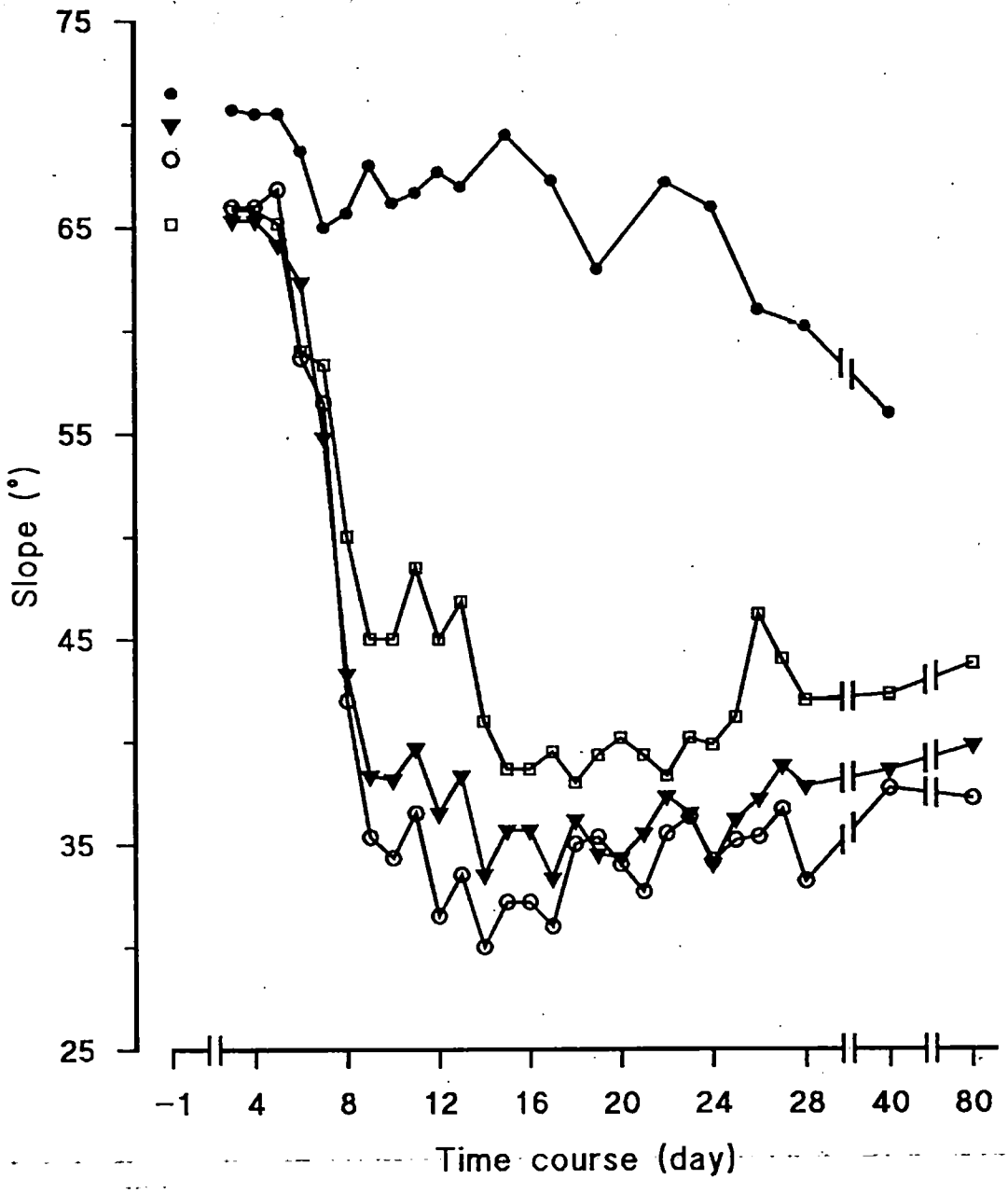

FIG 2-19. Slope test during the development of ataxia after BPAU and PMSF dosing. PMSF was given at either 1 day before the first BPAU dose (▼: PMSF-1d-BPAU), or 4 hours (O: BPAU-4h-PMSF), 1 day or 4 days after the second BPAU dose. Two control groups were given either two daily doses of BPAU (□: BPAU only) or a single dose of PMSF (●: PMSF control). The values from BPAU-1d-PMSF and BPAU-4d-PMSF come between the curves of BPAU-4h-PMSF and BPAU only control groups but not plotted in this figure for the clarity sake.

2.3.4 The effect of PMSF on BPAU disposition

2.3.4.1 On BPAU elimination

PMSF given either 1 day before or 4 hours after BPAU dose remarkably increased the BPAU levels in all tissues at 24 hours post BPAU, see FIG 2-20. The levels of BPAU in all observed tissues in BPAU-4h-PMSF group were significantly higher than that in BPAU control ($p<0.01$). The value in spinal cord in the PMSF-1d-BPAU group was 80 % higher than the BPAU control but not statistically significant. Taking spinal cord as an example, the BPAU level in the BPAU alone control group decreased to 6 % of its peak value at 24 hours after dosing. Whereas, the level in PMSF-1d-BPAU or in BPAU-4h-PMSF group decreased to 11% or 46% of the peak value at 24 hour respectively. PMSF obviously delayed BPAU elimination from tissues.

2.3.4.2 On the metabolism of BPAU

The effect of PMSF on M1 and M2 at 24 hours after BPAU are presented in FIG 2-21 and FIG 2-22. When PMSF was given 4 hours after BPAU, it significantly increased M1 level in tissues and decreased M2 concentration in serum at 24 hours after dosing. When PMSF was given 1 day before BPAU, it significantly increased M1 level in spinal cord at 24 hours after dosing and decreased M2 concentration by 13.5% which is not statistically significant.

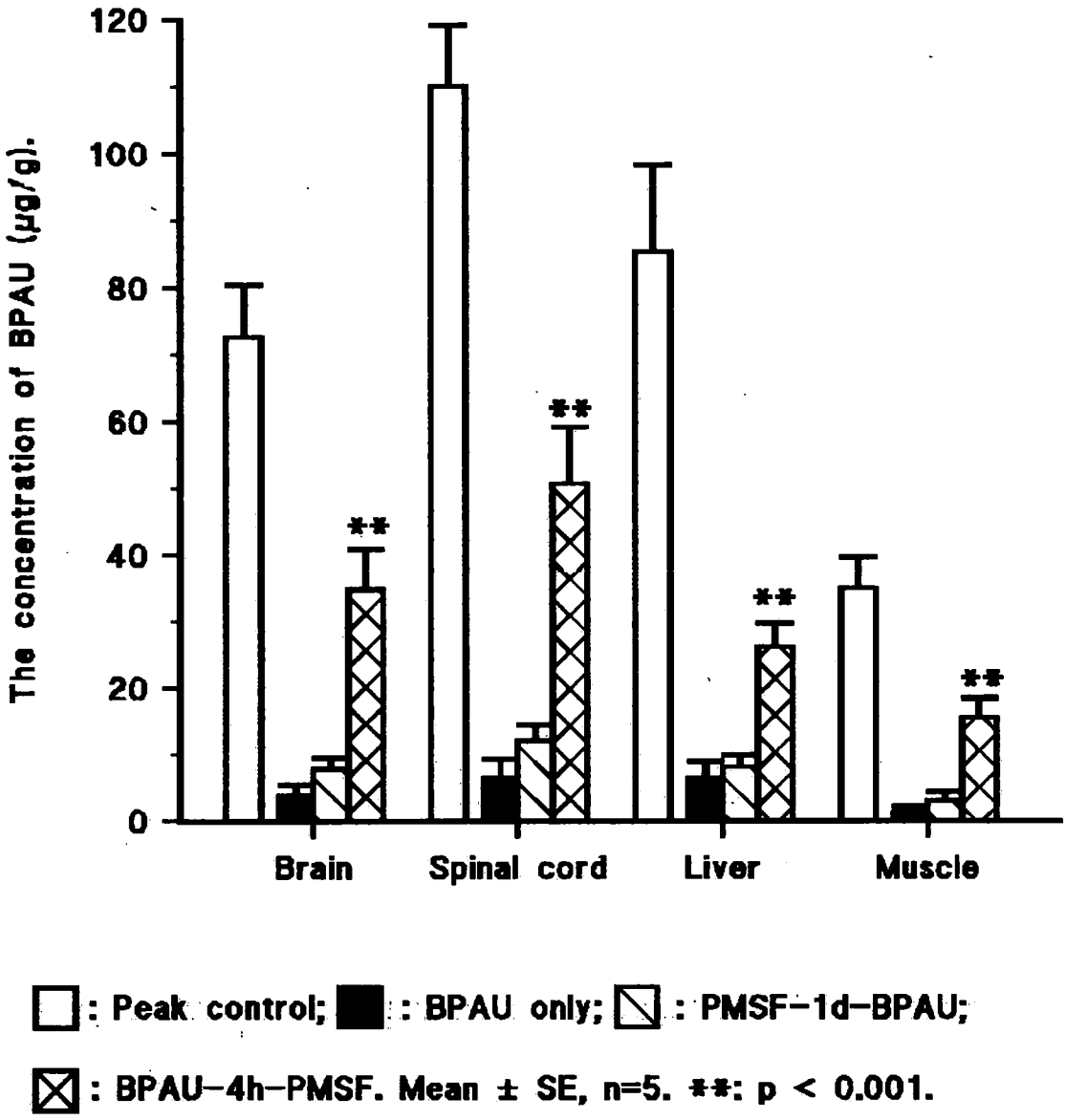

FIG 2-20. Effect of PMSF on BPAU elimination. Rats were given two daily doses of 150 mg/kg BPAU and co-administrated a single dose of 100 mg/kg PMSF at either 1 day before the first BPAU dosing (PMSF-1d-BPAU) or 4 hours after the second BPAU dosing (BPAU-4h-PMSF). The animals in above groups were killed at 24 hours after the second BPAU dosing. Two BPAU control groups were only given two daily doses of BPAU. They were used as either BPAU control in which animals were killed at 24 hours after the second BPAU dosing or peak control in which animals were killed at 6 hours after the second BPAU dosing.

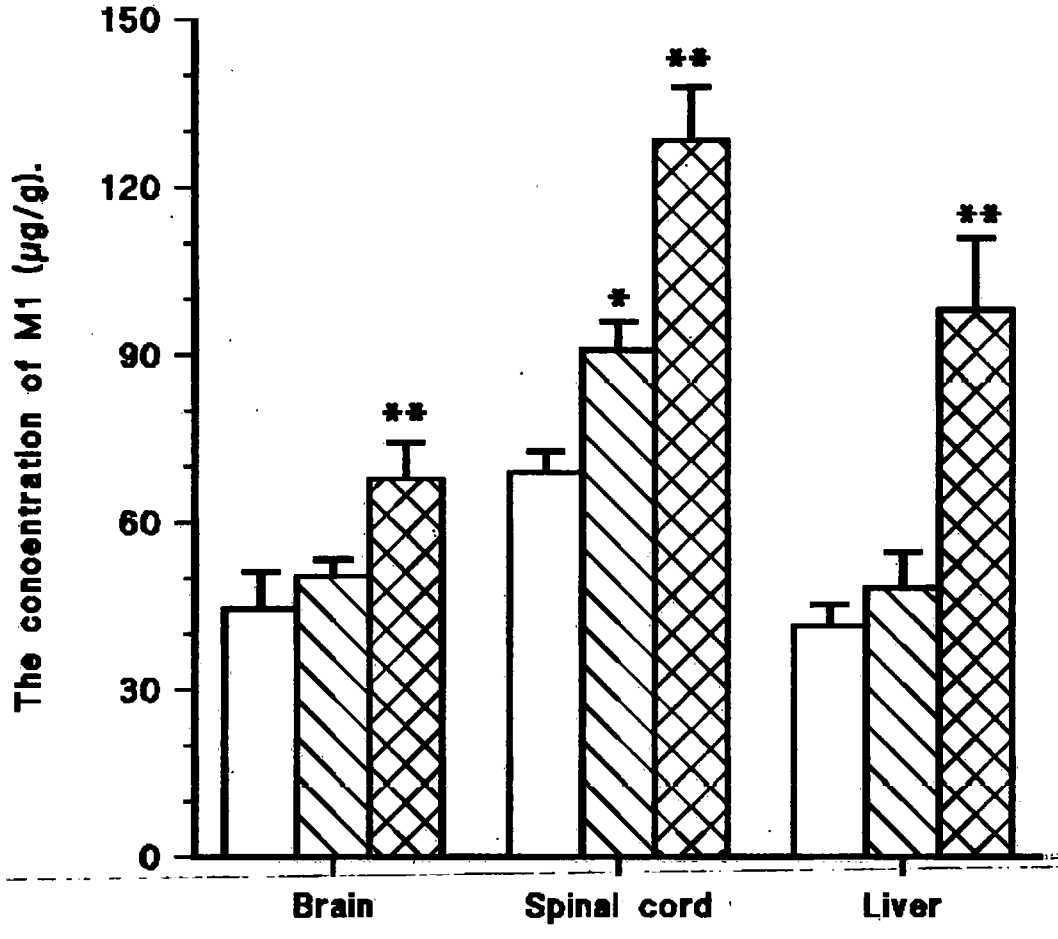

FIG 2-21. The effect of PMSF on M1 levels in brain, spinal cord and liver.

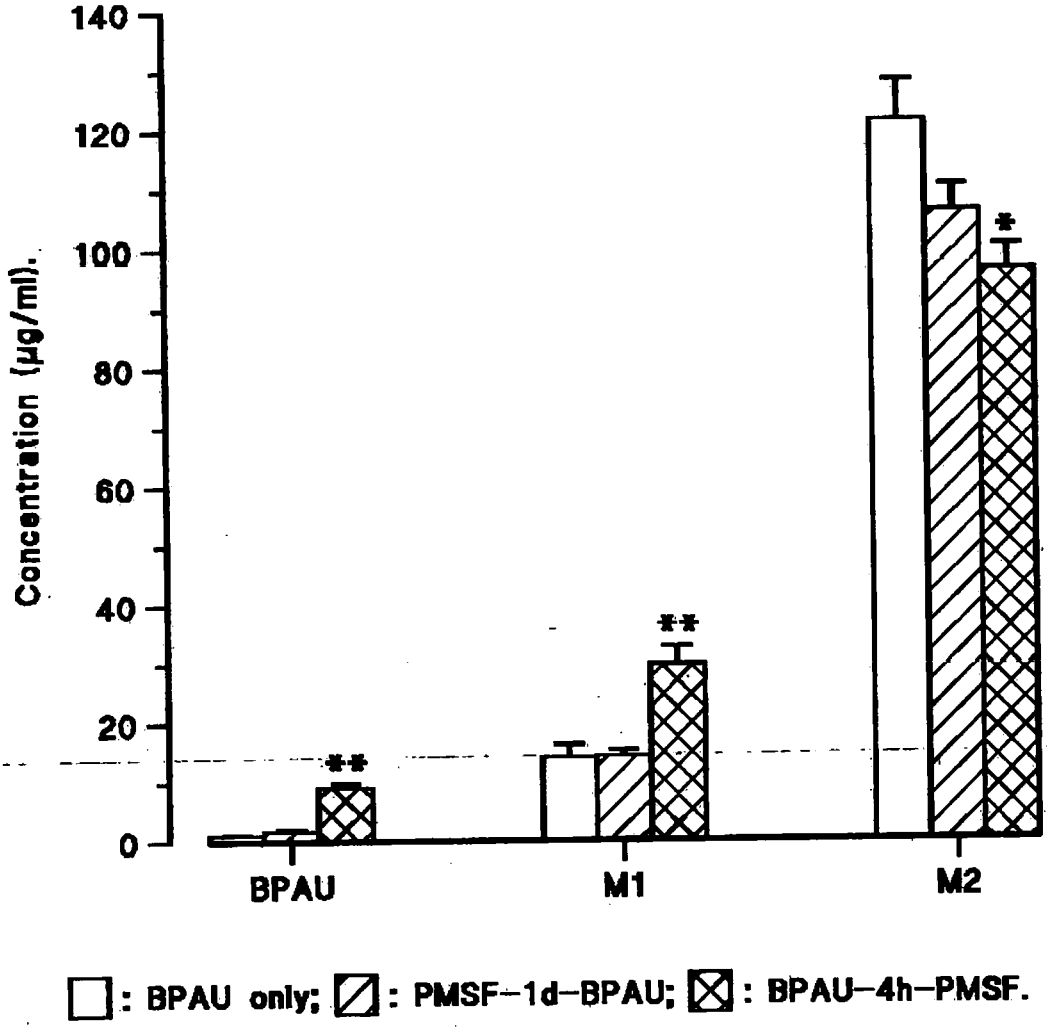

FIG 2-22. The effect of PMSF on BPAU, M1 and M2 concentrations in serum

2.3.4.3 On the pharmacokinetics of p-BPAU and its metabolites

About 30 % of dosed BPAU was found in faeces within first 24 hours and 4% of total dosage was detected between 24 and 48 hours after dosing. Only negligible amount of dosed BPAU was excreted from urine. PMSF did not affect BPAU absorption. The bioavailibilities in BPAU and BPAU+PMSF groups are similar, see table 2-3. But PMSF significantly changed the BPAU metabolism and elimination processes. It delayed BPAU elimination, increased M1 production and decreased M2, see FIG 2-23.

Table 2-3 Bioavailability of BPAU after oral dose

Treatment	Dosed amount (μg)	Absorbed amount (μg)	Bioavailability (%)
BPAU only	27.9 ± 0.7	18.4 ± 0.7	65.9
BPAU + PMSF	27.3 ± 1.6	17.8 ± 1.5	65.1

n=5.

The pharmacokinetic parameters of both groups are presented in table 2-4. PMSF significantly increased AUC and prolonged elimination half life.

Table 2-4. Comparison of pharmacokinetic parameters of a single oral dose of 150 mg/kg BPAU without or with PMSF at 4 hours after BPAU.

Treatment	k (h^{-1})	V (l)	AUC ($\mu g.ml^{-1}.h^{-1}$)	$T_{1/2}$ (hr)
BPAU alone	0.074	1.23 ± 0.16	103.7	9.4 ± 1.3
BPAU + PMSF	0.034	1.64 ± 0.25	202.4	20.5 ± 3.1*

k: elimination rate constant; V: apparent distribution volume; AUC: the area under the concentration-time curve; and $T_{1/2}$: elimination half life. Data are presented as Mean or Mean ± SE. *: $p<0.01$, n=5.

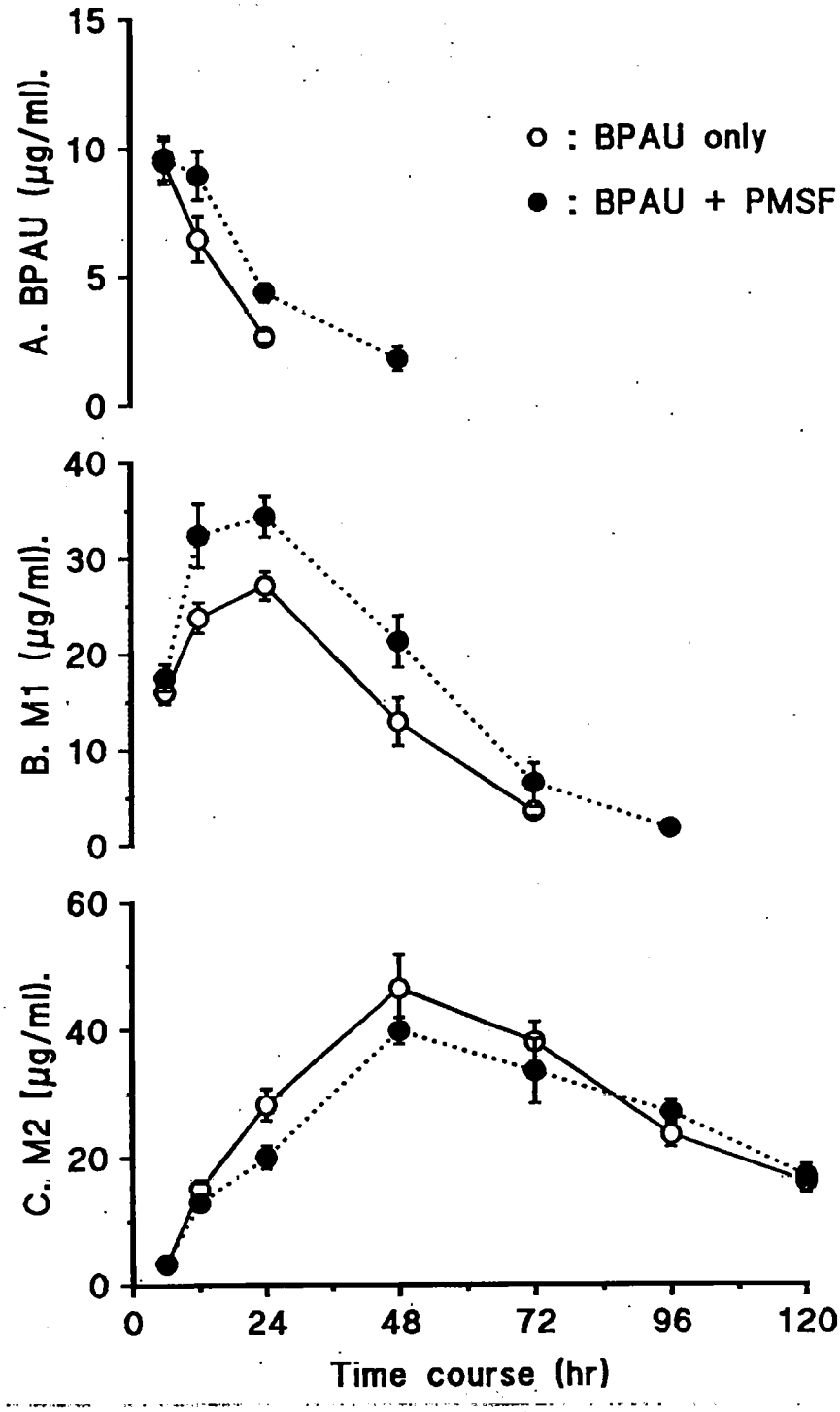

FIG 2-23. Concentration-time curves of BPAU and its metabolites in whole blood with or without PMSF dosing. Rats in the BPAU + PMSF group were given 150 mg/kg BPAU orally and co-administrated 100 mg/kg PMSF intraperitoneally at 4 hours after BPAU dosing. BPAU control was given the 150 mg/kg BPAU and the same volume of glycerinformal (solvent) as above group. The values are expressed as mean ± SE, n = 5.

Chemically, M1 and M2 are formed via different pathways. The possible sites for PMSF inhibition are shown in FIG 2-24. PMSF is likely to inhibit the initial step of M2 formation rather than the last step since accumulation of the intermediate was not detected.

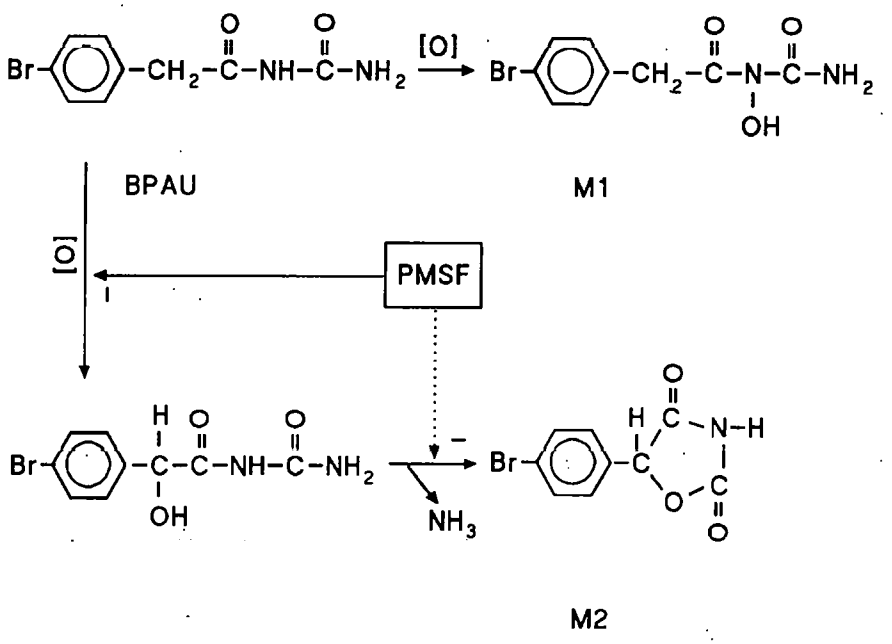

FIG 2-24 The possible inhibition sites of *p*-bromophenylacetylurea metabolism by phenylmethanesulphonyl fluoride.

PMSF: phenylmethanesulphonyl fluoride

BPAU: *p*-bromophenylacetylurea

M1: 3-hydroxy-5-(4-bromophenyl)-1,3-diazapentane-2,4-dione

M2: 4-(4-bromophenyl)-3-oxapyrrolidine-2,5-dione.

2.3.5 Age differences in the distribution and metabolism of BPAU

2.3.5.1 Differences in BPAU distribution

At 18 hours after a single oral dose of BPAU, the distribution of BPAU in serum and central nervous system in both 6-week and 1-year old rats is presented in FIG 2-25. In 6-week old rats, there is no significant difference in the BPAU distribution between brain and spinal cord. Whereas in 1-year old rats, BPAU in spinal cord is significantly higher than that in brain ($p<0.01$). The levels of BPAU in brain and serum were not significantly different between the two groups. However, BPAU in the spinal cord of 6-week old rats was significantly lower than that in 1-year old rats.

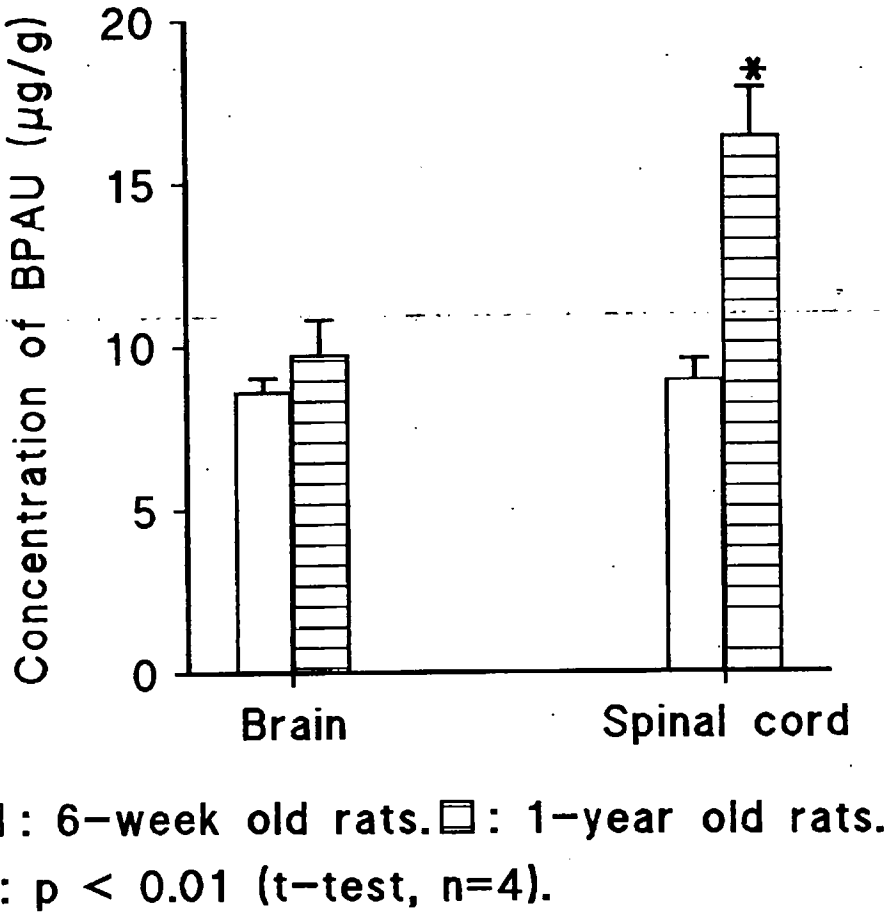

FIG 2-25. Age difference in BPAU distribution in brain and spinal cord.

2.3.5.2 Differences in metabolism

The difference of metabolite levels between 6-week and 1-year old rats is shown in FIG 2-26. M1 in spinal cord in 1-year old rats was significantly higher than that in 6-week old rats. In the brain, the level of BPAU in 1-year old rats was 23 % higher than that in 6-week old rats but was not statistically significant.

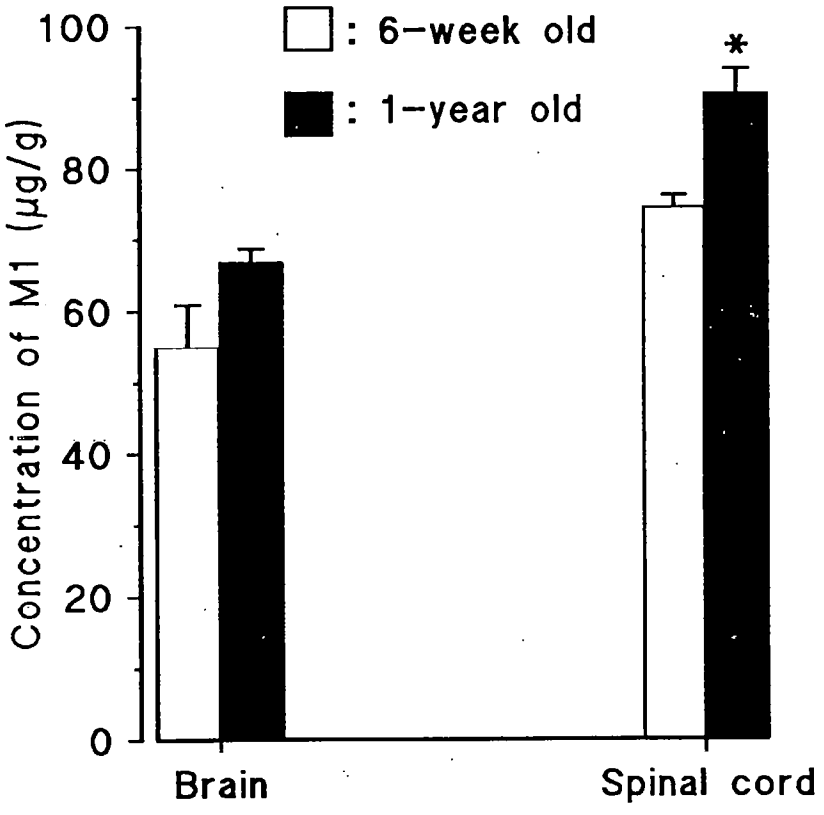

mean ± SE, n = 4. *: $p < 0.05$.

FIG 2-26. Age differences of M1 in brain and spinal cord between 6-week and 1-year old rats at 18 hours after dosing.

In serum, BPAU concentrations in both groups were similar, but M1 concentration in 1-year old rats was significantly higher than that in 6-week old rats, whereas M2 concentration in 1-year old rats significantly lower than that in 6-week old rats, see FIG 2-27. This indicates young rats produce more M2 but less M1, by contrast, old rats produce somewhat more M1 but markedly less M2.

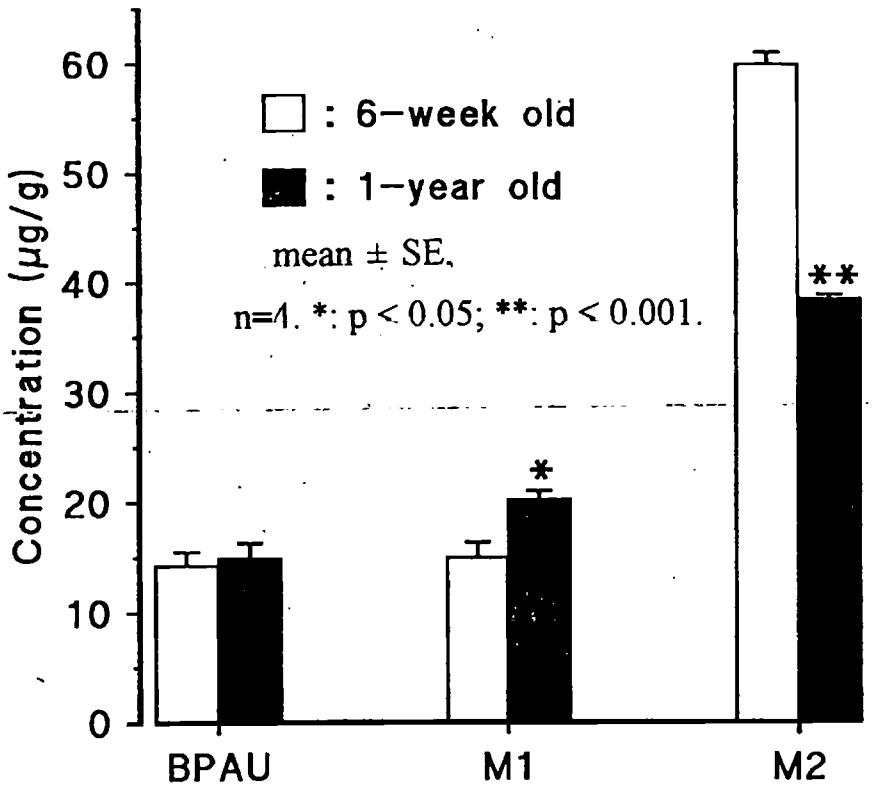

FIG 2-27. The comparison of BPAU and its metabolites in serum at 18 hours after dosing between 6-week and 1-year old rats.

2.4 DISCUSSION

2.4.1 Metabolic and pharmacokinetic factors in BPAU neurotoxicity

2.4.1.1 Pharmacokinetics of BPAU

Previous studies have shown that either a single higher dose or long-term repeated lower doses of BPAU caused the same clinical signs and pathological change (Diezel and Quadbeck, 1960; Cavanagh, 1968; Potkonjak, 1965). The mechanism of its neurotoxicity is totally unknown. This study investigated pharmacokinetic aspects of BPAU-induced neurotoxicity. The results revealed that the absorption, distribution and metabolism of BPAU in one way or another modified BPAU neurotoxicity.

This study shows that the absorption of BPAU is not complete either via ip or po doses possibly due to its poor solubility in water or other common solvents (Cavanagh, 1973). The bioavailability of po dose was found to be 65.9 %. The availability of ip dose of BPAU was difficult to be estimated because no iv dosing data was available. Since others have found that BPAU given by either ip or po route produced the similar degree of delayed ataxia at the same dosage (Cavanagh, *et al.*, 1968, Nagata, 1986), this suggests that the absorption of BPAU via the two routes are similar, which indicates that BPAU can be absorbed by simple diffusion to pass biological membranes. It would be expected to pass blood-brain barrier readily due to its lipophilic property (Caldwell, *et al.*, 1995). A quick absorption phase was observed over the first 6 hours following ip injection which was similar to po dose. However, some intraperitoneal residue of BPAU was seen even at 72 hours after injection. So, a slow absorption phase may occur after an ip dose, which

is different from the oral route in which most unabsorbed BPAU will be cleared from gut within 24 hours. The present results showed that the half life of BPAU in blood is significantly longer by ip injection than by po dose (Z test, $p<0.01$), see Table 2-1 and 2-4. The absorption difference significantly modified the rate constants of elimination and hence is responsible for the difference of half lives between ip and po doses.

BPAU reached peak value at 4 hours in blood and at 6 hours in tissues after ip injection. Lipid content in individual tissues plays an important role in the distribution of agents such as BPAU due to their lipophilic properties (Sipes, 1991). The central nervous system is rich in lipid (Spector, 1956). Accordingly, the levels of BPAU in brain and spinal cord are significantly higher than that in blood and muscles. Spinal cord reached the highest level in all observed tissues. The lipid content is also responsible for the distribution difference between spinal cord and whole brain as the spinal cord contains more lipid than whole brain (Spector, 1956). However, the level of BPAU in liver was significantly higher than in whole brain and muscles although liver contain less lipid than brain (Spector, 1956). This suggests that liver may have other ways to uptake and store BPAU. Perhaps, BPAU can bind to some proteins in liver (Sipes and Gandolfi, 1991).

The interaction between toxicant and target sites begins with distribution. The distribution depends on the physiochemical properties of toxicants and physiological and biochemical constitution of individual tissues, which determine the partition of a compound between blood and individual tissues. This study showed that the tissue/serum ratio of BPAU relates to the lipid content of individual tissues. It reflects an equilibrate state of partition between blood and tissues. The

greater the ratio, the easier for the compound to be absorbed by tissues and the more difficult for it to go back to blood. In this study, the highest ratio and longest half life were observed in spinal cord. This distribution feature of BPAU may partly explain why it specially caused spinal cord or peripheral nerve damage.

The concentration and persistence of a toxicant in target sites is directly relevant to the toxic response of individual tissues. In present study, each tissue observed is assumed to be a central compartment to describe the kinetics of BPAU in the particular tissue. Blood and biotransformation are taken as peripheral compartments. The results showed that after initial distribution, the kinetics of BPAU vary from tissue to tissue. BPAU in CNS has a longer half life than that in blood or non-nervous tissues, whereas BPAU in liver or muscle had a similar half life to that in blood, see Table 2-1. Therefore, as stated above, the initial distribution of BPAU mainly depends on its physiochemical properties and lipid content in individual tissues, whereas the elimination depends not only on lipid content but also the metabolic capacity in individual tissues.

This study shows that BPAU follows a one-compartment model in either serum or tissues when BPAU is given intraperitoneally. The rate constant k in tissues represents the total elimination rate which includes the rates of BPAU penetrating back to blood and its biotransformation *in situ*. It is not possible to estimate how much the biotransformation contributes to the total elimination rate from the present data. BPAU is a lipid soluble substance and easy to be absorbed by CNS. Biotransformation *in situ* is the major way for the elimination of lipophilic compounds (Sipes and Gandolfi, 1991).

It has well been demonstrated that spinal cord and peripheral nerves are the target sites of BPAU neurotoxicity (Cavanagh, *et al.*, 1968, Troncoso, *et al.*, 1982). This study has shown that BPAU reached the highest level and had a longest half life in spinal cord. Troncoso's work showed that rats given daily dose of 10 mg/kg BPAU continually for 8-10 weeks developed clinical ataxia (Troncoso, *et al.*, 1982). The pharmacokinetic explanation for this chronic toxicity was due to BPAU accumulation in nervous system. No matter what biochemical mechanism may be involved, this distribution and pharmacokinetic features of BPAU may partly be responsible for its selective neurotoxicity.

2.4.1.2 Metabolism of BPAU

A attempt to study the role of liver in the detoxification of BPAU was made by Chen (1971). His experiment was carried out by surgically cutting off part of the liver or by dosing carbon tetrachloride to damage liver before BPAU dosing and both treatments increased BPAU neurotoxicity. Therefore, liver was thought to be a major organ in BPAU detoxification (Chen, *et al.*, 1971). But prior to the present study, no documented data were available about BPAU metabolism. This study primarily identified three metabolites of BPAU by using HPLC, MS and NMR techniques and its metabolic pathway was proposed as well, see FIG 2-15.

M1 is a dominant metabolite of BPAU in all tissues measured. It has been identified as a hydroxylated metabolite, see FIG 2-8 and 2-9. BPAU is transformed into M1 in tissues by hydroxylation on the secondary N of BPAU. The distribution of M1 was similar to its parent compound BPAU. It reached peak values in tissues at 18 hours, which was a 12 hour delay compared to BPAU itself. This indicates

that M1 stays in tissues longer than its parent compound BPAU. Comparing with BPAU, M1 is more likely to accumulate in tissues when repeated doses are given. Therefore, M1 could potentially play a role in BPAU neurotoxicity.

The metabolic pathway of M2 is different from M1, see FIG 2-15. It is confirmed by NMR and accurate MS that a ring structure is formed after biotransformation. Contrary to M1, a high concentration of M2 was found in serum and urine but low levels in tissues. This indicates that M2 enters blood much quicker than M1 once it is formed and is excreted into urine. So, it is likely to be a detoxificated form of metabolite.

M3 was mainly found in urine. Its metabolic pathway is not clear so far. It may be formed via M1 or directly from BPAU by methylation in kidney because it had a very low level in blood or tissue and a high level was measured in urine. Therefore, it has less toxic potential than M1. Some further work is needed on its metabolic pathway.

Due to the lipophilic property of BPAU, redistribution is limited and biotransformation *in situ* may be the main way for its elimination from tissues. This study shows that the distribution pattern of metabolite M1 is similar to BPAU in each tissue. After primary distribution, the persistence of BPAU in individual tissues depends on metabolic capacity of these tissues. This may be responsible for the differences of half lives between different tissues. This study showed that the biotransformation of BPAU in liver was relatively quicker than brain and spinal cord. So, liver plays a role in general detoxification of BPAU.

Partial hepatectomy or damaging the liver by dosing carbon tetrachloride before administration of BPAU increased the degree of delayed ataxia (Chen, *et al.*,

1971). This may be due to both the decrease of liver metabolic capacity and relatively decrease of distribution volume and hence increase the level of BPAU in nervous system because BPAU level in liver is high and liver weight on average is 12-14 g, whereas the weight of central nervous system is 2.2-2.6g (brain weight is 1.7-1.9 g and spinal cord 0.5-0.7 g) if rats body weight are 200-250g. The same reason may be responsible for the increased neurotoxicity by damaging liver with carbon tetrachloride before BPAU dosing.

Chen (1971) found that pre-treatment with sodium phenobarbital before giving BPAU did not alter the degree of neurotoxicity and suggested that liver microsomal enzymes do not play a direct role in hepatic metabolism of BPAU. The present study has shown that M1 is formed by N-oxidation at the secondary N on BPAU. It has been demonstrated that the N-oxidation of secondary or tertiary amines is catalysed by flavin-containing monooxygenase (FMO) (Poulsen, *et al.*, 1974; Poulsen and Ziegler, 1977; Ziegler, 1980,1988, 1990; Sipes and Gandolfi, 1991). FMO activity is present in the liver at all mammals examined so far, and high activity has been observed in porcine (Ziegler and Poulsen, 1978) and human livers (Gold and Ziegler, 1973). In addition to liver, FMO activity was also detected in mammalian lung (Williams, *et al.*, 1984; Tynes, *et al.*, 1985), brain (Bhamre, *et al.*, 1993) and kidney (Tynes, *et al.*, 1985; Ziegler, 1988). There are multiple forms of FMO in human liver (Lemoine, *et al.*, 1990) and in rat brain (Bhamre et al, 1993). In the brain, FMO preferentially localises in the neuronal cell body (Bhamre, *et al.*, 1993). This is particularly important in toxicology if the metabolic activity produces a more toxic metabolite. Therefore, FMO may be a important enzyme in the formation of M1.

At least two steps were involved in M2 formation. The enzymes involved are not known. The first step is probably catalysed by the P450 enzyme system (Caldwell, *et al.*, 1995) and the subsequent reaction may be catalysed by a different enzyme to form a ring structure. This study has shown that the M2 pathway played an important role in BPAU detoxification. Therefore, any factors which inhibit M2 formation may increase BPAU toxicity.

In the halogenated derivatives of phenylacetylurea, only Br- and Cl- forms are neurotoxic. No neurotoxicities were observed in I- and F- forms (Diezel and Quadbeck, 1960; Brimijoin and Nagata, 1986) although they share a very similar chemical structure. Their chemical properties vary from each other, which may significantly influence their absorption, distribution or metabolism and hence modify their neurotoxicity.

In conclusion, this study has screened the distribution, pharmacokinetics and metabolism of BPAU in the rats. These factors well reflect the interaction between BPAU and body. Therefore, it provided a basic knowledge about the metabolic and pharmacokinetic behaviours of BPAU *in vivo* and a better understanding in its neurotoxicity.

2.4.2 Time-dependent promotion of BPAU neuropathy by PMSF

Organic phosphorous compound-induced delayed neuropathy can be intensified by some non-neurotoxic compounds (Lotti, *et al.*, 1991). This phenomenon was also seen in BPAU-induced delayed neuropathy (Ray and Johnson, 1992, Xu, *et al.*, 1994). The promotion mechanism is not known yet. This study showed that the increased clinical severity of BPAU-induced delayed ataxia

produced by PMSF depends on the time at which PMSF is given. A period from one day before to one day after BPAU dosing is a sensitive period to PMSF promotion. During this period, the closer the two compound were given, the more severe the ataxia. The effect of PMSF given one day before BPAU was much stronger than one day after BPAU. No effect was observed when PMSF was given 4 days after BPAU, although this time point was still within the latent period before expression of delayed neuropathy (a subclinical stage). These changes in severity coincided well with pharmacokinetic process. When PMSF was given 4 hours after BPAU, its effect fully overlapped with BPAU and hence produced most severe ataxia. Whereas at 24 hours after BPAU dosing, only 6 % of the peak value of BPAU was left in spinal cord and accordingly a minor effect was observed. Most BPAU had left body at 72 hours after dosing. We can imagine that at 4 days (96 hours) after BPAU dosing, no BPAU was available in tissues, and hence clinically no promotion was observed. A strong effect of PMSF was also seen when BPAU was given 1 day before BPAU dosing. This may be due to the effect of PMSF lasts a longer time in the body and overlap with BPAU more than it was given 1 day after BPAU. The effect of PMSF on NTE lasts several days (Lotti, *et al.*, 1991). This implies that PMSF may exhibit a long lasting effect on BPAU metabolism as well. This time-dependent character coincides well with pharmacokinetic process and clearly indicates that PMSF promotion depends on BPAU level in target tissues.

2.4.3 The effect of PMSF on BPAU disposition

This study has shown that the effect of PMSF on BPAU neuropathy had a time-dependent character, and suggested that the promotion may be caused by an

interaction between the two compounds. The question is how PMSF interacted BPAU metabolism and increased BPAU neurotoxicity. The further study showed that PMSF significantly changed the pharmacokinetic pattern of BPAU. It significantly delayed BPAU elimination. By 24 hours after dosing, BPAU decreased to 6 % of its peak value in the spinal cord in BPAU control, but it only decreased to 46 % of its peak value in BPAU + PMSF. This clearly indicates PMSF interfered with BPAU disposition.

2.4.4 Metabolic interaction between BPAU and PMSF and neurotoxic synergism

After having shown that PMSF interferes with BPAU disposition, a further question was how PMSF interfered with BPAU disposition. The answer may lead to a better understanding of the mechanism of the promotion. The primary findings in this study shows that PMSF can increase BPAU and its metabolite, M1 levels in tissues and decrease M2 concentration in blood. FIG 2-24 shows the proposed mechanism of metabolic interaction between BPAU and PMSF. BPAU is normally metabolised in tissues via two distinct pathways. PMSF inhibited M2 formation. Thus BPAU elimination was attenuated and more BPAU has to be metabolised via M1 pathway and hence increased BPAU and M1 levels. This can well explain why PMSF promotion depends on BPAU level and showed a time-dependent character. Thus metabolic interaction between BPAU and PMSF is probably sufficient to explain the promotion of BPAU-induced neuropathy by PMSF.

PMSF is commonly used as a protease inhibitor. It can also inhibit a carboxyl esterase which is known as neuropathy target esterase (NTE) (Johnson, 1969, 1974). The present study also indicates that PMSF may inhibit other enzymes.

PMSF can potentiate OPIDN. All OP neurotoxicants which cause delayed polyneuropathy are NTE inhibitors (Johnson, 1969, 1974; Lotti, *et al.*, 1991). It was thought that OP-induced delayed neuropathy and its promotion by PMSF related to NTE inhibition. PMSF is an NTE inhibitor but does not induce the subsequent change transfer needed initiate neuropathy. Hence PMSF itself can not produce delayed ataxia. BPAU is not a NTE inhibitor (personal communication with Dr Johnson) but it can induce a delayed neuropathy which is similar to OPIDN and its neurotoxicity can also be intensified by PMSF. Thus, the metabolic interaction between BPAU and PMSF demonstrated in this study provides a more likely explanation of their neurotoxic synergism than any potential interaction at the target site. Therefore, the promotion of BPAU-induced neurotoxicity by PMSF represents a distinct model in the studies of promotion phenomena.

2.4.5 Ataxia and its evaluation,

Ataxia is a clinical sign caused by central and/or peripheral nervous damage. In experimental animal models of neurotoxicity , the ataxia score has widely been used to evaluate the neurotoxicity of neurotoxicants to animals. It has been reported that body weight loss had a good correlation with ataxia score (Canavagh, *et al.*, 1968). This study shows that body weight loss was related not only to the severity of ataxia but to the process of recovery as well. In the PMSF-1d-BPAU group, the peak ataxia score was as high as in the BPAU-4h-PMSF group, but its body weight loss was less than in BPAU-4h-PMSF group during the whole period of 80 days observation. Similarly the recovery was better than that in BPAU-4h-PMSF.

PHARMACOKINETIC FACTORS IN THE NEUROTOXICITIES OF *p*-BROMOPHENYLACETYLUREA AND *m*-DINITROBENZENE

Jinsheng Xu

PH.D

1998

To attempt to find a more sensitive parameter to evaluate the muscle weakness, the slope test was also used in this study. The slope test was originally developed by Le Quesne (personal communication). This study indicated that the change of slope test took place 2 days earlier than the clinical signs of ataxia. This clearly indicates that the onset of clinical ataxia is preceded by muscle weakness. Therefore, the slope test has its own value in evaluating muscle weakness. However, when the slope value became lower than a certain degree, even a dead rat may stop slipping down. So it has its limit in reflecting more severe ataxia. Therefore, the slope test alone can not well reflect the higher degree of ataxia severity but it can be used as an auxiliary indicator to evaluate muscle weakness.

2.4.6 Age difference in BPAU metabolism

It was reported that adult rats were more susceptible to BPAU neurotoxicity than young rats (Chen, *et al.*, 1971). Our results show that there exist age differences in the distribution and metabolism of BPAU. The BPAU level in spinal cord in 1-year old rats was significantly higher than that in 6-week old rats. In addition, the relative production of M1 and M2 were dramatically different. Young rats produce more M2 and less M1 than 1-year old rats, see FIG 2-25. This metabolic difference may be responsible for the difference in BPAU distribution, and for the age-related susceptibility to BPAU neurotoxicity as it has been demonstrated in this study that the two metabolites M1 and M2 of BPAU are formed via different pathways (see FIG 2-24). M2 has been suggested to be a detoxicated metabolite and M1 may be a toxic metabolite, see 2.4.5. Therefore, pharmacokinetic factors possibly relating to an age-dependent decrease of M2

formation and the increase of M1 formation, and the overall increase in parent concentration are the main factors for age difference of susceptibility to BPAU neurotoxicity.

2.4.7 Summary

1. The interaction between BPAU and the body begins with absorption. The lipophilic property of BPAU and lipid content in individual tissues determines the exposure burden of individual tissues. BPAU reached the highest level and had a longest half life in spinal cord, which coincides well with its histopathological lesion.
2. BPAU is metabolised *in vivo* before it is eliminated from body. Three metabolites are primarily characterised and metabolic pathways have been proposed in this study. BPAU is metabolised *in vivo* via two distinct pathways, M1 ← BPAU → M2. The M2 pathway plays a important role in BPAU detoxification. Whereas M1 is suggested to be a toxic metabolite. M3 is also a less toxic metabolite because it was mainly found in urine.
3. PMSF significantly intensified BPAU-induced delayed neuropathy. Its effect showed a time-dependent character. The promotion effect of PMSF depends on the presence of BPAU at target sites. The nearer the two compounds were given in time, the more severe the delayed ataxia. PMSF can inhibit the M2 pathway and less BPAU will be metabolised overall, though there is an increase in the M1 pathway, and hence exaggerated BPAU neurotoxicity. The metabolic interaction between the two compounds underlies the promotion phenomenon and hence represent a distinct model in the studies of promotion phenomena.

4. The age differences in BPAU distribution and metabolism agree well with age related susceptibility to BPAU induced neuropathy. Young rats, which resist to BPAU neurotoxicity, have a lower level of BPAU in spinal cord and produce more M2 but less M1 than adult rats, which are more susceptible to BPAU neurotoxicity than young rats. This further confirms that metabolism and pharmacokinetics of BPAU are involved in the modification of its neurotoxicity.

In conclusion, pharmacokinetic factors play a important role in BPAU induced neuropathy; its promotion by PMSF; and its age-related susceptibility. Any factors which can change the distribution, persistence and metabolism of BPAU can significantly modify its neurotoxicity.

SECTION 3 METABOLISM AND PHARMACOKINETIC FACTORS OF *M*-DNB IN ITS NEUROTOXICITY

3.1 INTRODUCTION

3.1.1 *m*-Dinitrobenzene and its neurotoxicity

m-Dinitrobenzene (*m*-DNB) is widely used as an intermediate in the chemical synthesis of rubber chemicals, pesticides, dyes and explosives (Hartter, 1985). Its toxicity to man has been known for more than a hundred years. In common with other nitroaromatic compounds, *m*-DNB can cause methemoglobinemia both in animals (Kunz, 1942; Foster, *et al.*, 1987) and in man (Parke, 1961; DeBethizy and Rickert, 1984). It can also produce testicular toxicity (Cody, *et al.*, 1981; Levin and Dent, 1982; Cussum, *et al.*,1986), liver toxicity and neurotoxicity (Kunz,1942; Kiese, 1949; Lazerev and Levina, 1976; Philbert, *et al.*, 1987 and Romero, *et al.*, 1991).

The neurotoxicity of *m*-DNB in animals shows cerebral paralysis (Kunz, 1942 and Kiese, 1949). It has been demonstrated that *m*-DNB can selectively cause brain stem damage and this damage is easier to produce by repeated lower doses or infusion than by a bolus dose in the experimental animals (Philbert, *et al.*, 1987; Romero, *et al.*, 1991 and Nolan, *et al.*, 1995). In the study of *m*-DNB-induced neurotoxicity, it was noted that germ-free rats are more sensitive to *m*-DNB than conventional rats. Germ-free rats developed ataxia 24 h after a single dose whereas

conventional rats developed a similar degree of ataxia only after repeated oral doses (Philbert, *et al.*, 1987). Histopathological studies showed that the main lesions symmetrically distributed in rat brain stem (Philbert, *et al.*, 1987 and Romero, *et al.*, 1991). The vulnerable regions in brain stem include cerebellar roof, vestibular, superior olivary nuclei and the inferior colliculi. Frequent petechial haemorrhages were also observed in these regions. The earlier change probably occurred in glial cells and neuronal damage secondary to glial cells (Philbert, *et al.*, 1987 and Romero, *et al.*, 1991). *m*-DNB increased cerebral blood flow especially in the inferior colliculi (Romero, *et al.*, 1991). It was suggested that vascular bed may play an important role in the pathogenesis of these lesions, perhaps in parallel with early astroglial damage (Romero, *et al.*, 1991).

The species and age differences in susceptibility to *m*-DNB has been documented (Obasaju, *et al.*, 1991; Linder, 1990). Rats and Hamster differ in susceptibility to *m*-DNB-induced testicular toxicity and methemoglobinemia (Obasaju, *et al.*, 1991). The half life of *m*-DNB is 3.0 hours in rats and 2.7 hours in Hamsters (McEuen and Miller, 1991). The half life prolonged with ageing (Linder, 1990). This may be responsible for the susceptibility of old rats to *m*-DNB-induced testicular toxicity (Linder, 1990).

3.1.2 Metabolism of *m*-DNB *in vivo* and *in vitro*

In vivo and *in vitro* studies have shown that absorbed *m*-DNB undergoes biotransformation in body or in cultured tissues (Cossum, 1985; Rickert, 1987; Nystrom, 1987; McEuen and Miller, 1991). The metabolic pathways were proposed by several researchers (Comel, 1931; Roubal, 1946; Lipschitz, 1948; Parke, 1961;

Rickert, 1987). FIG 3-1 shows the metabolic pathways of *m*-DNB. 3-Nitroaniline (3-NA) is a major product of phase I metabolism of *m*-DNB in which NADPH-cytochrome P450 reductase is involved (Cossum and Rickert, 1985). 3-nitroaniline (3-NA) and 3-nitrophenyl-hydroxylamine were found in rabbit tissues after administration of *m*-DNB (Comel, 931).

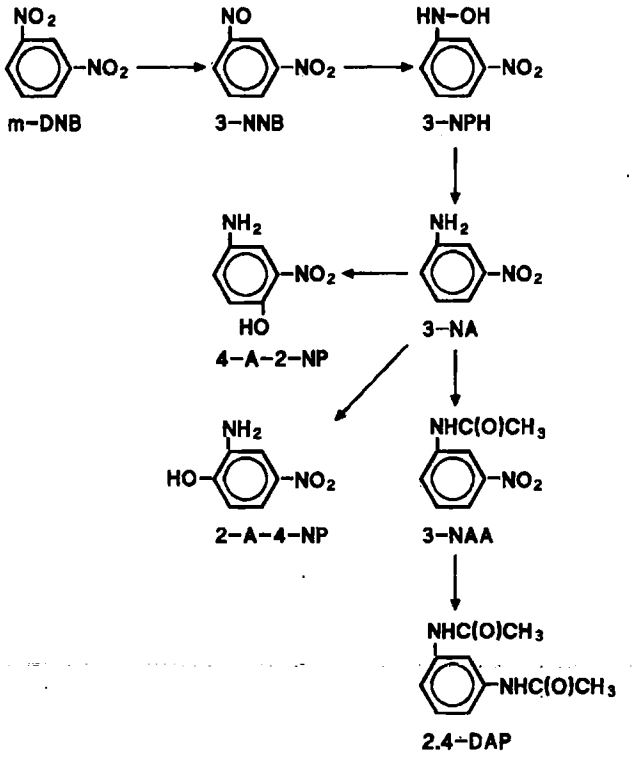

FIG 3-1. Major metabolic pathways of *m*-dinitrobenzene. *m*-DNB: *m*-dinitrobenzene; 3-NNB: 3-nitrosonitrobenzene; 3-NPH: 3-nitrophenyl-hydroxylamine; 4-A-2-NP: 4-amino-2-nitrophenol; 3-NA: 3-nitroaniline; 2-A-4-NP: 2-amino-4-nitrophenol; 3-NAA: 3-nitroacetaniline; 2,4-DAP: 2,4-diacetaminobenzene.

Whereas, the major metabolites of *m*-DNB in rabbit urine were 2,4-diacetaminophenol, 1,3-diaminobenzene, 3-nitroaniline (3-NA) and 2-amino-4-nitrophenol (Parke, 1961). Other metabolites found included 2,4-dinitrophenol, 4-amino-2-nitrophenol, 3-nitrosonitrobenzene (3-NNB), 3-nitrophenylhydroxylamine, and 3,3'-dinitroazoxy- benzene (Rickert, 1987). *m*-DNB in rat isolated hepatocytes was converted to 3-NA which accounted for 74 % of the added *m*-DNB (Cossum and Rickert, 1985). In rat testicular cell culture, two major metabolites 3-NA and 3-nitroacetanilide were found (Foster, 1987). In rat hepatocyte culture (Cossum and Rickert, 1985) and the brain slice incubation (Hu, *et al.*, 1995), 3-NA and small amount of 3-NNB were detected. Therefore 3-NA is a key metabolite either as a terminal metabolite or as a intermediate for the further metabolism of *m*-DNB.

Administrating 3-NA to rats and finding no testicular toxicity suggested that 3-NA is unlikely to be a toxic metabolite (Cosssum, *et al.*, 1986). However, 3-NNB was found to be more toxic than *m*-DNB itself (Foster, 1987). This suggests that the metabolic intermediates produced during the transformation from *m*-DNB to 3-NA may play an important role in *m*-DNB-induced testicular toxicity. Chemically, 3-NNB is not a stable intermediate. So, it is difficult to be detected *in vivo*. However, 3-NNB will be transformed into a relative stable metabolite 3-NA via 3-nitrophenylhydroxylamine, see FIG 3-1. Therefore, 3-NA may serve as a good indicator of the formation of toxic intermediates of *m*-DNB (McEuen and Miller, 1991).

3.1.3 Approaches of this study

m-DNB is a multi-target toxicant and can selectively cause brain stem damage. The dosing regimen of *m*-DNB significantly modified the susceptibility of individual target tissues. This suggests that pharmacokinetic factors in target sites may play an important role in its neurotoxicity. Although the metabolism and peripheral pharmacokinetics of *m*-DNB have been reported, its pharmacokinetic behaviour in individual target tissues has not been studied. This study investigates the metabolism and pharmacokinetics of *m*-DNB in individual target tissues and some cell types to look into the roles of these factors in *m*-DNB-induced neurotoxicity.

3.2. EXPERIMENTS

3.2.1 Chemicals

m-Dinitrobenzene (*m*-DNB), 3-nitroaniline (3-NA, 98%), 4-amino-2-nitrophenol and 2-amino-4-nitrophenol were obtained from Aldrich. 3-Nitrosonitrobenzene (3-NNB) was a gift from Dr M. K. Ellis (Zeneca Central Toxicology Laboratory). Trypsin, collagen, poly-L-lysine, cytosine β-D-arabinoside, foctal calf scrum (FCS) and the media of α-MEM and DMEM were purchased from Sigma; F-10 Ham's was obtained from Gibco. Other chemicals are as described in 2.2.1, Section 2.

3.2.2 Infusion-lesion model of *m*-DNB neurotoxicity

3.2.2.1. Animals and procedures

Intravenous infusions were made in conscious Fischer-344 (F344) rats, weight 250-280 g, via a catheter implanted into the external jugular vein. The catheter was placed under isofluorane anaesthesia and connected to a subcutaneous Alza osmotic minipump (Model 2ML1, alza Corporation) filled with *m*-DNB dissolved in DMSO. The total filling volume of each pump was 2114 ± 53 μl. The pumping rate was 10.26 ± 0.36 μl/h. The total dose for each infusion period was 30 mg/kg *m*-DNB. The concentration of *m*-DNB was adjusted to give the appropriate dosing rate over 6, 12, 24 hours, or 2, 4, 6, 8 or 14 days. Two rats were used for

each infusion period. Histopathological examination of each rat was done at the end of each infusion, see 3.2.2.2.

Five extra rats in 4-day infusion group were used for *m*-DNB measurement. The animals were killed by the inhalation of carbon dioxide at the end of 4-day infusion. Blood of each rat was sampled through heart immediately after the death of animals and anticoagulated with heparin. Brain and spinal cord were removed. The brain was dissected into cerebral cortex, brain stem and cerebellum. Brain stem was further dissected into the regions of colliculi, pons and medulla oblongata. Sample preparation and analysis: see 3.2.3.2 and 3.2.5.

3.2.2.2 Histopathological observation

Rats for histopathological observation were killed at 24 hours after the end of infusion by perfusion fixation under deep halothane anaesthesia. The ascending aorta was cannulated and following a brief wash with saline, perfused with 10 % formalin, 2 % acetic acid for 12 min at a pressure of 120 mmHg. The brain and cervical spinal cord were removed after storage of the intact head at 4 °C for 24 hours, sliced coronally into 5 blocks and wax embedded. Composite blocks were step serial sectioned at 7 μm and stained with haemotoxylin and eosin. Some large area semithin plastic sections were prepared from 4 % glutaraldehyde in 0.1 M sodium cacodylate buffer (pH 7.2).

Lesion severity was graded from no abnormalities (-) through scattered vacuolation (+) and confluent areas of vacuolation within brain stem nuclei (++), to involvement of whole nuclei (+++).

3.2.3 Metabolism and pharmacokinetics of *m*-DNB

3.2.3.1 Animals and procedures

Groups of 5 female F344 rats, weight 250-300 g, were dosed with 10 mg/kg *m*-DNB in DMSO through tail lateral vein. The animals were killed at the time points of 0.5, 1, 2, 4, 8 and 18 hour(s) after dosing. Two control rats were only given an equal volume of DMSO and they were killed at either 2 or 18 hours after injection. Animals were killed by inhalation of carbon dioxide at the end of experiments. Blood samples were collected through the heart immediately after animal death and anticoagulated with heparin. Liver, testis, brain and spinal cord were removed. The brain was dissected into cerebral cortex, brain stem and cerebellum. Brain stem was further dissected into the regions of colliculi, pons and medulla oblongata. All the samples were weighed and stored at -20 °C until analysis.

3.2.3.2 Sample preparation

The collected anticoagulated blood samples were centrifuged at 3000 g for 10 min. Plasma (1 ml) was taken from each sample and mixed with 4 ml solution of methanol/DMSO (95:5 by volume). Tissues were homogenated in methanol/DMSO solution at 100 mg tissue per ml solution. All samples were centrifuged at 6000 g for 20 min. Supernatant was taken and centrifuged at 9000 g with Eppendorf centrifuge for 5 min. *m*-DNB and its metabolites were determined by HPLC. HPLC analytical condition see 3.3.2.6.

The recovery of *m*-DNB in the analytical system was studied by homogenizing fresh rat brain in methanol/DMSO (95:5 % by volume) containing

standard *m*-DNB (1 μg/ml). Seven samples were tested. The percentage of recovery was calculated by dividing the detected amount by the added amount.

3.2.4 *m*-DNB metabolism in endothelial cells and astrocytes

3.2.4.1 Astrocyte primary culture

3.2.4.1.1 Buffers and culture reagents

Buffer D1: This buffer consisted of a Ca- and Mg-free Hank's Balanced Salt Solution (HBSS) containing 140 mM NaCl, 5.4 mM KCl, 0.67 mM Na_2HPO_4, 0.22 mM KH_2PO_4, 17 mM glucose, 22mM sucrose, 10 mM HEPES buffer, 100U/ml penicillin G and 100 μg/ml streptomycin. It was adjusted to pH 7.4 with 1 M NaOH, sterilised by filtration through a 0.22 μm filter and stored at 4 °C until use within 2 days.

Trypsin solution was made up fresh and consist of a 1.25 mg/ml trypsin solution in buffer D1 sterilised by filtration through a 0.22 μm filter.

Collagen stock was a 0.3 mg/ml rat tail collagen solution in 0.1 % (v/v) glacial acetic acid to help dissolve collagen.

Poly-L-lysine stock consisted of a 1 mg/ml poly-L-lysine [hydrobromide] (MW 75,000 - 150,000) in 0.1 M borate buffer made up with 3.1 mg/ml H_3BO_3 and 4.75 mg/ml $Na_2B_4O_7$ adjusted to pH 8.5. The solution was sterilised by filtration through a 0.22 μm filter and stored at -20 °C until use. The poly-L-lysine solution is prepared by diluting the stock solution to 10 μg/ml in sterile borate buffer on the day of the isolation procedure.

Cytosine arabinoside stock (Ara C): β-D-arabinoside was dissolved in HBSS at a concentration of 1 mM and sterilised by filtration through a 0.22 μM filter. The

solution was diluted 1:100 in culture medium to give a final concentration of 10 μM.

3.2.4.1.2 Culture medium

Dulbecco's Modified Eagle's Medium (DMEM) was used throughout the culture. It contains 10 % foetal bovine serum, 2 mM glutamine, 1 mM sodium pyruvate, 0.057 mM sodium ascorbate, 26 mM sodium bicarbonate, 100 U/ml penicillin G and 100 μg/ml streptomycin. The medium was sterilised by filtration through a 0.22 μm filter and stored at 4 °C until use within 1-1.5 months.

3.2.4.1.3 Preparation of growth surface

Astrocytes were routinely grown on 25 cm^2 tissue culture flasks which had been previously coated with poly-L-lysine on its own or in combination with collagen for a more durable cell attachment on glass coverslips. Prior to seeding cells, the flask surfaces were coated with 3 ml of poly-L-lysine at room temperature for 1 hour. Excess poly-L-lysine was removed by washing three times with HBSS.

3.2.4.1.4 Isolation of cells

1) F344 rat pups at either day 0 or day 2 were used. The pups were soaked in 70 % ethanol and were killed by decapitation with scissors. The pup heads were placed in the centre of a lint soaked with buffer D1 and held with a pair of big forceps. The skin was cut along the midline with a scalpel. The soft skull was also cut on the midline with another scalpel to avoid contamination and separated the bone with a pair of curved forceps. The whole brain was removed and transferred to a 50 ml beaker containing ice-cold buffer D1.

2) Brains were transferred to a 60 mm diameter plastic dish containing 5 ml of buffer D1. The brain was held with the small straight forceps and the cerebrum was cut off at the superior colliculi level with the small curved forceps. The brain was sliced longitudinally along the midline and separated into two hemispheres. Midbrain structures, the hippocampus and the choroid plexus were pinched off with a small curved forceps until just cerebral cortex was left. The two cortices were transferred to a moist lint and picked off meninges and surface vessels with blunt curved forceps. The cortices were then transferred to a 60 mm plastic dish containing 5 ml of buffer D1 and placed on ice.

3) Dissected tissues were then chopped finely with a surgical scalpel. Trypsin solution (5 ml) was added to disaggregate the tissue suspension at 37 °C for 30 min. Following the incubation period, trypsin was inactivated by adding an equal volume of serum-containing nutrient medium for 5 min and then spun 5 min at 1,500 rpm. The supernatant was decanted and the brain pellets were resuspended in 2 ml culture medium. The tissue was further dissociated to form a cell suspension by trituration through a fine-bore fire-polished Pasteur pipette and sedimentation. Cells were then filtered by gravity through a sterile 73.5 μm metal sieve to get rid of big cell clumps and diluted with culture medium for counting in a haemocytometer. Cells were then seeded at a plating density of 25,000 cells/cm^2 (usually each cortex will give around two or three 25 cm^2 flasks).

3.2.4.1.5 Maintenance of the cultures

The culture medium was replaced with fresh medium 24 h after seeding and subsequently every 2-3 days. The cells were incubated at 37 °C in a water saturated

atmosphere of 95 % air 5% CO_2. At sub-confluence (days 7-9 after plating), cell contaminants on top of the monolayer were separated from type I astrocytes by shaking on a vibrax SR/VXR7 shaking system (Camlab Ltd., Cambridge, U.K.) at 37 °C for 24 h. Detached cells, consisting mainly of oligodendrocytes, type 2 astrocytes and 0-2A progenitors, were aspirated off and the culture medium was replaced. Further purification of the cell cultures was achieved at confluence (day 14-16 after plating) by adding cytosine arabinoside (10 μM) to the culture medium for 5 days to kill contaminating dividing cells.

3.2.4.1.6 Exposure to *m*-DNB

Monolayer astrocytes were incubated in the medium containing 100 μM *m*-DNB for 4, 8 or 24 hours. Both cells and media were collected at the end of each time point for the measurements of *m*-DNB and its metabolites. Four flasks were used at each time point. The cell-free control flasks were added medium containing 100 μM *m*-DNB and blank control flasks with cells were added culture medium without *m*-DNB.

3.2.4.2 Endothelial cell line

Mouse endothelial cells (RBE4, P.50, clone A3) were seeded in 25 cm^2 plastic flasks at a plating density of 25,000 cells/cm^2. The cells were maintained in the medium of α-MEM (Sigma): F10 Ham's (Gibco) (1:1) plus 10 % foetal calf serum (FCS) and the flasks were incubated under standard condition (37 °C, 5 % CO_2 and 95 % air) until a monolayer was completed in each individual flask. The

metabolic study of *m*-DNB was carried out by replacing the culture medium by the medium containing 100 μM *m*-DNB. Cells and 0.5 ml of medium were collected at the end of each time point for the measurements of *m*-DNB and its metabolites. Four flasks were used at each time point. The cell-free control flasks were added medium containing 100 μM *m*-DNB and blank control flasks with cells were added culture medium without *m*-DNB.

3.2.4.3 Neuroblastoma cell line

The cells of neuroblastoma (mouse N1E 115) were seeded in 25 cm^2 flasks at a plating density of 25,000 cells/cm^2 and incubated in the medium of 10 % FCS in DMEM under the standard culture condition until a monolayer was formed. Then, the cells were exposed to the medium containing 50 μM *m*-DNB. 100 μl medium was taken at either 4, 8 or 24 hours after exposure for the determination of *m*-DNB and its metabolites.

3.2.4.4 Procedures and analysis of samples

The monolayer cells in each flask were trypsinized and collected with a 5 ml centrifuge tube. Then the cells were transferred into pre-weighted 1.5 ml Eppendorf tube after centrifuging. The Eppendorf tubes were centrifuged at 9000 g for 3 min and medium in tubes was drawn out. The sample weight of each flask was obtained by the difference between the tube weight with cells and the weight of empty tube. Then the cells were homogenised in 100 μl methanol for 3-5 min and then centrifuged at 9000 g for 5 min. The supernatant of each sample was kept for HPLC analysis.

Each sample of media taken from above experiments was mixed with equal volume of methanol. Then they were centrifuged at 9000 g for 5 min. The supernatant of each sample was kept and analysed by HPLC. The HPLC analytical condition see 2.6.

3.2.5 Study of 3-nitrosonitrobenzene stability

3-nitrosonitrobenzene (3-NNB) is an important intermediate in *m*-DNB metabolism, see FIG 3-1. But in *in vivo* study, it is difficult to detect. This spiking study was to study its stability in tissue extraction.

Two male F344 rats, weight approximately 200 g, were used. One of them was dosed with 30 mg/kg of *m*-DNB iv and was killed by CO_2 at 2 hours after dosing. The other rat was not dosed and was killed by CO_2 as well. The brains were taken out immediately and stored in -20 °C fridge. The analysis were carried out within one week.

Rat brains were homogenised in methanol according to the ratio of 100 mg tissue per ml. 3-NNB, *m*-DNB and/or 4-amino-2-nitrophenol in DMSO were added to the extraction to make either 5 or 10 μg/ml spiked extraction. The two brain tissues were also extracted by 5 % TCA and then 3-NNB was added to make 10 μg/ml extraction. Samples were analysed by HPLC. The analytical condition see 3.2.6.1.

3.2.6 HPLC analytical condition

3.2.6.1 Gradient

HPLC system: Waters HPLC system with a Controller 600, a tuneable absorbance detector 486, and an autosampler plus 717. The column was a S5 ODS2 250 × 4.6 mm (Spherisorb), and the detector wavelength was 254 nm; The mobile phase (A= water, B= acetonitrile) used a gradient: maintained 5 % B for 1 min and then directly changed to and maintained at 50 % B at a velocity of 1ml/min for 19 min. The injected volume of each sample was 25 or 50 μl.

3.2.6.2 Isocratic

HPLC (Philips, Pye Unicam, PU4010 pump, LDC/Milton Roy Spectromonitor III). Column: S5 ODS2 250 X 4.6 mm (Spherisorb); Wavelength: 254 nm; Mobile phase: 30% acetonitrile in 0.1 mM ammonium acetate; Velocity: 1 ml/min. The injected volume of each sample was 50 μl.

The HPLC profile of *m*-DNB and its metabolites are shown in FIG 3-2.

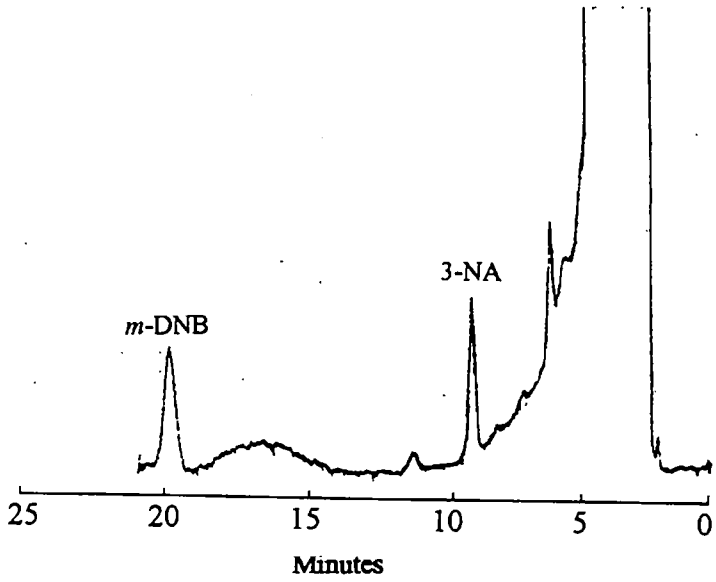

A: Isocratic condition.

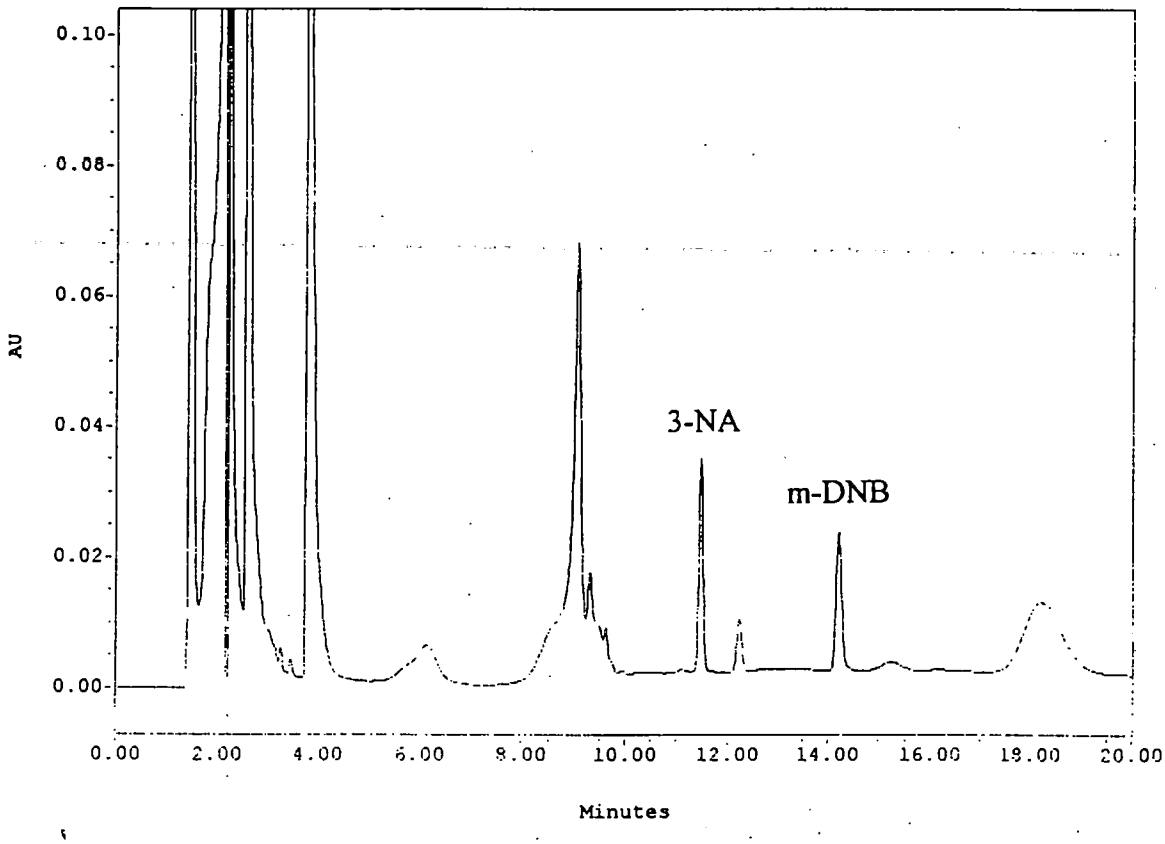

B: Gradient condition.

FIG 3-2. The HPLC profiles of *m*-DNB and its metabolites.

3.2.7 Statistics and pharmacokinetics

3.2.7.1 Statistics

Anova analysis was used for the comparisons of the concentration of *m*-DNB or its metabolites in different tissues and the blood/tissue ratio. Student-t test was employed for two sample comparison. The standard error of elimination rate constants were calculated according to the method given by Mead and Curnow (1987). The Z test was used for half life comparison. The statistics were carried out by computer on the statistics programme of MINITAB 10.2.

3.2.7.2 Pharmacokinetics

Pharmacokinetic data were analysed according to the methods and equations given by Gibaldi & Perrier (10). *m*-DNB follows apparent first order absorption and elimination kinetics and one-compartment open model was employed. The concentration (C_t) of *m*-DNB at any time (t) after a single iv dose was estimated by

$$\log C_t = \log C_0 - kt/2.303 \qquad (1)$$

where k is the rate constant of elimination phase.

The plasma concentration (C_i) of *m*-DNB at any time (T_i) during the infusion was estimated by the following equation

$$C_i = r_i(1-e^{-kTi})/k.V \qquad (2)$$

where r_i is the infusion rate; V is the apparent distribution volume.

The time (t_d) from the end of infusion to decline to a certain concentration was calculated by the equation transformed from (1)

$$t_d = 2.303(\log C_0 - \log C_t)/k \qquad (3)$$

The details of the calculations of pharmacokinetic parameters are in the *Appendix*.

3.3. RESULTS

3.3.1 Pharmacokinetics of *m*-DNB

3.3.1.1 Distribution

m-DNB was determined by HPLC method. The recovery of this analytical system was 92.2 ± 3.7% (n=7). Following a bolus iv dose, *m*-DNB reached its peak value in tissues at 1 hour. The peak levels in different regions of the central nervous system are significantly higher than those in liver and testis. *m*-DNB does not evenly distribute in CNS. Its levels in spinal cord and different regions of brain stem are 15-52 % higher than those in cerebral cortex and cerebellum, see FIG 3-3 and 3-4.

3.3.1.2 Pharmacokinetics

The pharmacokinetic parameters of *m*-DNB in blood and individual tissues were estimated. *m*-DNB given intravenously followed apparent first order absorption and elimination kinetics in plasma and tissues of rats. FIG 3-3, 4 and 5 show the concentration-time curves of *m*-DNB and its metabolite 3-NA in plasma and different tissues. *m*-DNB reached its peak value in tissues at 1 hour and 3-NA reached its peak value at 2 hours after iv injection. Most *m*-DNB had been eliminated at 18 hours after dosing. The concentration-time data were transformed into logarithm of concentration versus time data and the kinetic models were identified. All the data from either plasma or tissues were best fitted by a one-compartment model, see A-II-A, Appendix.

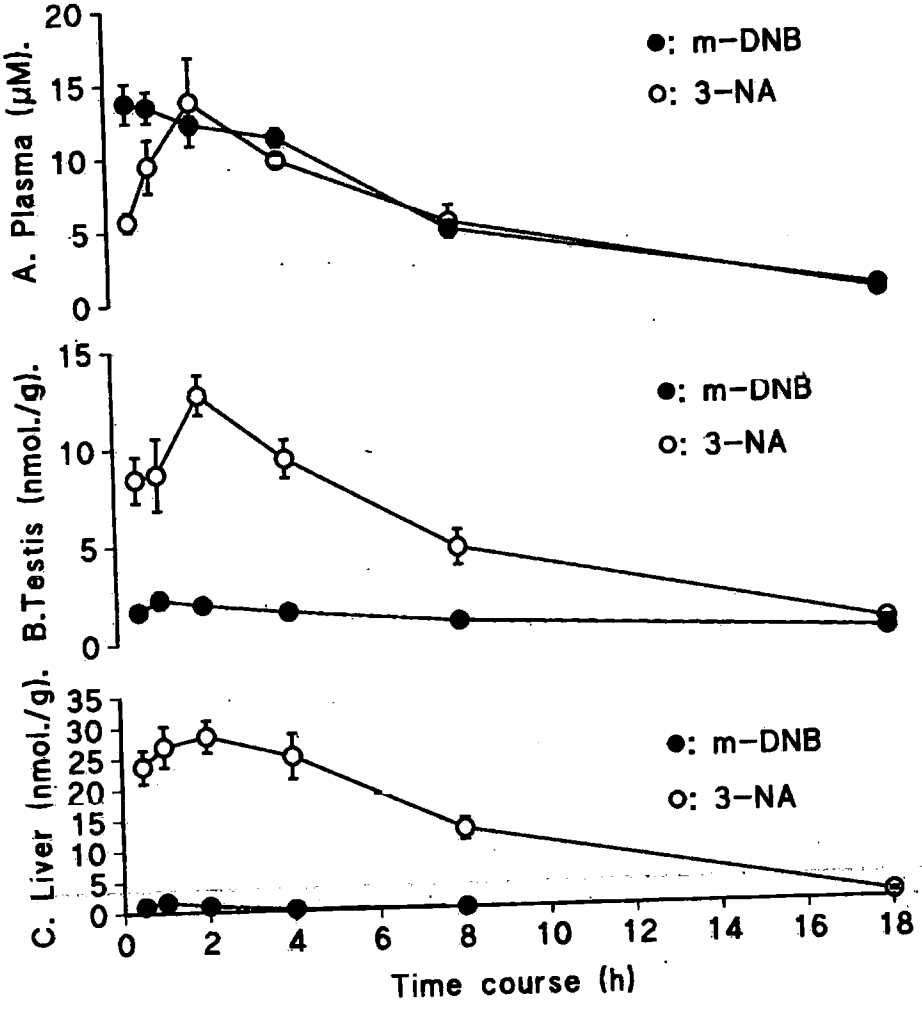

FIG 3-3 Concentration-time curves of *m*-dinitrobenzene and 3-nitroaniline in plasma, testis and liver. The data were obtained by giving a single iv dose of 10 mg/kg *m*-DNB. The values are presented as mean ± SE, n=5.

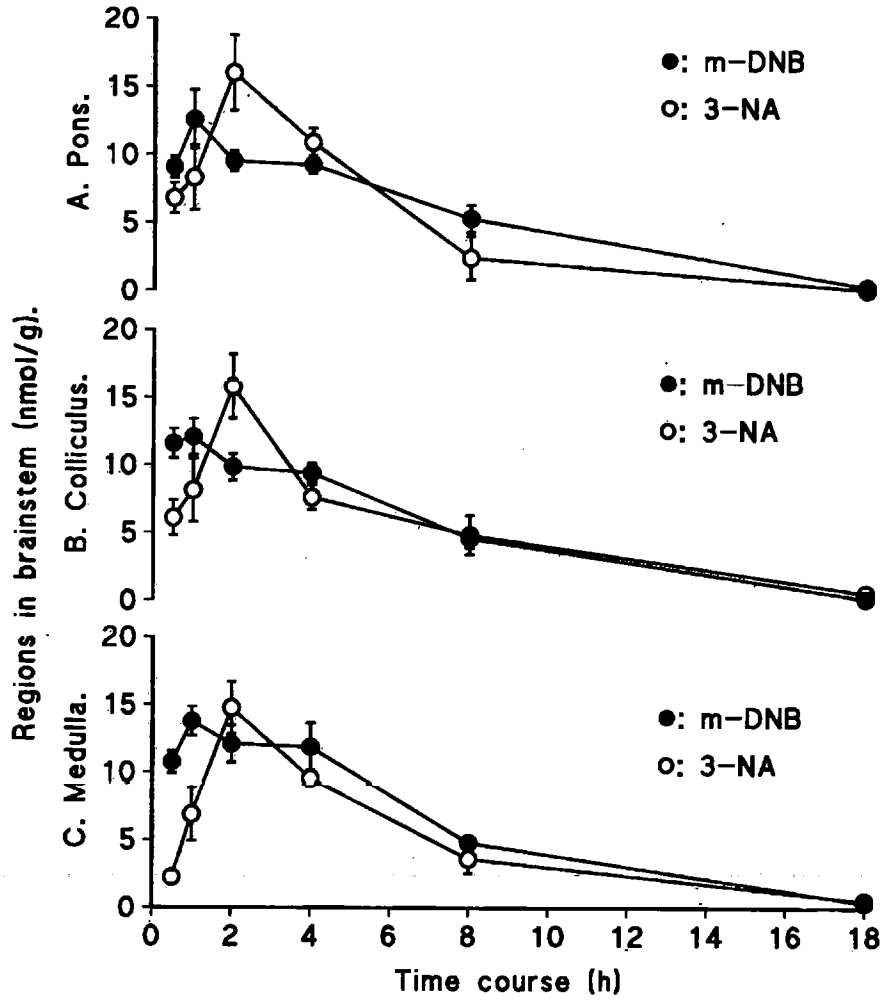

FIG 3-4 Concentration-time curves of *m*-dinitrobenzene and 3-nitroaniline in the regions in brain stem. The data were obtained by giving a single iv dose of 10 mg/kg *m*-DNB. The values are presented as mean ± SE, n=5.

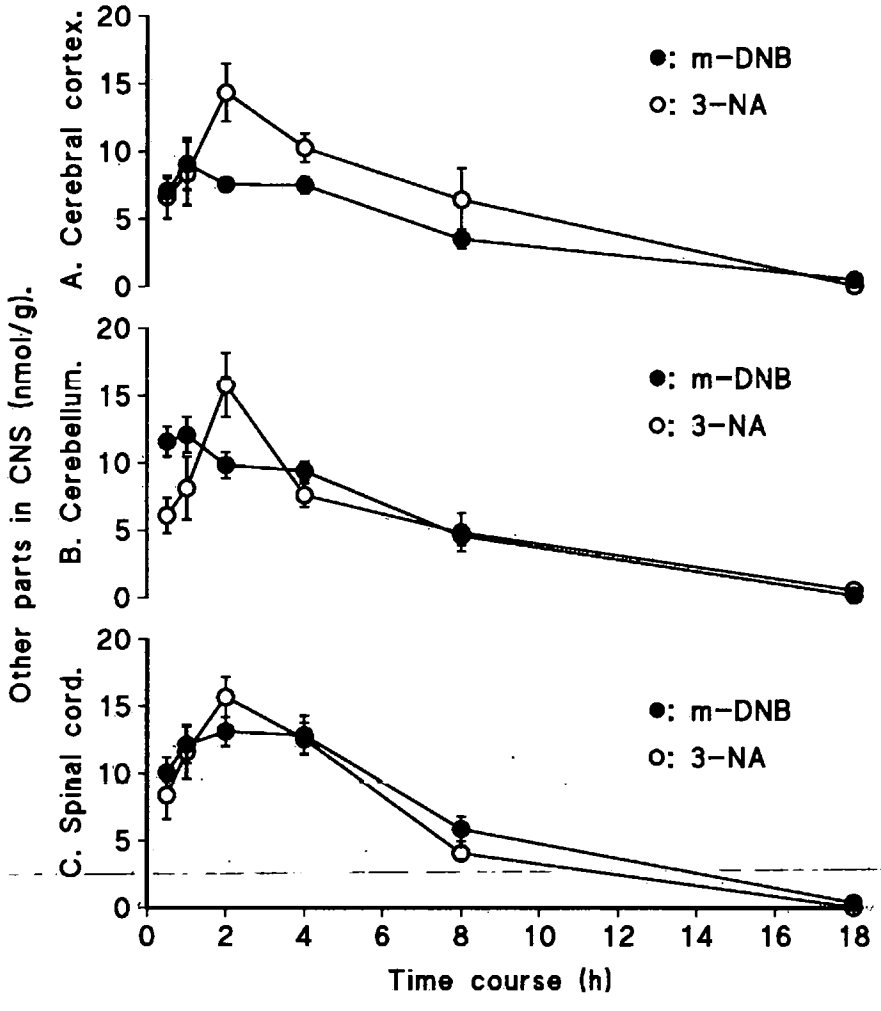

FIG 3-5 Concentration-time curves of *m*-dinitrobenzene and 3-nitroaniline in cerebral coetex, cerebellum and spinal cord. The data were obtained by giving a single iv dose of 10 mg/kg *m*-DNB. The values are presented as mean ± SE, n=5.

Fitting these data using non-linear least square regression yields straight lines for the elimination phase, and the kinetic parameters were determined according to the equations given by Gibaldi & Perrier (1975). The parameters of *m*-DNB in blood are presented in Table 3-1.

Table 3-1. The pharmacokinetic parameters of *m*-DNB in plasma following a single iv dose of 10mg/kg.

X_0 (mg)	C_0 (mg/l)	V (l)	k (h^{-1})	AUC ($mg.hr^{-1}.l^{-1}$)	$T_{1/2}$ (h)
2.76	2.79	0.989	0.237	11.78	2.92 ± 0.12

k: elimination rate constant; V: apparent distribution volume; AUC: the area under the concentration-time curve; and $T_{1/2}$ elimination half life. Half-life is presented as Mean ± SE, n=5.

Table 3-2. The pharmacokinetic parameters of *m*-DNB in tissues

Tissue	C_0 (μg/ml)	k (h^{-1})	$T_{1/2}$ (h)	AUC ($\mu g.ml^{-1}.h^{-1}$)
Medulla	3.66	0.237 ± 0.010	3.0 ± 0.2	17.7
Pons	3.21	0.238 ± 0.015	2.9 ± 0.2	15.8
Colliculi	3.17	0.237 ± 0.013	2.9 ± 0.2	15.2
Cerebellum	2.88	0.228 ± 0.018	3.0 ± 0.2	14.4
Cortex	2.07	0.203 ± 0.019	3.4 ± 0.3	11.9
Spinal cord	4.09	0.222 ± 0.053	3.1 ± 0.6	19.4
Liver	2.20	0.546 ± 0.072	1.3 ± 0.2**	0.7
Testis	2.29	0.152 ± 0.031	4.6 ± 0.8*	2.7

C_0 is the concentration estimated from the extrapolated line of -k/2.303 when time t is zero; k: the apparent first-order elimination rate constant. $T_{1/2}$ is the half life of elimination phase. AUC: the area under the concentration-time curve. Data are presented as mean ± SE, (n=5).*: $p<0.05$; **: $p< 0.01$ (Z test) for liver or testis comparing with brain areas.

The half lives and AUC of *m*-DNB in tissues are shown in Table 3-2. The half life in liver was significantly shorter than that in blood and other tissues. Whereas the half life in testis was significantly longer than that in blood and other tissues. The half lives in different regions of CNS are similar to that in blood. AUC in central nervous system was much higher than that in non-nervous system.

3.3.1.3 *m*-DNB metabolism *in vivo*

The main metabolite of *m*-DNB detected in all tissues was 3-NA. Its distribution in the central nervous system paralleled that of *m*-DNB after 2 hours. However, liver

Table 3-3 The pharmacokinetic parameters of 3-NA

Tissue	k (h^{-1})	$T_{1/2}$ (h)
Blood	0.155 ± 0.041	4.47 ± 0.45
Medulla	0.260 ± 0.048	2.66 ± 0.41
Pons	0.213 ± 0.047	3.26 ± 0.58
Colliculi	0.215 ± 0.055	3.22 ± 0.66
Cerebellum	0.242 ± 0.047	2.86 ± 0.46
Cortex	0.206 ± 0.031	3.37 ± 0.44
Spinal cord	0.147 ± 0.034	3.98 ± 0.64
Liver	0.147 ± 0.012	4.70 ± 0.70
Testis	0.184 ± 0.068	3.77 ± 0.61

k: the apparent first-order elimination rate constant. $T_{1/2}$ is the half life of elimination phase of 3-NA. Data are presented as Mean ± SE, n=5.

reached the highest concentration of 3-NA which is 16 times higher than *m*-DNB. 3-NA reached its peak value in tissues at 2 hours after iv injection. This was a one hour delay compared with its parent compound, *m*-DNB, see FIG 3-3, 4 & 5. The half lives of 3-NA in different tissues are presented in Table 3-3.

3.3.1.4 Infusion studies

Distribution pattern: A total intravenous dose of 30 mg/kg *m*-DNB was infused within 4 days. *m*-DNB in plasma and tissues were measured at the end of infusion. The concentration of *m*-DNB was 2.8 ± 0.4 μM in plasma, 3.8 ± 0.4 nmol/g in medulla oblongata, 3.6 ± 0.5 nmol/g in colliculi, 2.6 ± 0.5 nmol/g in pons, 2.4 ± 0.4 nmol/g in cerebellum, and 2.3 ± 0.3 nmol/g in cerebral cortex. The distribution pattern of *m*-DNB in the brain after infusion is similar to that after bolus iv dose.

Tissue/plasma ratio: In order to compare the relative distribution between different tissues and accumulation between bolus dosing and infusion, tissue/plasma ratio was calculated. Tissue/plasma ratio for each tissue was obtained by dividing the peak value (μg/g) of *m*-DNB in each tissue by its concentration (μg/ml) in plasma at the same time point. The tissue/plasma ratios of tissues in infusion were generally higher than that in bolus dose, see FIG 3-6, and the ratios in colliculi and medulla oblongata in infusion were significantly higher than in bolus dose. This indicates that infusion allowed more *m*-DNB to accumulate in central nervous system than a single bolus dose, especially in some regions of brain stem.

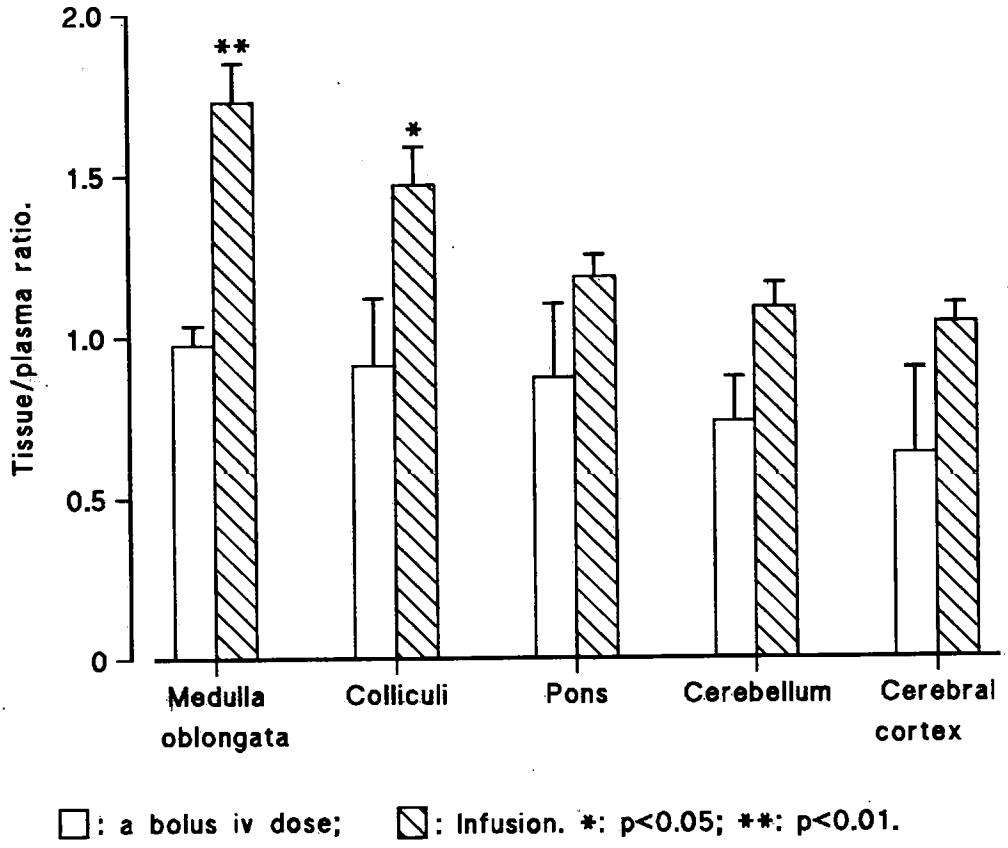

FIG 3-6 Comparisons of tissue/plasma ratios in different regions in brain between infusion and bolus doses. The infusion study was done by infusing 30 mg/kg *m*-DNB to rats over 4 days. *m*-DNB levels in plasma or tissues were measured at the end of experiment. The ratios from bolus dose are the tissue peak values versus the plasma value at the same time point after a single iv dose of 10mg/kg *m*-DNB. The tissue/plasma ratio of each tissue was obtained by dividing tissues concentration (μg/mg) by plasma concentration (μg/ml). The data are presented as mean ± SD, n= 5.

3.3.2 Infusion-lesion model of *m*-DNB-induced neurotoxicity

A total of 30 mg/kg of *m*-DNB was infused over either 6, 12 or 24 hours, or 2, 4, 6, 8 or 14 days. The histopathological lesions in each infusion are shown in Table 3-4. To illustrate how the blood concentration of *m*-DNB relates to its histological lesion, the theoretical infusion curve for each infusion period was calculated based on pharmacokinetic parameters and constants given in table 3-1. The concentration-time curves of infusion are shown in FIG 3-7.

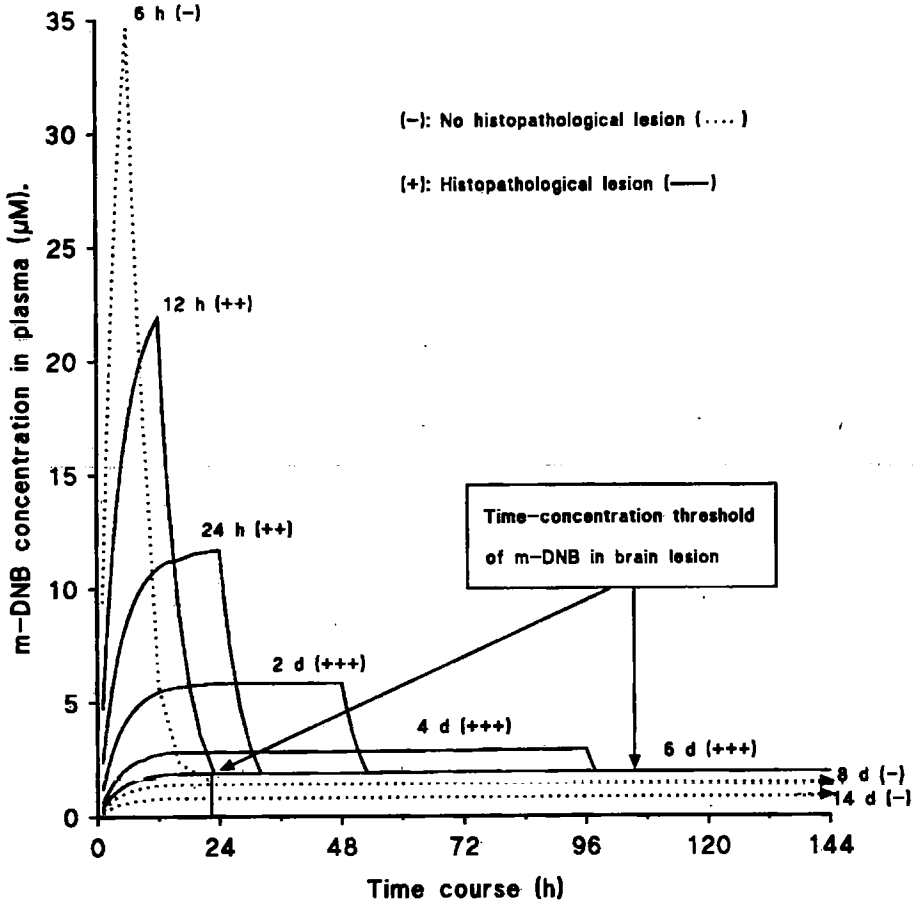

FIG 3-7. The infusion-lesion model of *m*-DNB neurotoxicity: Theoretical concentration-time curves of *m*-DNB in the infusions of different periods and their correspondent histopathological lesions.

Table 3-4. Dosing regimen of *m*-DNB and its lesion scores

Duration	Pathological score	Ataxia score*
Bolus	-	0
	-	0
6 hours	-	0
	-	0
12 hours	-	0
	+++	4
1 day	+	3
	++	5
2 days	+++	2
	+++	2
4 days	+++	1
	+++	1
	+++	3
	+++	2
6 days	++	1
	+++	1
8 days	-	2
	-	2
14 days	-	2
	-	2

*: the evaluation system of ataxia score see 2.2.5.2.1, Section 2.

The plasma steady-state level of *m*-DNB at the end of the 4-day infusion was 2.8 ± 0.4 μM. The predicted value was 2.9 μM which is within the normal range of the real value. Thus it is reasonable to estimate the infusion curve of *m*-DNB in plasma by using the pharmacokinetic rate constants and parameters obtained from the above pharmacokinetic study. The infusion curves were plotted according to the equation (2) stated in 3.2.7.2 in this section. When the infusions end, *m*-DNB will decline according to equation (1). All the theoretical curves of infusions are presented in FIG. 3-7. As shown in FIG 3-7, the steady state level of 6-day infusion is 1.95 μM which is the minimum plasma concentration associated with lesion

formation. Therefore this concentration is taken as the plasma concentration threshold of lesion. The time (T_d) needed to decline from the end level or steady state of infusion to 1.95 μM was next estimated by the equation (3), see 3.2.7.2. Thus the time (T_m) over which plasma concentration was maintained above threshold can be estimated by $T_d + T_i$ (T_i is infusion time). T_m in each case of infusion is presented in table 3-5.

Table 3-5. The time maintaining the level of *m*-DNB above lesion threshold in each infusion.

Infusion group	T_i (h)	T_d (h)	T_m (h)
6 h	6	12.8	18.8
12 h*	12	10.7	22.7
24 h*	24	8.0	32.0
2 d*	48	4.9	52.9
4 d*	96	1.8	97.8
6 d*	144	0.0	144.0

T_i is the infusion time; T_m is the time over which plasma concentration was maintained above the neuropathic threshold; T_d: the time needed from the end level or steady state of infusion declining to lesion threshold, 1.95 μM. *: lesion produced.

3.3.3 Metabolism of *m*-DNB *in vitro*

3.3.3.1 Metabolism of *m*-DNB in astrocytes and endothelia cells

Cell culture studies show that the cell types of endothelial cells,

astrocytes and neuroblastomal cells are all able to metabolise *m*-DNB. 3-NA was the main metabolite detected in both media or cells, see FIG 3-8 and 3-9.

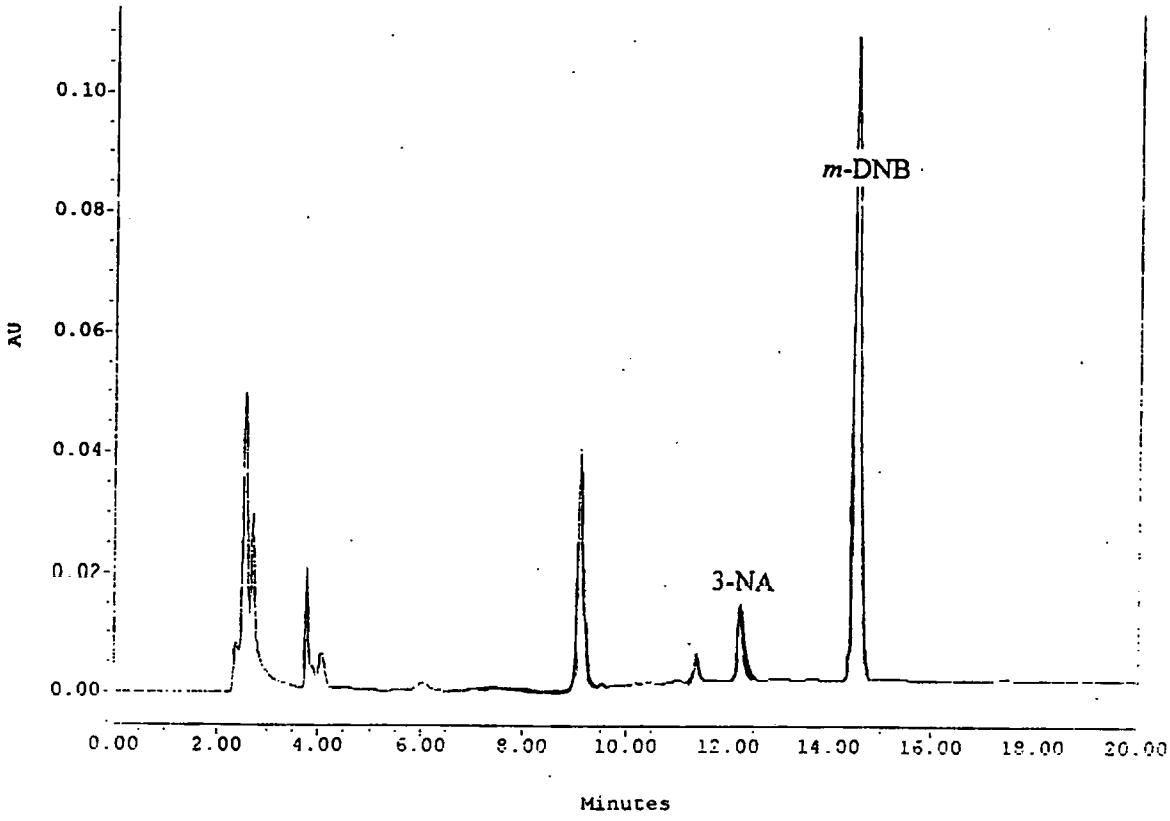

FIG 3-8. Chromatogram of *m*-DNB and its metabolites in the medium of endothelial cells at 24 hours after incubation.

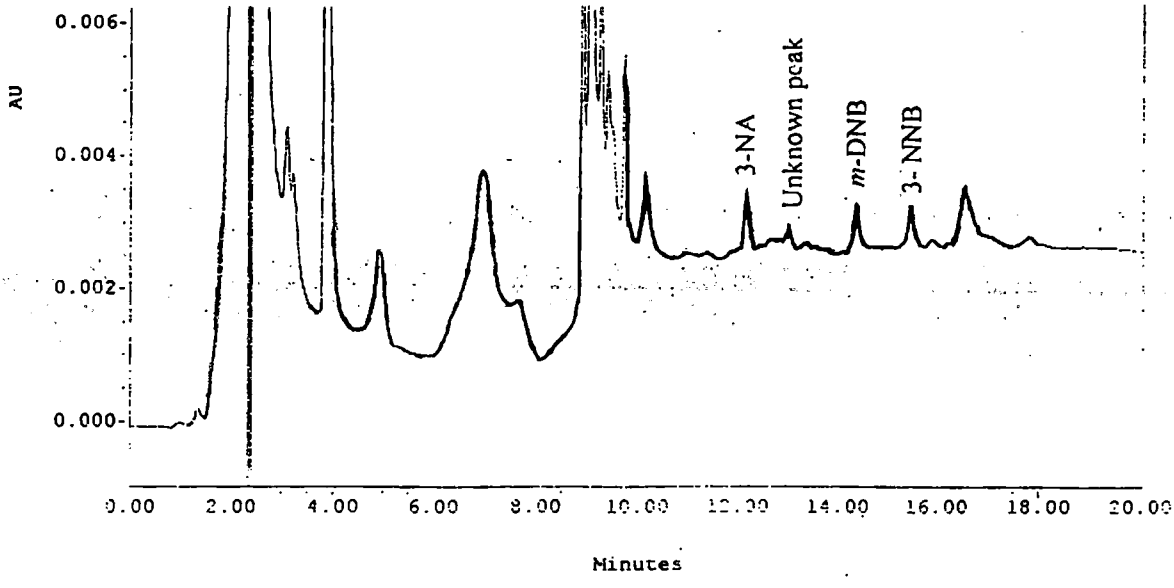

FIG 3-9. **Chromatogram of *m*-DNB and its metabolites in washed endothelial cells at 4 hours after incubation.**

3-NA accumulated in media in a constant rate. A active intermediate 3-NNB was detected in either endothelial cells or astrocytes at 4-hour, but not at 8 or 24 hours, see FIG 3-9. One unidentified peak was also detected, see FIG 3-8 and 3-9. The unknown peak came out after 3-NA in HPLC graphs and it was mainly detected at 4 and 8 hour incubation, but not at 24 hours. The concentration-time curves of *m*-DNB and 3-NA in medium are shown in FIG 3-10. The decreasing levels of *m*-DNB and corresponding increase in 3-NA in the medium are presented in Table 3-6. These changes were quicker than those seen in astrocyte medium but they are not statistically significant.

The spontaneous loss of *m*-DNB culture dishes with a initial concentration of 100 μM was 4.3-8.3 % in the control cell-free medium. This loss presumably reflected evaporation, or movement in to the plastic dishes. No metabolites were detected in the cell-free control media. The control values of *m*-DNB at 24 hours were taken as 100 % to calculate the active loss due to metabolism.

Table 3-6. Biotransformation of *m*-DNB in cultured endothelia cells and astrocytes

Cell type	% of *m*-DNB loss	Loss rate of *m*-DNB ($nmol.g^{-1}.h^{-1}$)	Production rate of 3-NA ($nmol.g^{-1}.h^{-1}$)
Endothelia	46.5 ± 1.9[a]	875 ± 78	135 ± 11
Astrocyte	41.5 ± 0.5	837 ± 151	122 ± 22

a: values are presented as Mean ± SE.

One flask of neuroblastomal cells cultured with a initial concentration of 25 μM *m*-DNB showed a net *m*-DNB loss rate of 632.4 nmol/g/ h and a 3-NA production rate of 116.9 nmol/g/h during the first 24-hour culture. This clearly showed the metabolic ability of neuroblastomal cells for *m*-DNB.

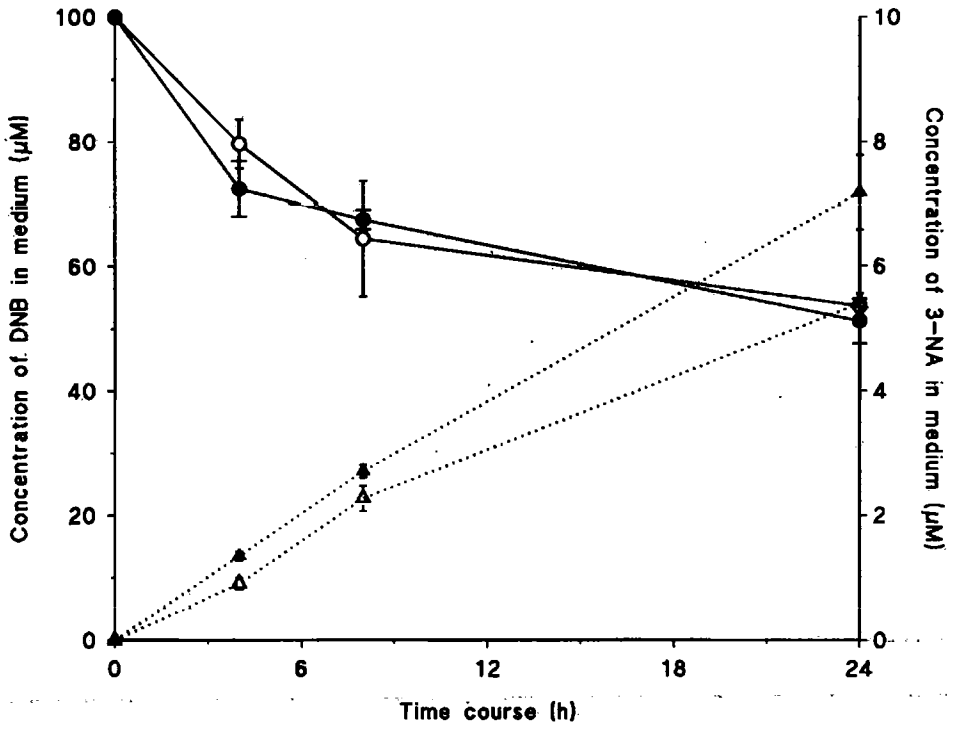

FIG 3-10. Concentration-time curves of *m*-DNB and 3-NA in the media of astrocytes and endothelial cells after exposing to an initial concentration of 100 μM *m*-DNB. The data are presented as mean ± SE, n = 4.

The levels of *m*-DNB and its metabolite 3-NA in cells are presented in FIG 3-11. Their levels in endothelial cells at all time points were similar. In astrocytes, the level of *m*-DNB at 24 hours was significantly higher than that at 4 or 8 hours after exposure ($p<0.01$).

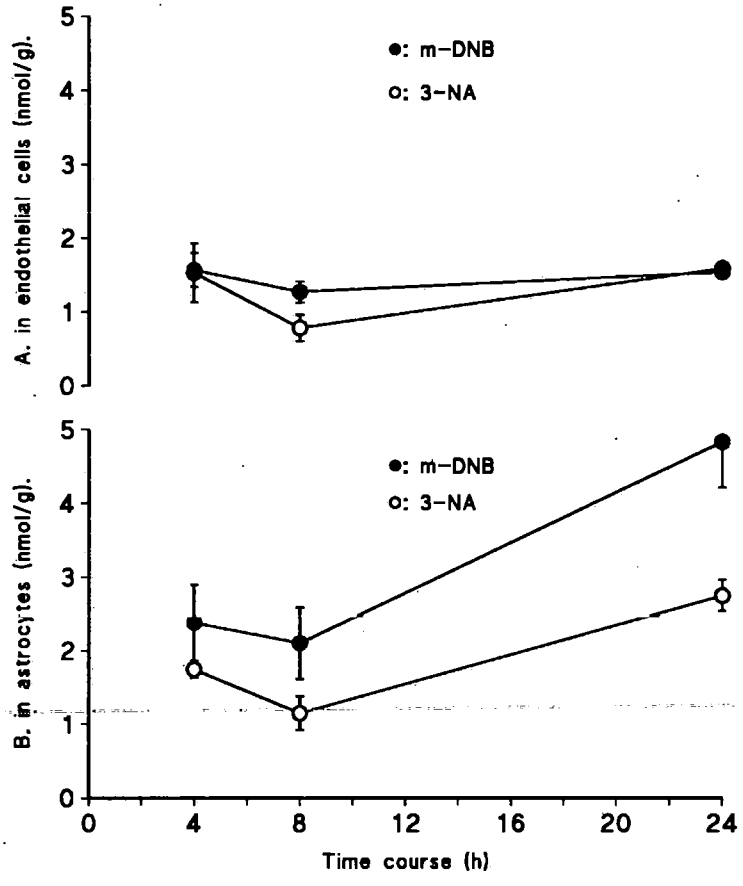

FIG 3-11. Concentration-time curves of *m*-DNB and 3-NA in astrocytes and endothelial cells after exposing to an initial concentration of 100 μM. *m*-DNB. The data are presented as mean ± SE, n = 4.

3.3.3.2 Stability of 3-NNB in brain extract

FIG 3-12 shows the HPLC profile of *m*-DNB and 3-NNB standards in methanol. It indicates that 3-NNB is stable in methanol.

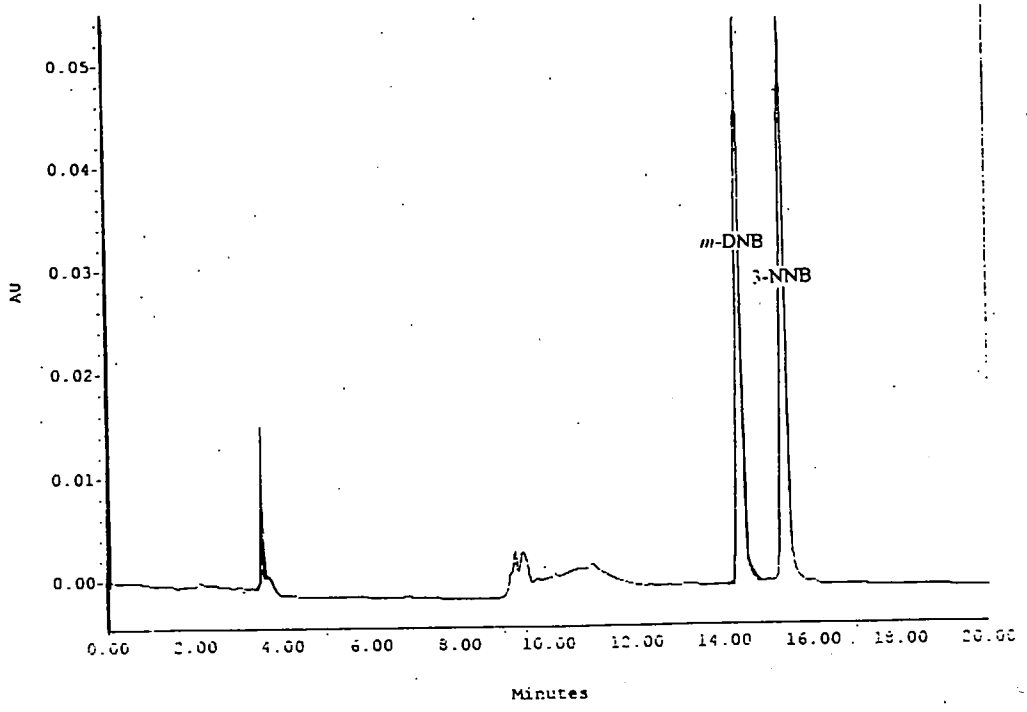

FIG 3-12. Chromatogram of m-DNB and 3-NNB in methanol.

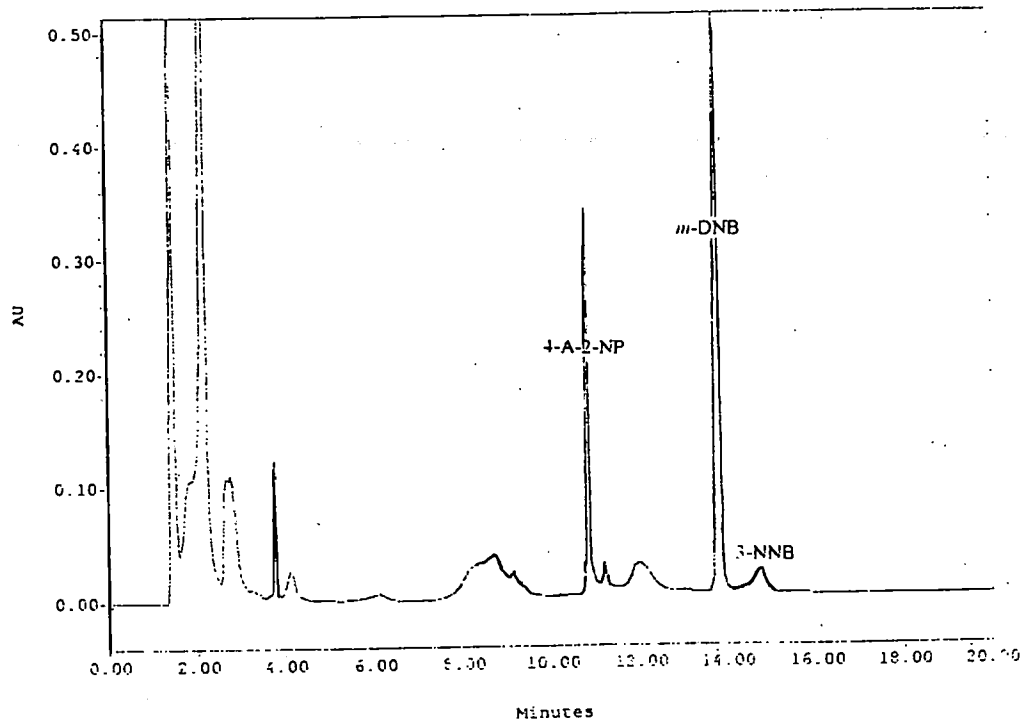

FIG 3-13. Chromatogram of *m*-DNB and 3-NNB in brain extract. *m*-DNB remains but 3-NNB degrades to 4-A-2-NP.

When *m*-DNB and 3-NNB were added to the extraction of fresh brain tissue, the peak of *m*-DNB remained unchanged but only a small peak of 3-NNB left and a new peak appeared at the retention time of 10.8 min, see FIG 3-13. This indicates that most 3-NNB has been degraded into a new metabolite.

When equal amount of *m*-DNB, 3-NNB and 4-amino-2-nitrophenol standards were spiked to brain extraction, again the peak of *m*-DNB was not changed but the peak of 3-NNB was nearly disappeared. However, the peak of 4-amino-2-nitrophenol was nearly doubled, see FIG 3-14. This means that the retention time of degraded product is identical to that of the authentic standard of 4-amino-2-nitrophenol. This HPLC profile highly suggests that the degraded product of 3-NNB is 4-amino-2-nitrophenol.

3-NNB was also spiked with the extraction of brain tissue from the rat dosed with 30 mg/kg. The chromatogram showed the same result as in the fresh tissue extraction. 3-NNB was quickly degraded and a new peak appeared at the retention time of 10.8 min as well. This suggests that the new peak is not a normally detectable metabolite of *m*-DNB *in vivo*.

However, when brain tissue was extracted with 5 % TCA solution and then it was spiked with 3-NNB, 3-NNB was not changed. This means 3-NNB is stable under the extraction conditions used to prepare brain tissue for HPLC using TCA.

Both 4-amino-2-nitrophenol and 2-amino-4-nitrophenol are metabolites of *m*-DNB, see FIG 3-1. Both standards were tested in the HPLC analytical system used in this study. Although they have similar chemical structure, their HPLC performance were different. 4-Amino-2-nitrophenol had a very sharp peak at the retention time 10.8 min, whereas 2-amino-4-nitrophenol had a broader flat peak

which was difficult to recognise. Therefore, spiked 3-NNB in brain extract was likely to be transformed to 4-amino-2-nitrophenol rather than 2-amino-4-nitrophenol.

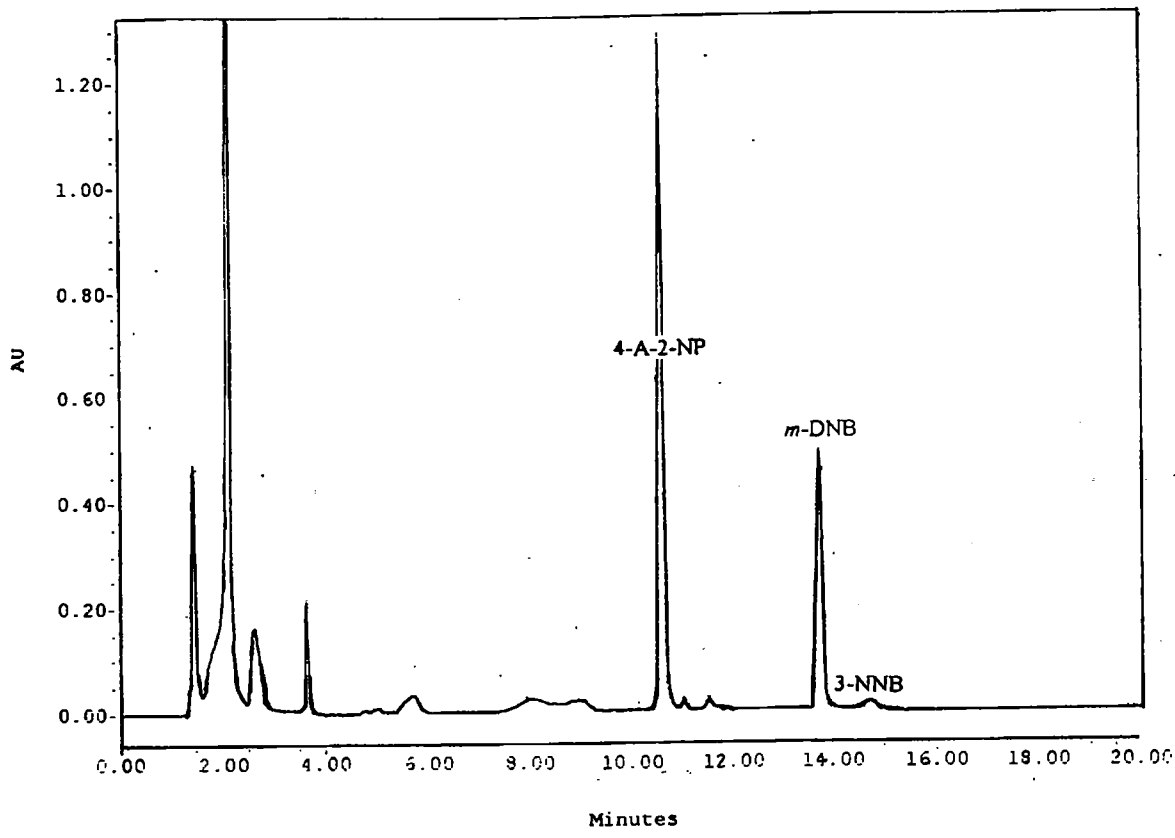

FIG 3-14. Chromatogram of *m*-DNB, 3-NNB and 4-amino-2-nitrophenol in brain extract. *m*-DNB remained but the peak of 3-NNB is greatly reduced and the peak of 4-amino-2-nitrophenol is doubled.

3.4 DISCUSSION

3.4.1 Pharmacokinetics of *m*-DNB in individual tissues

It has been reported that there are age and species differences in the whole body absorption and elimination of *m*-DNB (McEuen and Miller 1991; Brown, *et al.*, 1994). However, little is known about *m*-DNB distribution and elimination in individual tissues. This study investigated the absorption, distribution, metabolism and elimination of *m*-DNB in different target tissues of the rat. The result shows that after initial distribution, the peak level of *m*-DNB was higher in CNS than that in other tissues. *m*-DNB levels in the regions in brain stem were higher than that in other regions. In agreement with this, this distribution profile correlates well with regional lipid content of brain (Gospe, *et al.*, 1988). Brain stem is the target site of *m*-DNB-induced neurotoxicity (Philbert, *et al.*, 1987; Nolan, *et al.*, 1995). The gross distribution of *m*-DNB agrees with the histopathlogical lesions and might be responsible (at least in part) for the selective regional vulnerability to *m*-DNB neurotoxicity. The present study also shows that *m*-DNB in different tissues follows different elimination rates. The half life of *m*-DNB in blood is 2.9 hr which is in agreement with 3.0 hours obtained by McEuen and Miller (1991) and similar to 3.3 hours reported by Brown (1994) from 75-day-old group of Sprague-Dawley rats. This study shows that the half lives in different regions in the central nervous system of rats ranged from 2.9 to 3.1 hours, which were very similar to that in blood. However the half life in liver was significantly shorter than that in blood or other tissues. By contrast, in testis the half life was significantly longer than that in blood or other tissues. Hence *m*-DNB in liver and testis did not follow the same

kinetics as in blood. These indicate that pharmacokinetic behaviour of the compound varied from tissue to tissue, and that the pharmacokinetic data obtained from blood could not be extrapolated to individual tissues. The pharmacokinetic differences between tissues reflect the physiological and biochemical differences in *m*-DNB distribution and elimination, and may contribute to the differences in tissue susceptibility to *m*-DNB.

m-DNB is a lipophilic compound. The central nervous system (CNS) is rich in lipid. So *m*-DNB can be absorbed by CNS by simple diffusion and tends to accumulate in CNS. Whatever the mechanism of *m*-DNB toxicity might be, the level and duration of *m*-DNB in target tissues are primarily responsible for its toxic lesions. This has been shown in species or age differences in susceptibilities to *m*-DNB in testicular toxicity. Rats are more sensitive than hamster to *m*-DNB testicular toxicity. When the same dosage of 25 mg/kg *m*-DNB was given to both species, the blood peak concentration measured in hamster was only half of the rats' value (Obasaju, *et al.*, 1991). Old rats are more sensitive to *m*-DNB than younger rats (Linder, *et al.*, 1990). The age difference in *m*-DNB pharmacokinetics has been reported, the half life of *m*-DNB in Sprague-Dawley rats being 1.91 hours in 31-day-old group and 4.53 hours in 120-day-old group rats (Brown, *et al.*, 1994). Germ-free rats are more susceptible to *m*-DNB induced neurotoxicity than conventional ones. A single oral dose of 25 mg/kg *m*-DNB which did not produce neurotoxicity in conventional rats produced brain lesion in germ-free rats because germ-free rats have no microbial nitroreductase activity in gut to remove *m*-DNB prior to absorption (Philbert, *et al.*,1987). In addition, although a single dose of 30 mg/kg *m*-DNB can not produce neurotoxicity in conventional rats, when the same

dosage was split into several doses, it caused brain lesion (Philbert, *et al.*, 1987). Our infusion studies showed that when a total dose of 30 mg/kg *m*-DNB was infused within 6 hours, it did not produce brain lesions. However, when the same dosage was infused over from 12 to 144 hours, the brain histopathological damage was produced. This indicates that once a threshold of *m*-DNB is exceeded, time factor will play a more important role than a transiently high concentration in producing brain damage.

Compared with *m*-DNB-induced neurotoxicity, a single dose of 25 mg/kg *m*-DNB which can not produce brain damage can produce testicular damage in the conventional rat. This study showed that *m*-DNB has a significantly longer half life in testis than that in blood or CNS. Therefore, the pharmacokinetic differences may partly be responsible for the susceptibility of testis to *m*-DNB.

3.4.2 Infusion-lesion model of *m*-DNB

m-DNB is a multi-target toxicant. Repeated doses readily produced neurotoxicity (Philbert, *et al.*, 1987). This implied that pharmacokinetic factors play a role in *m*-DNB neurotoxicity. In infusion-lesion model, we studied the link between blood concentration and brain lesion. Theoretically, there must be a dose threshold in any chemical induced lesion. In our experiments, when a total dose of 30mg/kg *m*-DNB was infused within 6 days, the plasma concentration was 1.95 μM which caused brain damage. When the same dosage was infused within either 8 or 14 days, the plasma concentration were 1.5 and 0.8 μM respectively, which did not produce brain damage, see FIG 3-7. Therefore, the *m*-DNB concentration of 1.95 μ M was considered as the blood concentration threshold of brain lesion. However,

when the same total dose was infused within 6 hours, the plasma concentration reached as high as 34.7μM and the T_m was 18.8 hours which did not produce histopathological damage in brain either. But damage was observed when the same total dosage was infused within 12 hours or up to 6 days when the plasma concentration was from 21.9 μM to 1.95 μM and the T_m was 22.3 to 144 hours, see table 3-5. This clearly shows that a longer T_m has more neurotoxic potential than a instantaneously higher blood concentration for *m*-DNB neurotoxicity. Thus the time factor plays an important role in *m*-DNB neurotoxicity once a threshold is exceeded. This study also showed that infusion can cause *m*-DNB accumulation in brain because the tissue/plasma ratio in brain after infusion was significantly higher than that after a bolus dose. This may have been because a constant blood concentration provided a constant source of *m*-DNB for metabolic activation to nitrosonitrobenzene. This might explain why split doses or infusion more readily produced brain lesions than a bolus dose (Philbert, *et al.*, 1987; Nolan, *et al.*, 1995). This model may suggest that long-term exposing to a low level of *m*-DNB will increase the potential of neurotoxicity.

3.4.3 *In vivo* and *in vitro* metabolism of *m*-DNB

This study showed that 3-NA was the major metabolite of *m*-DNB phase I metabolism *in vivo* and in cultured cells. It was reported that 3-NA accounted for 74 % radioactivity of dosed *m*-DNB in rat urine (Cossum and Rickert, 1985; McEuen and Miller, 1991). However after oral administration of *m*-DNB to F-344 rats, 3-aminoacetanilide (3-AA) excretion accounted for 21% of dosed *m*-DNB (Nystrom and Rickert, 1987). But 3-AA was not detected in either rat or hamster after ip

administration (McEuen and Miller, 1991), nor after iv injection in the present study. This metabolic difference caused by different dosing routes suggests that *m*-DNB after oral administration could have been catalysed by the gastrointestinal tract microflora before absorption (Richert, 1987). This may explain why germ-free rats are more susceptible to *m*-DNB-induced neurotoxicity than conventional rats (Philbert, *et al.*, 1987).

The present study shows that 3-NA in liver was 17-fold higher than its parent compound, *m*-DNB and the half life of *m*-DNB in liver was significantly shorter than that in blood and other tissues, see table 3-2. These clearly indicate rapid transformation of *m*-DNB in liver. This is in agreement with Cossum and Rickert's findings that *m*-DNB is a P450-NADPH-reductase dependent substrate (Cossum and Rickert, 1985). Liver is rich in this enzyme system. Therefore it is easy to understand the rapid metabolism of *m*-DNB in liver. In addition, P450 enzyme system generally distributes in many extrahepatic tissues. Lung, kidney, gastrointestinal mucosa, brain and spinal cord all possess P450 isoenzymes (Caldwell, 1995; Anandatheerthavarada, *et al.*, 1993; Haglund, 1984). With *in vitro* studies, it has been demonstrated that besides liver, testis (Foster, 1987) and brain slices (Hu, *et al.*, 1995) all have the ability to transform *m*-DNB into 3-NA. This study shows that cultured endothelial cells, astrocytes, or neuroblastomal cells were all able to metabolise *m*-DNB into 3-NA, see FIG 3-8 and 3-9. This study also shows that the distribution of 3-NA in CNS is similar to its parent compound, *m*-DNB. The distribution feature of 3-NA might reflect the *in situ* metabolism of *m*-DNB. This suggests that the *in situ* metabolism of *m*-DNB may play a important role in its elimination from individual tissues, especially from CNS.

It is difficult to estimate the metabolic rate of a foreign compound in individual tissues *in vivo*. However, integrating the concentrations of parent compound and its elimination half life as well as the concentration of metabolite enable us to estimate the relative metabolic activity of each individual tissue. The lowest level and the shortest half life of *m*-DNB together with the highest 3-NA level in liver clearly indicate the rapid metabolism of *m*-DNB in liver. 3-NA in testis was also significantly higher than *m*-DNB. 3-AN is different from *m*-DNB in physiochemical properties. It is more water soluble than *m*-DNB. Testis contains more water and less lipids than liver and brain (Spector, 1956). Therefore the redistribution of 3-AN may partly contribute to the concentration of 3-NA in testis. On the other hand, the lowest level and the longest half life of *m*-DNB in testis indicate the slow metabolism of *m*-DNB in testis.

3.4.4 3-Nitrosonitrobenzene

3-Nitrosonitrobenzene is a common intermediate in the metabolism of either *p*- or *m*-DNB (Cossum and Rickert, 1985). It is normally difficult to detect *in vivo*. But when a high concentration of *p*- or *m*-DNB was co-cultured with microsomes, 4- or 3-NNB was detected at early incubation stage but not later (Cossum and Rickert, 1985). The present study found a similar metabolic phenomenon with *m*-DNB in the cultured endothelial cells or astrocytes. 3-NNB was present in endothelial cells or astrocytes at 4 hour incubation but not at 8 or 24 hour incubation, see FIG 3-9. 3-NNB could also be detected in brain slices incubated with *m*-DNB (Hu, *et al.*, 1995). This evidence demonstrated that 3-NNB must have been produced during the metabolism of *m*-DNB.

In order to study the stability of 3-NNB, 3-NNB was spiked with the methanol extraction of fresh brain tissue or the brain tissue dosed with *m*-DNB. To our surprise, 3-NNB was quickly degraded into 4-amino-2-nitrophenol in brain extraction. However, 3-NNB was stable in methanol. It was also stable in the extraction by 5 % TCA solution. This clearly suggested that there must be something in the extraction which can initiate the chemical reaction of 3-NNB and transforms it into 4-amino-2-nitrophenol. Further work has demonstrated that ascorbic acid can initiate above reaction in room temperature (personal communication from Hu, *et al.*, 1995). When equal molar ascorbic acid was added to the 3-NNB standard solution, 3-NNB was completely converted into 4-amino-2-nitrophenol. However, when glutathione (GSH) was added to the 3-NNB standard solution, 3-NNB was degraded into 3-NA. The evidence from this chemical reaction indicates that 3-NNB is normally difficult to detect in *in vivo* studies because ascorbic acid and GSH in normal tissues are sufficient to neutralise 3-NNB. On the other hand, if ascorbic acid is involved in the transformation of 3-NNB, 4-amino-2-nitrophenol should be detected in tissue extraction but, in fact, 4-amino-2-nitrophenol was not detected *in vivo*. Therefore ascorbic acid is unlikely to play an important role in neutralising 3-NNB. But GSH may be involved in the detoxification of 3-NNB. It has been demonstrated that depleting GSH in brain can increase the susceptibility of brain towards *m*-DNB (Hu, *et al.*, 1996). Therefore, normally, 3-NNB can be quickly removed by GSH or/and other mechanism once it is produced. When the detoxification system fails to remove 3-NNB in time, it will accumulate in cells and cause damage.

3.4.5 Metabolism of *m*-DNB and its neurotoxicity

m-DNB is converted into 3-nitroaniline (3-NA) through multiple steps, see FIG 3-1. It has been suggested that the process of conversion of an aromatic nitro group to an amine is likely to proceed through a number of reactive intermediates (Mason and Josephy, 1984). This study indicates that *m*-DNB is quickly converted to 3-NA in liver. *m*-DNB is a P450-NADPH-reductase dependent substrate (Cossum and Rickert, 1985). Brain microsomal P450 levels are approximately 2.5-4 % of the specific contents of the hepatic tissue (Warner, 1988). But mitochondrial P450 content in brain is significantly higher than the microsomal P450 content, in contrast to the liver (Walther, *et al.*, 1986; Bhagwar, *et al.*, 1995). Brain exhibits regional differences in the distribution of P450. Maximal P450 levels have been detected in olfactory lobes, cerebellum and brain stem (Anandatheerthavarada, *et al.*, 1993). On the other hand, the endogenous nucleophile, glutathione is relatively low in brain stem (Ravindranath, 1989). Therefore, the presence of high amounts of P450 in brain stem coupled with the low levels of glutathione may render the brain stem particularly vulnerable to damage through P450-mediated bioactivation of xenobiotics to reactive electrophilic metabolites (Ravindranath, 1995). This might explain the selective susceptibility of brain stem to *m*-DNB.

Cossum, *et al.*, (1987) showed that while a single ip dose of *m*-DNB caused testicular lesions, an equal molar dose of 3-NA had no effect when administered *in vivo* in conventional rats. But damage was produced by 3-NNB. *In vivo* and *in vitro* studies of the conjugated metabolite, 3-nitroacetanilide (3-NAA) also showed no testicular toxicity (Foster, *et al.*, 1987; McEuen and Miller, 1991). In rat testicular cell culture, it has been demonstrated that 3-NNB is more toxic than *m*-DNB itself

(Foster, *et al.*, 1987). This might suggest that metabolic activation may be the common mechanism in either testicular toxicity or neurotoxicity induced by *m*-DNB. Thus, the results obtained from the infusion-lesion model may be explained by the toxic effect of *m*-DNB not directly depending on *m*-DNB level in the target site but more directly depending on the level of its toxic intermediate. The level of the toxic intermediate depends on two factors, its production rate and removal rate. It may not be proportional to the level of *m*-DNB because of the metabolic saturation. In this case, a lower concentration with a longer exposure time can provide a constant source of activated intermediate and hence have more toxic potential than a higher concentration with a shorter exposure time. This might explain how dosing regimen modifies susceptibility of rats to *m*-DNB.

3.4.6 Summary

This study investigated the metabolic and pharmacokinetic behaviour of *m*-DNB in individual target tissues, and an infusion-lesion model of *m*-DNB-induced neurotoxicity.

1. *m*-DNB reached higher concentrations in the vulnerable regions in the brain stem than in other parts in the CNS. *m*-DNB in different tissues follows different pharmacokinetic process after systematic exposure to a single dose of *m*-DNB. The half lives in brain regions are similar to that in blood but different from those in testis or liver. This indicates that blood concentration of *m*-DNB is important in maintaining a certain level of it in brain.
2. *In vivo* and *in vitro* metabolism studies show that *m*-DNB was mainly transformed into 3-NA. The activated intermediate, 3-NNB, was detected in the

cultured astrocytes and endothelial cells. This indicates that 3-NNB must have been produced during *m*-DNB metabolism.

3. The infusion-lesion model has revealed that once a blood threshold of lesion is exceeded, the time over which *m*-DNB exceeds its threshold toxic level is crucial in producing brain lesion, but not a instantaneous higher concentration. This suggests that, up to a point, long-term exposure to a low level of *m*-DNB will increase the potential of neurotoxicity.

In conclusion, the metabolic and pharmacokinetic factors of *m*-DNB have a strong influence on its neurotoxicity. Absorbed *m*-DNB is metabolised in tissues before it is eliminated from body. This biotransformation is a important way for tissues to eliminate the lipophilic compound and, on the other hand, produces an activated intermediate, 3-NNB, which can cause cell damages if it is not cleared by cells. Glutathione can reduce 3-NNB to 3-nitroaniline and detoxify it. Brain stem contains relatively lower level of glutathione and higher level of P450 than some other regions in CNS and, therefore, is particularly vulnerable to damage through P450-mediated bioactivation of *m*-DNB. Long-term exposure to a certain low level of *m*-DNB is readily able to produce neurotoxicity. This may be due to the depletion of glutathione or other factors. Therefore the dosing regimen can significantly modify the pharmacokinetics of *m*-DNB and hence modify its neurotoxicity.

SECTION 4. GENERAL DISCUSSION

4.1 Introduction

Over 100 years ago, a German pathologist, Franz Nissl observed that particular agents consistently resulted in characteristic injury to neurons of defined areas of the brain. His studies stimulated later pathologists to propose the hypothesis that the cells in particular regions of the brain, by virtue of unique biochemical or anatomic features, are vulnerable to intoxication by certain classes of xenobiotics and not by others. This theory became known as *pathoclisis* (Vogt, *et al.*, 1922). The basis of pathoclisis is the tremendous regional heterogeneity in brain. Each region may have its distinct physiological and biochemical properties which, in turn, may have a distinct response towards neurotoxicants. This part of the thesis will discuss the aspects of metabolism and pharmacokinetics in the selective neurotoxicities induced by BPAU and *m*-DNB.

4.2 Distribution and neurotoxicity

Both BPAU and *m*-DNB can induce selective neurotoxicities in defined regions or parts in the nervous system. BPAU can produce delayed ataxia. The typical onset of BPAU induced delayed ataxia took place at day 7 or afterwards after dosing. The major pathological damages can be observed in spinal cord and peripheral nerves in rats after either a single higher dose or repeated lower doses of BPAU (Cavanagh, *et al.*, 1968; Fossom, *et al.*, 1985). *m*-DNB can cause brain stem damage in the rats after repeated lower doses or infusion (Philbert, *et al.*, 1987;

Nolanet, *et al.*, 1995). In common, both compounds reached higher levels at their target sites within the CNS.

The distribution patterns of xenobiotics mainly depends on their physiochemical properties and lipid content of individual tissues. Both BPAU and *m*-DNB are lipophilic compounds. The central nervous system (CNS) is rich in lipids. Therefore, lipophilic compounds readilly distribute to and accumulate in CNS. On the other hand, the CNS is far from a homogenous organ in lipid content as well as histological structure and physiological function. It has been demonstrated that the regional lipid content of brain correlates well with the regional distribution levels of toluene, a lipophilic neurotoxicant (Gospe, *et al.*, 1988). The regional distribution of *m*-DNB is similar to toluene. Thus all toxicants have their own physiological properties and distribution patterns and hence may produce distinct effects. Obviously, the distribution features of BPAU and *m* DNB at least partly play a role in their selective neurotoxicities.

4.3 Duration and neurotoxicity

Duration of a toxicant in target sites is another important factor in chemical-induced lesions. Dosing regimen, in fact, mainly modifies the duration of a toxicant in target sites. This study showed that a single dose of 30 mg/kg of *m*-DNB can not induce neurotoxicity (Nolan, *et al.*, 1995). However, if the same total dose is split into 4 smaller doses within 24 hours, brain damage is produced (Philbert, *et al.*, 1987). The half lives of *m*-DNB in different regions of CNS are similar to that in blood. This indicates that the elimination rate of *m*-DNB in brain parallel with that in blood. Therefore, blood concentration is important in maintaining a certain level

of *m*-DNB in brain and in producing neurotoxicity. This study has demonstrated, in the infusion-lesion model, that once a concentration threshold is exceeded, a certain minimum time threshold is also needed, it being easier to produce lesion by infusion than with á instant high blood concentration (see Fig. 3-7 and table 3-4&5, Section 3). In addition, this study has also shown that the distribution pattern of a single iv dose of 10 mg/kg *m*-DNB in different regions of brain was similar to that of an infusion but the tissue/plasma ratios in infusion were significantly higher in some regions than that in single dose, see FIG 3-6. This implies that the dosing regimen does not influence the distribution pattern of *m*-DNB within the brain, but infusion allows *m*-DNB to accumulate in brain in comparison with a single bolus dose and hence prolongs exposure time. This may partly explain why repeated doses or infusion of *m*-DNB is easier to produce lesion than a single dose (Philbert, *et al.*, 1987; Nolanet, *et al.*, 1995).

The similar phenomenon was also seen in BPAU-induced neuropathy. A single dose of either 100, 200 or 400 mg/kg BPAU produced different degrees of delayed ataxia within 1-2 week(s) after dosing (Diezel and Quadbeck, 1960; Canavagh, 1968; Fossom, 1985; Nagata, 1986). However, rats were given a daily dose of either 40 or 10 mg/kg BPAU for two or six months induced the similar clinical ataxia to that in single higher doses (Fossom, *et al.*, 1985). This obviously indicates that the repeated lower daily doses allow BPAU or its toxic effects to accumulate in target sites and prolong exposure time until a certain lesion threshold is exceeded and produce lesions. Therefore, a toxicant may have its own distinct distribution feature no matter how it is dosed but the dosing regimen can dramatically change the duration of a toxicant and hence can modify its toxicity.

On the other hand, the pharmacokinetics of a toxicant in different tissues varies. This may greatly modify the susceptibility of individual tissues to the toxicant. The present study has shown that, after initial distribution, the half lives of BPAU in brain and spinal cord are longer than that in blood, muscle or liver (see table 2-1, Section 2). *m*-DNB is a multi-target toxicant. Testis is more susceptible than other tissues. A single dose of 25 mg/kg *m*-DNB is high enough to produce testicular toxicity (Linder, *et al.*, 1990). In agreement with this, the half life of *m*-DNB in testis was longer than in other tissues (see table 3-2, Section 3). Thus the pharmacokinetic behavior of a toxicant in individual tissues, in fact, is a matter of its duration in these tissues and hence modifies their susceptibility to the toxicant.

In addition, some factors such as age and metabolic inhibitors can modify the elimination of a toxicant and, therefore, modify the toxicity of the toxicant. The present study has demonstrated that the elimination of BPAU from spinal cord in 1-year old rats, which are more susceptible to BPAU neurotoxicity than young ones (Chen and Cavanagh, 1971), was slower than 6-week old rats (see 2.3.5.2, Section 2). PMSF interfered with BPAU metabolism and prolonged BPAU half lives in target sites and hence intensified BPAU-induced delayed ataxia (see 2.3.4, Section 2).

In brief, the persistence, or maintaining time of a certain level, of a toxicant in target sites is an important factor in the susceptibility of individual tissues to toxicants. Dosing regimen, the physiological and biochemical properties of individual tissues and some factors can influence the duration of neurotoxicants and hence modify their neurotoxicities.

Another example of time-dependent neurotoxicity is provided by organophosphates. A distinctive feature of the toxicology of organophosphorus agents is that, because of the covalent nature of the enzyme-organophosphate reaction and of the covalent nature of the ageing reaction, the extent of their biological effects is dependent on product of both concentration and time (Johnson, 1992). This is contrast to the reversible equilibrium reactions commonly seen in pharmacology, which eventually come to a time-independent steady state. Thus with organophosphorus agents high concentration, short time effects and low concentration, long time effects can be equivalent. This gives a special significance to the rate of biological disposal of organophosphates, which can not only limit the duration, but also the severity of effects.

Several mechanisms may be involved in the toxic damage due to the persistence of a toxicant in target sites. We assume that any cells have their own tolerant limits or thresholds to a particular toxicant. Long-term exposing to a certain level of a toxicant will allow no time for cells to recovery and surpass the tolerant limits of cells due to the depletion of endogenous detoxicants, such as glutathione depletion which may result in free radical mediated damage (Halliwell, 1989, 1992), and prolonged specific enzyme inhibition which will disturb normal functions of cells. Therefore, persistence of a neurotoxicant in target sites is an important aspect in producing neurotoxicity.

4.4 Metabolism and neurotoxicity

Metabolism is the process whereby body actively acts on xenobiotics. Non polar, highly lipophilic compounds may be retained for longer periods in tissue

lipids since these are relatively low in xenobiotic metabolic capacity (Caldwell, *et al.*, 1995). Most of these compounds may undergo enzymatic metabolism which may introduce or uncover a functional group suitable for subsequent conjugation or for excretion. However, the introduced functional group may greatly change both the physicochemical properties and biological effect of a toxicant. As a result, its toxicity may be reduced or increased. The increase of biological effect after metabolism is also called metabolic activation (Caldwell, *et al.*, 1995).

Metabolic activation is believed to play an important role in *m*-DNB-induced testicular toxicity (Nystrom and Richert, 1987). By *in vitro* study of testicular toxicity, it has been demonstrated that 3-NNB, a intermediate of *m*-DNB, is more toxic than *m*-DNB itself (Foster, *et al.*, 1987). The metabolites of *m*-DNB, 3-NA and 3-NAA did not induce testicular lesions (Foster et al, 1987; McEuen and Miller, 1991). 3-NNB is a important step of *m*-DNB metabolism and it is transformed into 3-NA (see FIG 3-1, Section 3). Therefore the present of 3-NA indicates that 3-NNB must have been produced during *m*-DNB metabolism. Chemically, 3-NNB is a reactive intermediate. Our *in vivo* and *in vitro* studies have demonstrate that brain tissue can actively metabolize *m*-DNB (see Section 3). Therefore *m*-DNB induced neurotoxicity is believed to be caused by its activated intermediate(s). This may explain why a lower blood concentration of *m*-DNB maintained a longer time is more neurotoxic than a more transient higher concentration (see Fig. 3-7). This phenomenon may indicate that *m*-DNB-induced neurotoxicity is not directly caused by *m*-DNB itself, but its activated intermediate. A higher level of *m*-DNB may not increase the product of such an intermediate if there is a metabolic saturation. However, a certain level of *m*-DNB maintained over a longer time could allow the

activated intermediate or its lesion to accumulate in cells, and hence produce neurotoxicity.

m-DNB is a P450-NADPH-reductase dependent substrate (Cossum and Rickert, 1985). P450 levels in olfactory lobes, cerebellum and brain stem are higher than in other regions (Anandatheerthavarada, *et al.*, 1993). *In vitro* study has shown that glutathione can directly degrade 3-NNB into 3-NA. Artificially depleting glutathione in brain stem increased regional susceptibility to *m*-DNB (personal communication with Hu, 1996). This indicates that glutathione may play an important role in protecting brain from m-DNB-induced damage. The presence of high amounts of P450 and relatively low levels of glutathione in the brain stem (Ravindranath, *et al.*, 1989), may render the brain stem particularly vulnerable to the damage through P450-mediated bioactivation of *m*-DNB. In the present study, the activated intermediate of *m*-DNB, 3-NNB was detected by *in vitro* study (see 3.3.3.1, Section 3). Therefore, metabolic activation is likely to involve in *m*-DNB-induced neurotoxic damage.

Metabolism also plays a role in BPAU-induced neurotoxicity. The current study has primarily demonstrated that BPAU is metabolised to M1, M2 and M3 *in vivo* (see Fig. 2-15, Section 2). Although there is no, so far, direct data to show the toxicity of M1, the following three points may suggest that the M1 pathway may increase BPAU neurotoxicity whereas M2 pathway plays a important role in BPAU detoxification. The first evidence is that pharmacokinetically, M1 reached a high levels in tissues and stayed in tissues much longer than its parent compound, BPAU (see Section 2), whereas M2 reached very high concentration in serum but very low levels in tissues. These two metabolites are formed via different pathways and can

be excreted through urine. The distribution pattern of these two metabolites clearly suggested their different biological importance. The second evidence was from the promotion study of BPAU neuropathy by PMSF. PMSF which can significantly intensify BPAU-induced delayed ataxia interferes with BPAU metabolism. It increased BPAU and M1 levels in tissues and decreased M2 concentration in serum. PMSF inhibited the M2 pathway and increased M1 production and parent accumulation and hence increased BPAU neurotoxicity (see Section2). The third evidence was obtained from the comparison study of age-dependent metabolism of BPAU. It was reported that adult rats are more susceptible to BPAU than young ones (Chen and Cavanagh, 1971). This study has demonstrated that adult rats produce more M1 and retain more parent but less M2 than young rats (see Section 2). Therefore, BPAU metabolism plays an important role in its delayed neurotoxicity either by influencing the concentration of parent BPAU in tissues, or possibly by generating a toxic metabolite.

In conclusion, this study clearly shows that BPAU and *m*-DNB undergo metabolism before they are excreted. Their neurotoxicities closely related to their metabolism. This may suggest a common process for the neurotoxicities induced by some lipophilic neurotoxicants.

4.5 Metabolic interaction and neurotoxic synergism

Co-exposure to two or more compounds can produce a more severe neurotoxicity than exposure to these individual compounds. The most rescent disastrous incidence in man which may be related to such effect is the Gulf-War syndrome which claimed approximately 30,000 victims out of three quarter of a

million troops (Aboudonia, *et al.*, 1996). It has now been demonstrated in hens that co-exposure to just sub-toxic levels of a anti-nerve agent (pyridostigmine bromide), the insect repellent DEET, and the insecticide permethrin produced more severe neurotoxicity than exposure to these individual agents (Aboudonia, *et al.*, 1996). It is possible that exposure to multiple agents was responsible for Gulf-war syndrome (Aboudonia, *et al.*, 1996) although it is far from clear if the levels of exposure encountered by troops would have been high enough to allow the pharmacokinetic saturation effects seen in the hen studies. Another phenomenon which has puzzled neurotoxicologists for the last decade is the 'promotion'. This term was originally used to describe the phenomenon that organophosphorous compound induced delayed neuropathy (OPIDN) can be promoted (or enhanced) by some non-neurotoxicants (Lotti, *et al.*, 1991; Veronesi and Padilla, 1985; Pope and Padilla, 1990; Lotti, *et al.*, 1991). Phenylmethanesulfonyl fluoride (PMSF) is a commonly used potentiator. The mechanism of OPIDN is believed to relate to irreversible inhibition and subsequent aging of NTE. Similarly to OPs, PMSF can also inhibit NTE, but itself does not induce delayed neuropathy. When PMSF was given before OP administration, it could protect animals from OPIDN. This protective effect of PMSF was thought to be due to a reversible pre-occupation of NTE to prevent it from subsequently binding irreversible NTE inhibitor. However, when it was given after OPs, it could enhance OPIDN. Interestingly, *p*-bromophenylacetylurea (BPAU) can not inhibit NTE (Johnson, 1969) but can induce clinically delayed ataxia in rats closely similar to OPIDN in chicken (Cavanagh, *et al.*, 1968). BPAU-induced delayed neuropathy can also be intensified by PMSF (Johnson and Ray, 1992; Xu, *et al.*, 1993). This suggests that PMSF can also act on a site other than

NTE to promote either OPIDN (Fioroni, *et al.*, 1995) or BPAU-induced delayed neuropathy. The promotion site is still unknown in the case of OPIDN.

The current study has shown that, in the case of BPAU, the promotion of delayed neuropathy by PMSF is due to the metabolic interaction between the two compounds (see Fig. 2-24). PMSF can inhibit the M2 pathway, which plays an important role in BPAU detoxification, leading to parent accumulation and increased M1 production (which might be a toxic metabolite) and hence intensified BPAU neurotoxicity. PMSF is well known as a protease inhibitor. This study clearly indicates that PMSF may also inhibit enzymes which are involved in xenobiotic metabolism.

In short, neurotoxic synergy is a particular phenomenon seen when animals or humans are simultaneously co-exposed to two or more chemicals. Previous studies have not established a understandable explanation for its mechanism. This study demonstrated a distinct model of metabolic interaction and promotion of neuropathy. It may have general importance in understanding the promotion phenomenon of neurotoxicities.

4.6 Summary

Metabolic and pharmacokinetic factors in the neurotoxicities of BPAU and *m*-DNB were investigated. The approach in this study is different from conventional studies focusing strictly on the site of action. It focuses instead on the pharmacokinetic behaviour of the neurotoxicants, BPAU and *m*-DNB, and metabolic factors in their neurotoxicities.

1. The distribution of the two neurotoxicants is a relatively passive process which depends on their physicochemical properties and the biochemical and physiological institutions of individual target sites. In common, both BPAU and *m*-DNB are lipophilic compounds and they reached higher concentrations in target sites in the CNS. In contrast, the metabolic processes of the two neurotoxicants in body are active process. These processes may play a crucial role for some neurotoxicants to produce toxic damage. Both BPAU and *m*-DNB are metabolised in tissues before they are excreted. Their metabolism closely relates to their neurotoxicities.
2. The identification and characterization of BPAU metabolites, M1, M2 and M3, represent the significant progress in this study. Two major metabolic pathways have been proposed: M1⇐ BPAU ⇒M2. M3 may be formed either directly from BPAU or via M1. PMSF increased M1 and decreased M2, with a net reduction in BPAU disposal, and hence intensified BPAU-induced delayed neuropathy. On this basis, the metabolic interaction between BPAU and PMSF was clarified and an understandable mechanism of the promotion of BPAU-induced delayed neuropathy by PMSF was established. It may have general importance in understanding neurotoxic synergism between two or more toxicants. The study of BPAU metabolism in the rats of different ages showed that 1-year old rats produced more M1 and less M2 than 6-week old rats. This also provided a mechanistic understanding in age-dependent susceptibility to BPAU.
3. *In vivo* and *in vitro* studies have demonstrated that *m*-DNB can be metabolised in brain. The major metabolite is 3-NA. The activated intermediate 3-NNB was detected in cell culture. This suggests that 3-NNB must have been produced

during *m*-DNB metabolism and may play an important role in *m*-DNB-induced neurotoxicity. The infusion-lesion model has revealed that once a threshold of *m*-DNB is exceeded, the time during which *m*-DNB is maintained above the threshold is an important factor in producing brain lesion, rather than a higher instantaneous blood concentration. This model may explain why repeated doses or infusion more readily induce neurotoxicity and suggests long-term exposure to a lower level of *m*-DNB will increase the potential of neurotoxicity.

In conclusion, pharmacokinetic factors play important roles in inducing and modifying the neurotoxicities induced by either BPAU and *m*-DNB. It suggests that metabolism and pharmacokinetic approaches have a great potential in understanding the mechanism of the neurotoxicities induced by neurotoxicants.

4.7 Possible future studies

4.7.1 BPAU enzymatic metabolism

As indicated in Section 2, BPAU was metabolized *in vivo* into M1, M2 and M3. PMSF can inhibit the M2 pathway and increase the M1 pathway and hence exaggerate BPAU neurotoxicity. Furthermore, old rats which are susceptible to BPAU neurotoxicity produced more M1 and less M2 than younger ones. It would be interesting to know what enzymes are involved in the two metabolic pathways and what are their biological importance in the detoxification of toxicants. It may have general importance in studying the potential intoxication or detoxification of drugs or other xenobiotics.

4.7.2 The biochemical mechanism of brain cells tolerating *m*-DNB-induced neurotoxicity

The current study has revealed that brain damage induced by *m*-DNB depends on not only its concentration but also the time during which a certain concentration is maintained. In other words, there exist two factors, concentration threshold and time threshold, in *m*-DNB-induced neurotoxicity. Conventional studies pay much attention to dosage which relates to the concentration in target sites but little attention to the time threshold which may represent the critical factor for target cells. The tolerance limit varies from tissue to tissue and from species to species of animals. The question is what mechanism lies behind the toleration or susceptibility of individual tissues to *m*-DNB. The regional distribution of some enzyme systems, the cellular specificity of the toxicant, and the biochemical mechanism of detoxification in target cells are far from clear. These factors are important in understanding the interaction between target cells and *m*-DNB, or related compounds. Therefore some further work is needed on these areas to clarify the response, toleration and recovery or degeneration of target cells after *m*-DNB exposure.

APPENDIX: CALCULATIONS OF PHARMACOKINETIC PARAMETERS

A-I. BPAU

A-I-A. A illustration of the model analysis and exponential regressions of BPAU pharmacokinetics.

Following a single ip dose of 150 mg/kg BPAU, the absorption and elimination processes of BPAU showed the first order kinetics in both serum and individual tissues. Therefore, the pharmacokinetic data of BPAU from serum is taken as a example here to show its model analysis. FIG A-1 illustrates the semi-logrithmic versus concentration-time curve of BPAU in serum. The data is best fitted with an one-compartment model.

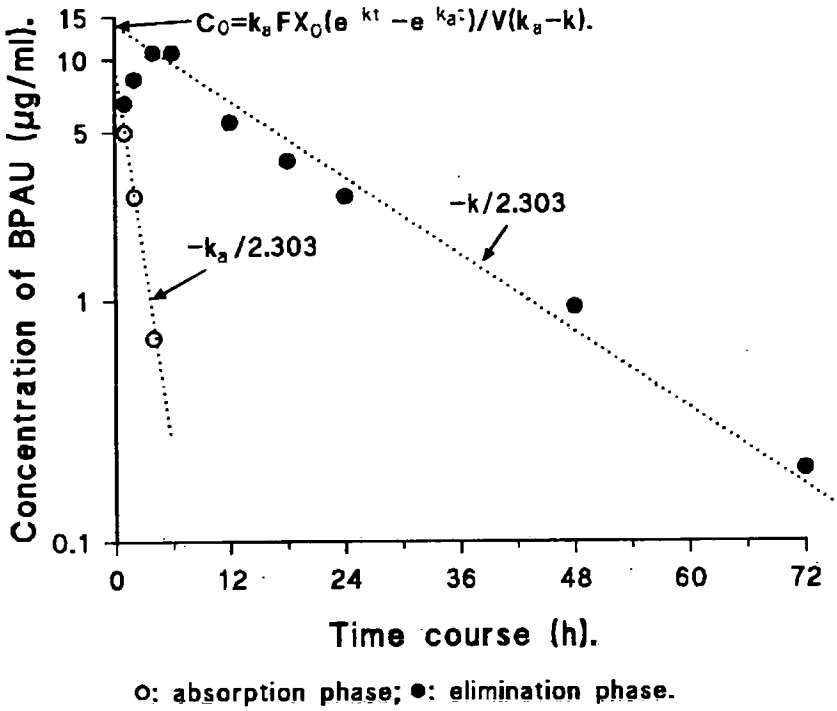

FIG A-1. A illustration of non-linear fitting and model analysis of BPAU pharmacokinetics — data from serum after a single ip dose.

The exponential regressions of BPAU pharmacokinetic data and calculations of elimination rate constants were carried out on a computer using the statistical software

MINITAB 10. The rate constants and half lives were calculated according to the equations given by Gibaldi & Perrier (1982) and the standard error of rate constant in each tissue was obtained using the method given by Mead & Curnow (1987). The exponential regression of the absorption phase was done using the residual method given by Gibaldi & Perrier (1982).

A-I-B. Calculations of the pharmacokinetic parameters of BPAU in serum and individual tissues after a single ip dose

A-I-B-a. Serum

1. Correlation and regression of pharmacokinetic data:

$r = -0.967$; $r^2 = 0.935$. $p<0.001$.

$A = C_0 = 11.39$ (μg/ml)

$B = -0.0255$

$k = 2.303 \times 0.0255 = 0.0587$

where r is the correlation coefficient, A is the concentration when time t=0, B is the slope, and k is the elimination rate constant.

2. Analysis of variation of BPAU exponential regression:

The results of variation analysis are shown in Table A-1.

Table A-1. Analysis of variation of BPAU exponential regression in serum.

Source	DF	SS	MS	F	P
Regression	1	3.447	3.447	14.0	0.001
Error	22	5.406	0.246*		
Total	23	8.853			

*: S_{tc}.

3. Standard error of slope:

$SE_{(k)} = \sqrt{(S_{tc} / S_{tt})} = \sqrt{(0.246/12672)} = 0.0044$

where $SE_{(k)}$ is the standard error of slope; S_{tc} is the mean of the error of square variance (see Table A-1: *); S_{tt} is the sum of squares of time.

$$k_{se} = 2.303 SE_{(k)} = 2.303 \times 0.0044 = 0.0101$$

where k_{se} is the standard error of rate constant.

4. Half life

$$t_{1/2} = 0.693/k \pm [0.693/k - 0.693/(k+k_{se})]$$

$$= 0.693/0.0587 \pm [0.693/0.0587 - 0.693/(0.0587+0.0101)]$$

$$= 11.8 \pm 1.7 \text{ (h)}$$

A-I-B-b. Brain

1. Correlation and regression of pharmacokinetic data:

$r = -0.939$; $r^2 = 0.882$. $p<0.001$.

$A = C_0 = 28.3$ (μg/g)

$B = -0.0194$

$k = 2.303 \times 0.0194 = 0.0447$

2. Analysis of variation of BPAU exponential regression:

The results of variation analysis are show in Table A-2.

Table A-2. Analysis of variation of BPAU exponential regression in brain.

Source	DF	SS	MS	F	P
Regression	1	4.774	4.774	163.5	0.000
Error	22	0.6425	0.029*		
Total	23	5.416			

*: S_{tc}.

3. Standard error of slope:

$$SE_{(k)} = \sqrt{(S_{tc} / S_{tt})} = \sqrt{(0.029/12672)} = 0.0015$$

$k_{se} = 2.303SE_{(k)} = 2.303 \times 0.0015 = 0.0035$

4. Half life

$t_{1/2} = 0.693/k \pm [0.693/k - 0.693/(k+k_{se})]$

$= 0.693/0.0447 \pm [0.693/0.0447 - 0.693/(0.0447+0.0035)]$

$= 15.5 \pm 1.1$ (h)

A-I-B-c. Spinal cord

1. Correlation and regression of pharmacokinetic data:

$r = -0.917$; $r^2 = 0.841$. $p<0.001$.

$A = C_0 = 44.3$ (μg/g)

$B = -0.0193$

$k = 2.303 \times 0.0193 = 0.0444$

2. Analysis of variation of BPAU exponential regression:

The results of variation analysis are shown in Table A-3.

Table A-3. Analysis of variation of BPAU exponential regression in spinal cord

Source	DF	SS	MS	F	P
Regression	1	4.696	4.696	116.9	0.000
Error	22	0.8834	0.040*		
Total	23	5.579			

*: S_{tc}.

3. Standard error of slope:

$SE_{(k)} = \sqrt{(S_{tc} / S_{tt})} = \sqrt{(0.040/12672)} = 0.0018$

$k_{se} = 2.303SE_{(k)} = 2.303 \times 0.0018 = 0.0041$

4. Half life

$t_{1/2} = 0.693/k \pm [0.693/k - 0.693/(k+k_{se})]$

$= 0.693/0.0444 \pm [0.693/0.0444 - 0.693/(0.0444+0.0041)]$

$= 15.6 \pm 1.3$ (h)

A-I-B-d. Liver

1. Correlation and regression of pharmacokinetic data:

$r = -0.887$; $r^2 = 0.787$. $p<0.001$.

$A = C_0 = 42.7$ (μg/g)

$B = -0.0269$

$k = 2.303 \times 0.0269 = 0.062$

2. Analysis of variation of BPAU exponential regression:

The results of variation analysis are shown in Table A-4.

Table A-4. Analysis of variation of BPAU exponential regression in liver.

Source	DF	SS	MS	F	P
Regression	1	8.386	8.386	136.6	0.000
Error	22	1.351	0.061*		
Total	23	9.737			

*: S_{tc}.

3. Standard error of slope:

$SE_{(k)} = \sqrt{(S_{tc} / S_{tt})} = \sqrt{(0.061/12672)} = 0.0022$

$k_{se} = 2.303 SE_{(k)} = 2.303 \times 0.0022 = 0.0051$

4. Half life

$t_{1/2} = 0.693/k \pm [0.693/k - 0.693/(k+k_{se})]$

$= 0.693/0.062 \pm [0.693/0.062 - 0.693/(0.062+0.0051)]$

$= 11.2 \pm 1.1$ (h)

A-I-B-e. Muscle

1. Correlation and regression of pharmacokinetic data:

$r = -0.976$; $r^2 = 0.953$. $p<0.001$.

$A = C_0 = 17.6$ (μg/g)

$B = -0.0259$

$k = 2.303 \times 0.0259 = 0.0597$

2. Analysis of variation of BPAU exponential regression:

The results of variation analysis are shown in Table A-5.

Table A-5. Analysis of variation of BPAU exponential regression in muscle.

Source	DF	SS	MS	F	P
Regression	1	6.923	6.923	42.2	0.000
Error	22	3.608	0.164*		
Total	23	10.531			

*: S_{tc}.

3. Standard error of slope:

$SE_{(k)} = \sqrt{(S_{tc} / S_{tt})} = \sqrt{(0.164/12672)} = 0.0036$

$k_{se} = 2.303 SE_{(k)} = 2.303 \times 0.0036 = 0.0082$

4. Half life

$t_{1/2} = 0.693/k \pm [0.693/k - 0.693/(k+k_{se})]$

$= 0.693/0.0597 \pm [0.693/0.0597 - 0.693/(0.0597+0.0082)]$

$= 11.6 \pm 1.4$ (h)

A-I-B-f. BPAU only, in whole blood after a single oral dose

1. Correlation and regression of pharmacokinetic data:

$r = -0.8725$; $r^2 = 0.761$. $p<0.001$.

$A = C_0 = 14.8$ (μg/ml)

$B = -0.032$

$k = 2.303 \times 0.032 = 0.074$

2. Analysis of variation of BPAU exponential regression:

The results of variation analysis are shown in Table A-6.

Table A-6. Analysis of the variation of exponential regression in blood—BPAU+PMSF

Source	DF	SS	MS	F	P
Regression	1	0.858	0.858	41.46	0.000
Error	13	0.269	0.021*		
Total	14	1.128			

*: S_{tc}.

3. Standard error of slope:

$$SE_{(k)} = \sqrt{(S_{tc}/S_{tt})} = \sqrt{(0.021/3888)} = 0.0023$$

$$k_{se} = 2.303 SE_{(k)} = 2.303 \times 0.0023 = 0.0054$$

4. Half life

$$t_{1/2} = 0.693/k \pm [0.693/k - 0.693/(k+k_{se})]$$

$$= 0.693/0.074 \pm [0.693/0.074 - 0.693/(0.074+0.0054)]$$

$$= 9.4 \pm 0.7 \text{ (h)}$$

A-I-B-g. BPAU + PMSF, in whole blood after a single oral dose

1. Correlation and regression of pharmacokinetic data:

$r = -0.8892$; $r^2 = 0.7906$. $p<0.001$.

$A = C_0 = 11.2$ (μg/ml)

$B = -0.0147$

$k = 2.303 \times 0.0147 = 0.034$

2. Analysis of variation of BPAU exponential regression:

The results of variation analysis are shown in Table A-7.

Table A-7. Analysis of the variation of exponential regression in blood—BPAU only.

Source	DF	SS	MS	F	P
Regression	1	0.809	0.089	29.51	0.000
Error	16	0.438	0.027*		
Total	17	1.247			

*: S_{tc}.

3. Standard error of slope:

$SE_{(k)} = \sqrt{(S_{tc} / S_{tt})} = \sqrt{(0.027/3888)} = 0.0026$

$k_{se} = 2.303 SE_{(k)} = 2.303 \times 0.0026 = 0.006$

4. Half life

$t_{1/2} = 0.693/k \pm [0.693/k - 0.693/(k+k_{se})]$

$= 0.693/0.0339 \pm [0.693/0.0339 - 0.693/(0.0339+0.006)]$

$= 20.4 \pm 3.1$ (h)

A-I-C. Area under concentration-time curve (AUC) of BPAU

In tissues, the pharmacokinetic characteristics of BPAU are similar to that in blood after ip or po dose. There is an absorption phase which allows the xenobiotic to enter

tissues from blood. Therefore, the estimation of AUC in tissues is different from that in blood after iv dose. The estimation of AUC in each tissue is calculated using the trapezoidal rule (Martin, 1986). The trapezoidal rule is illustrated in FIG A-2, here the data from serum is plotted and taken as a example.

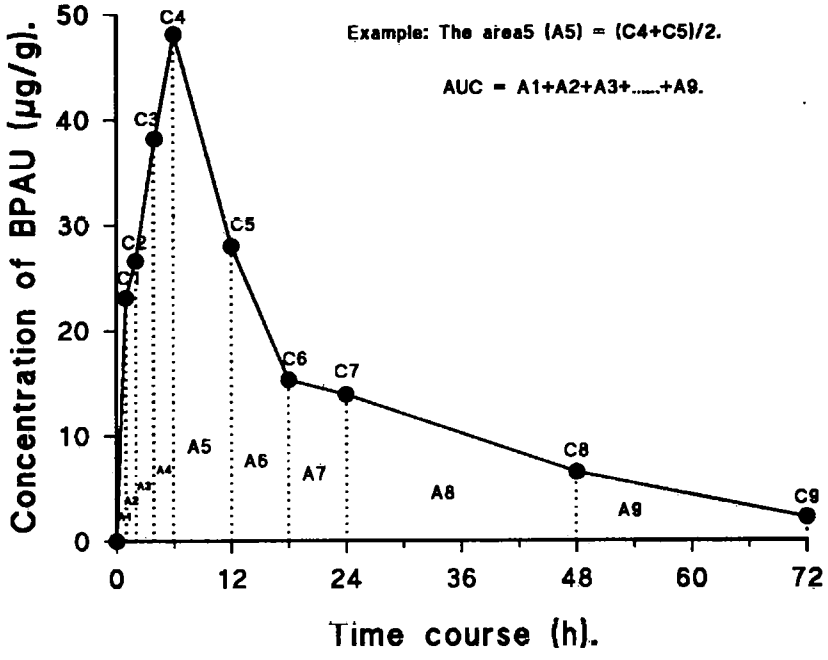

FIG A-2. A illustration of AUC calculation of BPAU in individual tissues using trapezoidal rule — data from spinal cord after a single ip dose.

A-I-C-a. Serum, ip dose

$$AUC = (0+6.6)/2 + (6.6+8.3)/2 + 2(8.3+10.7)/2 + 2(10.7+10.7)/2 + 6(10.7+5.5)/2 + 6(5.5+3.8)/2 + 6(3.8+2.7)/2 + 24(2.7+0.94)/2 + 24(0.94+0.2)/2$$

$$= 204.5\ (\mu g.\ ml^{-1}.\ h^{-1})$$

A-I-C-b. Brain, ip dose

AUC = (0+16.7)/2 + (16.7+17.5)/2 + 2(17.5+24.1)/2 + 2(24.1+30.2)/2 + 6(30.2+18.1)/2

+ 6(18.1+9.8)/2 + 6(9.8+8.7)/2 + 24(8.7+5.0)/2 + 24(5.0+1.1)/2

= 643.1 ($\mu g. g^{-1}. h^{-1}$)

A-I-C-c. Spinal cord, ip dose

AUC = (0+23.1)/2 + (23.1+26.6)/2 + 2(26.6+38.2)/2 + (38.2+48.1)/2 + 6(48.1+28.0)/2 +

6(28.0+15.3)/2 + 6(15.3+13.9)/2 + 24(13.9+ 6.5)/2 + 24(6.5+2.2)/2

= 982.5 ($\mu g. g^{-1}. h^{-1}$)

A-I-C-d. Liver, ip dose

AUC = (0+24.1)/2 + (24.1+29.1)/2 + 2(29.1+38.0)/2 + 2(38.0+ 38.4)/2 + 6(38.4+22.1)/2

+ 6(22.1+13.6)/2 + 6(13.6+10.4)/2 + 24(10.4+3.9)/2 + 24(3.9+0.7)/2

= 769.6 ($\mu g. g^{-1}. h^{-1}$)

A-I-C-e. Muscle, ip dose

AUC = (0+8.5)/2 + (8.5+9.8)/2 + 2(9.8+10.3)/2 + 2(10.3+12.5)/2 + 6(12.5+11.2)/2 +

6(11.2+5.1)/2 + 6(5.1+4.3)/2 + 24(4.3+1.5)/2 + 24(1.5+0.2)/2

= 294.5 ($\mu g. g^{-1}. h^{-1}$)

A-I-C-f. BPAU alone, in whole blood — oral dose

AUC = 6(0+9.48)/2 + 6(9.48+6.48)/2 + 6(6.48+2.66)/2

= 103.7 ($\mu g. ml^{-1}. h^{-1}$)

A-I-C-g. BPAU + PMSF, in whole blood — oral dose

AUC = 6(0+9.64)/2 + 6(9.64+8.96)/2 + 6(8.96+4.58)/2 + 24(4.58 + 1.84)/2

= 202.4 ($\mu g. ml^{-1}. h^{-1}$)

A-II. *m*-DNB

A-II-A. Model determination of *m*-DNB pharmacokinetics

Following a single ip dose of 10 mg/kg *m*-DNB, the absorption and elimination processes of BPAU showed the first order kinetics in both serum and individaul tissues. Therefore, the pharmacokinetic data of *m*-DNB from serum is taken as a example here to show its model analysis. FIG A-3 illustrates the semi-logrithmic versus concentration-time curve of *m*-DNB in serum. The data is best fitted with a one-compartment model.

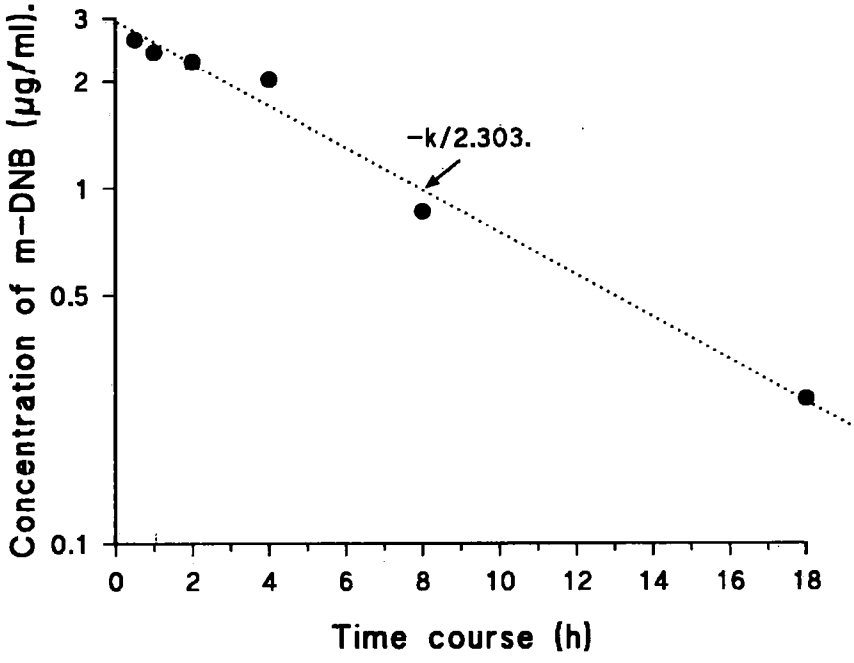

FIG A-3. A illustration of non-linear fitting and model analysis of *m*-DNB pharmacokinetics — data from plasma after a single iv dose.

A-II-B. Exponential regressions and calculations of the pharmacokinetic parameters of *m*-DNB in serum and individual tissues after a single ip dose

The exponential regressions of *m*-DNB pharmacokinetic data and calculations of elimination rate constants were carried out as described for BPAU, see A-I-B.

A-II-B-a. Whole blood

1. Correlation and regression of pharmacokinetic data:

$r = -0.975$; $r^2 = 0.951$. $p<0.001$.

$A = C_0 = 2.79$ (μg/ml)

$B = -0.103$

$k = 2.303 \times 0.103 = 0.237$

2. Analysis of variation of *m*-DNB exponential regression:

The results of variation analysis are shown in Table A-8.

Table A-8. Analysis of variation of *m*-DNB exponential regression in whole blood.

Source	DF	SS	MS	F	P
Regression	1	11.876	11.876	536.5	0.000
Error	28	0.620	0.022*		
Total	29	12.496			

*: S_{tc}.

3. Standard error of slope:

$$SE_{(k)} = \sqrt{(S_{tc} / S_{tt})} = \sqrt{(0.022/1111)} = 0.0044$$

where $SE_{(k)}$ is the standard error of slop; S_{tc} is the mean of the error of square variance (see Table A-8: *); S_{tt} is the sum of squares of time.

$$k_{sc} = 2.303 SE_{(k)} = 2.303 \times 0.0044 = 0.0101$$

where k_{sc} is the standard error of rate constant.

4. Half life

$t_{1/2} = 0.693/k \pm [0.693/k - 0.693/(k+k_{se})]$

$= 0.693/0.237 \pm [0.693/0.237 - 0.693/(0.237+0.0101)]$

$= 2.9 \pm 0.1$ (h)

A-II-B-b. Plasma

1. Correlation and regression of pharmacokinetic data:

$r = -0.959$; $r^2 = 0.0.920$. $p<0.001$.

$A = C_0 = 3.2$ (μg/ml)

$B = -0.0976$

$k = 2.303 \times 0.0976 = 0.224$

2. Analysis of variation of m-DNB exponential regression:

The results of variation analysis are shown in Table A-9.

Table A-9. Analysis of variation of *m*-DNB exponential regression in plasma.

Source	DF	SS	MS	F	P
Regression	1	8.998	8.998	179.6	0.000
Error	23	1.152	0.050*		
Total	24	10.150			

*: S_{tc}.

3. Standard error of slope:

$SE_{(k)} = \sqrt{(S_{tc} / S_{tt})} = \sqrt{(0.05/956)} = 0.0072$

$k_{se} = 2.303 SE_{(k)} = 2.303 \times 0.0072 = 0.0166$

4. Half life

$t_{1/2} = 0.693/k \pm [0.693/k - 0.693/(k+k_{se})]$

$= 0.693/0.224 \pm [0.693/0.224 - 0.693/(0.224+0.0166.)]$

$= 3.1 \pm 0.2$ (h)

A-II-B-c. Medulla

1. Correlation and regression of pharmacokinetic data:

$r = -0.943$; $r^2 = 0.889$. $p<0.001$.

$A = C_0 = 3.7$ (μg/g)

$B = -0.1003$

$k = 2.303 \times 0.1003 = 0.231$

2. Analysis of variation of m-DNB exponential regression:

The results of variation analysis are shown in Table A-10.

Table A-10. Analysis of variation of *m*-DNB exponential regression in medulla.

Source	DF	SS	MS	F	P
Regression	1	9.610	9.610	187.5	0.000
Error	23	1.179	0.051*		
Total	24	10.798			

*: S_{tc}.

3. Standard error of slope:

$SE_{(k)} = \sqrt{(S_{tc} / S_{tt})} = \sqrt{(0.051/956)} = 0.0073$

$k_{sc} = 2.303 SE_{(k)} = 2.303 \times 0.0073 = 0.0168$

4. Half life

$t_{1/2} = 0.693/k \pm [0.693/k - 0.693/(k+k_{sc})]$

$- 0.693/0.231 \pm [0.693/0.231 - 0.693/(0.231+0.0168)]$

$= 3.0 \pm 0.2$ (h)

A-II-B-d. Pons

1. Correlation and regression of pharmacokinetic data:

$r = -0.959$; $r^2 = 0.920$. $p<0.001$.

$A = C_0 = 3.2$ (μg/g)

$B = -0.1033$

$k = 2.303 \times 0.1033 = 0.238$

2. Analysis of variation of m-DNB non-linear regression:

The results of variation analysis are shown in Table A-11.

Table A-11. Analysis of variation of *m*-DNB exponential regression in pons.

Source	DF	SS	MS	F	P
Regression	1	10.21	10.210	263	0.000
Error	23	0.98	0.039*		
Total	24	11.10			

*: S_{tc}.

3. Standard error of slope:

$$SE_{(k)} = \sqrt{(S_{tc}/S_{tt})} = \sqrt{(0.039/956)} = 0.0064$$

$$k_{se} = 2.303 SE_{(k)} = 2.303 \times 0.0064 = 0.015$$

4. Half life

$$t_{1/2} = 0.693/k \pm [0.693/k - 0.693/(k+k_{se})]$$

$$= 0.693/0.238 \pm [0.693/0.238 - 0.693/(0.238+0.015)]$$

$$= 2.9 \pm 0.2 \text{ (h)}$$

A-II-B-e. Coliculi

1. Correlation and regression of pharmacokinetic data:

$r = -0.969$; $r^2 = 0.939$. $p<0.001$.

$A = C_0 = 3.2$ (μg/g)

$B = -0.103$

$k = 2.303 \times 0.103 = 0.237$

2. Analysis of variation of m-DNB exponential regression:

The results of variation analysis are shown in Table A-12.

Table A-12. Analysis of variation of *m*-DNB exponential regression in coliculi.

Source	DF	SS	MS	F	P
Regression	1	10.150	10.150	357	0.000
Error	23	0.653	0.028*		
Total	24	10.803			

*: S_{tc}.

3. Standard error of slope:

$SE_{(k)} = \sqrt{(S_{tc} / S_{tt})} = \sqrt{(0.028/956)} = 0.0055$

$k_{se} = 2.303 SE_{(k)} = 2.303 \times 0.0055 = 0.0127$

4. Half life

$t_{1/2} = 0.693/k \pm [0.693/k - 0.693/(k+k_{se})]$

$= 0.693/0.237 \pm [0.693/0.237 - 0.693/(0.237+0.0127)]$

$= 2.9 \pm 0.2$ (h)

A-II-B-f. Cerebellum

1. Correlation and regression of pharmacokinetic data:

$r = -0.938$; $r^2 = 0.880$. $p<0.001$.

$A = C_0 = 2.9$ (μg/g)

$B = -0.099$

$k = 2.303 \times 0.099 = 0.228$

2. Analysis of variation of m-DNB exponential regression:

The results of variation analysis are shown in Table A-13.

Table A-13. Analysis of variation of *m*-DNB exponential regression in cerebellum.

Source	DF	SS	MS	F	P
Regression	1	9.37	9.370	165.6	0.000
Error	23	1.30	0.057*		
Total	24	10.67			

*: S_{tc}.

3. Standard error of slope:

$$SE_{(k)} = \sqrt{(S_{tc} / S_{tt})} = \sqrt{(0.057/956)} = 0.0077$$

$$k_{se} = 2.303 SE_{(k)} = 2.303 \times 0.0077 = 0.018$$

4. Half life

$$t_{1/2} = 0.693/k \pm [0.693/k - 0.693/(k+k_{se})]$$

$$= 0.693/0.228 \pm [0.693/0.228 - 0.693/(0.228+0.018)]$$

$$= 3.0 \pm 0.2 \text{ (h)}$$

A-II-B-g. Cerebral cortex

1. Correlation and regression of pharmacokinetic data:

$r = -0.915$; $r^2 = 0.837$. $p<0.001$.

$A = C_0 = 2.07$ (μg/g)

$B = -0.088$

$k = 2.303 \times 0.088 = 0.203$

2. Analysis of variation of m-DNB exponential regression:

The results of variation analysis are shown in Table A-14.

Table A-14. Analysis of variation of *m*-DNB exponential regression in cerebral cortex.

Source	DF	SS	MS	F	P
Regression	1	7.32	7.320	106	0.000
Error	23	1.59	0.069*		
Total	24	8.91			

*: S_{tc}.

3. Standard error of slope:

$$SE_{(k)} = \sqrt{(S_{tc} / S_{tt})} = \sqrt{(0.069/956)} = 0.0084$$

$$k_{se} = 2.303 SE_{(k)} = 2.303 \times 0.0084 = 0.019$$

4. Half life

$$t_{1/2} = 0.693/k \pm [0.693/k - 0.693/(k+k_{se})]$$

$$= 0.693/0.203 \pm [0.693/0.203 - 0.693/(0.203+0.019)]$$

$$= 3.4 \pm 0.3 \text{ (h)}$$

A-II-B-h. Spinal cord

1. Correlation and regression of pharmacokinetic data:

$r = -0.940$; $r^2 = 0.884$. $p<0.001$.

$A = C_0 = 4.1$ (μg/g)

$B = -0.096$

$k = 2.303 \times 0.096 = 0.221$

2. Analysis of variation of m-DNB exponential regression:

The results of variation analysis are shown in Table A-15.

Table A-15. Analysis of variation of *m*-DNB exponential regression in spinal cord.

Source	DF	SS	MS	F	P
Regression	1	13.20	13.200	176	0.000
Error	23	1.72	0.075*		
Total	24	14.92			

*: S_{tc}.

3. Standard error of slope:

$$SE_{(k)} = \sqrt{(S_{tc} / S_{tt})} = \sqrt{(0.075/1418)} = 0.023$$

$$k_{se} = 2.303 SE_{(k)} = 2.303 \times 0.023 = 0.053$$

4. Half life

$$t_{1/2} = 0.693/k \pm [0.693/k - 0.693/(k+k_{se})]$$

$$= 0.693/0.221 \pm [0.693/0.221 - 0.693/(0.221+0.053)]$$

$$= 3.1 \pm 0.6 \text{ (h)}$$

A-II-B-i. Liver

1. Correlation and regression of pharmacokinetic data:

$r = -0.904$; $r^2 = 0.817$. $p<0.001$.

$A = C_0 = 0.46$ (μg/g)

$B = -0.237$

$k = 2.303 \times 0.237 = 0.546$

2. Analysis of variation of m-DNB exponential regression:

The results of variation analysis are shown in Table A-16.

Table A-16. Analysis of variation of *m*-DNB exponential regression in liver.

Source	DF	SS	MS	F	P
Regression	1	1.310	1.310	58.1	0.000
Error	14	0.293	0.023*		
Total	15	1.603			

*: S_{tc}.

3. Standard error of slope:

$$SE_{(k)} = \sqrt{(S_{tc} / S_{tt})} = \sqrt{(0.023/23.3)} = 0.031$$

$$k_{ec} = 2.303 SE_{(k)} = 2.303 \times 0.031 = 0.071$$

4. Half life

$$t_{1/2} = 0.693/k \pm [0.693/k - 0.693/(k+k_{ec})]$$

$$= 0.693/0.546 \pm [0.693/0.546 - 0.693/(0.546+0.071)]$$

$$= 1.3 \pm 0.2 \text{ (h)}$$

A-II-B-j. Testis

1. Correlation and regression of pharmacokinetic data:

$r = -0.7346$; $r^2 = 0.540$. $p<0.0025$.

$A = C_0 = 0.438$ (μg/g)

$B = -0.066$

$k = 2.303 \times 0.066 = 0.152$

2. Analysis of variation of m-DNB exponential regression:

The results of variation analysis are shown in Table A-17.

Table A-17. Analysis of variation of *m*-DNB exponential regression in testis.

Source	DF	SS	MS	F	P
Regression	1	0.623	0.623	23.21	0.000
Error	18	0.484	0.027*		
Total	19	1.107			

*: S_{tc}.

3. Standard error of slope:

$$SE_{(k)} = \sqrt{(S_{tc} / S_{tt})} = \sqrt{(0.027/144)} = 0.014$$

$$k_{sc} = 2.303 SE_{(k)} = 2.303 \times 0.014 = 0.032$$

4. Half life

$$t_{1/2} = 0.693/k \pm [0.693/k - 0.693/(k+k_{sc})]$$

$$= 0.693/0.152 \pm [0.693/0.152 - 0.693/(0.152+0.032)]$$

$$= 4.6 \pm 0.8 \text{ (h)}$$

A-II-C. The Area under concentration-time curves (AUC) of *m*-DNB in blood after a single iv dose

In one-compartment model, when a single iv dose of *m*-DNB is given, the AUC is estimated by the following equation (Gibaldi & Perrier, 1982).

$$AUC = dose/(V.k)$$

where V is apparent distribution volume; *k* is elimination rate constant.

$$V = dose/C_0$$

where C_0 is the concentration when t = 0.

Dose = 2.76 (mg/rat)

C_0 = 2.79 (mg /L)

$V = 2.76/279 = 0.989$ (L)

$AUC = 2.76/(0.989 \times 0.237)$

$= 11.8$ ($mg.L^{-1}.h^{-1}$)

$= 11.8$ ($\mu g.ml^{-1}.h^{-1}$)

A-II-D. The Area under concentration-time curves (AUC) of *m*-DNB in individual tissues after a single iv dose

In tissues, the pharmacokinetics of *m*-DNB are similar to blood after an oral dose. There is an absorption phase which allows *m*-DNB enter tissues from blood. Therefore, the estimation of AUC in tissues is different from that in blood after iv dosing. The estimation of AUC in each tissue is calculated using the trapezoidal rule (Martin, 1986). The trapezoidal rule is illustrated in FIG A-4. The concentration-time data of *m*-DNB from medulla is plotted and taken as a example.

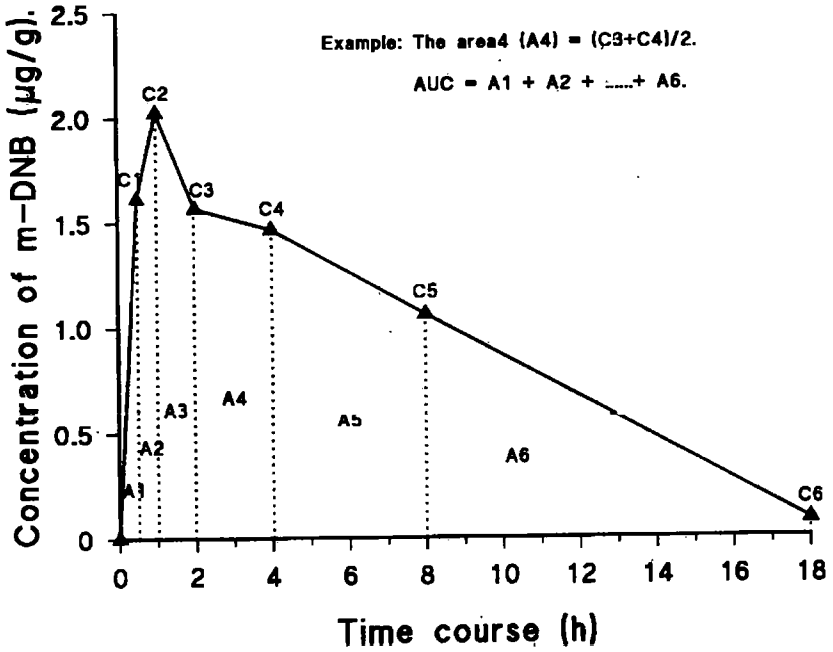

FIG A-4. A illustration of AUC calculation of *m*-DNB in individual tissues using trapezoidal rule — data from pons after a single iv dose.

A-II-D-a. Medulla

AUC = 0.5(0+2.016)/2 + 0.5(2.016+2.311)/2 + (2.311+2.046)/2 + 2(2.046+ 1.992)/2 +

4(1.992+0.803)/2 + 10(0.803+0.062)/2

= 17.7 ($\mu g.g^{-1}.h^{-1}$)

A-II-D-b. Pons

AUC = 0.5(0+1.524)/2 + 0.5(1.524+2.113)/2 + (2.113+1.597)/2 + 2(1.597+ 1.55)/2 +

4(1.55+0.884)/2 + 10(0.884+0.037)/2

= 15.8 ($\mu g.g^{-1}.h^{-1}$)

A-II-D-c. Coliculi

AUC = 0.5(0+1.948)/2 + 0.5(1.948+2.028)/2 + (2.028+1.653)/2 + 2(1.653+1.578)/2 +

4(1.578+0.765)/2 + 10(0.765 + 0.037)/2

= 15.2 ($\mu g.g^{-1}.h^{-1}$)

A-II-D-d. Cerebral cortex

AUC = 0.5(0+1.187)/2 + 0.5(1.187+1.522)/2 + (1.522+1.268)/2 + 2(1.268+ 1.258)/2 +

4(1.258+0.586)/2 + 10(0.586+0.077)/2

= 11.9 ($\mu g.g^{-1}.h^{-1}$)

A-II-D-e. Cerebellum

AUC = 0.5(0+1.299)/2 + 0.5(1.299+1.758)/2 + (1.758+1.582)/2 + 2(1.582 + 1.528)/2 +

4(1.528+0.745)/2 + 10(0.745+0.05)/2

= 14.4 ($\mu g.g^{-1}.h^{-1}$)

A-II-D-f. Spinal cord

AUC =0.5(0+1.690)/2 + 0.5(1.69+2.042)/2 + (2.042+2.206)/2 + 2(2.206 + 2.158)/2 +

4(2.158+0.984)/2 + 10(0.984+0.067)/2

= 19.4 ($\mu g.g^{-1}.h^{-1}$)

A-II-D-g. Liver

AUC = 0.5(0+0.18)/2 +0,5(0.18+0.286)/2 + (0.286+0.166)/2 + 2(0.166+0.041)/2 +

4(0.041+0)/2

= 0.7 ($\mu g.g^{-1}.h^{-1}$)

A-II-D-h. Testis

AUC = 0.5(0+0.278)/2 + 0.5(0.278+0.389)/2 + (0.389+0.329)/2 + 2(0.329+0.256)/2 +

4(0.256+0.145)/2 + 10(0.145+0)/2

= 2.7 ($\mu g.g^{-1}.h^{-1}$)

PUBLICATIONS AND ACADEMIC COMMUNICATIONS

1. Xu J., Chan M and Ray D. E. (1997): Metabolism of m-dinitrobenzene in astrocytees and endothilial cells, (which was presented at BTS meeting, 24-26 March, 1997, Warwick and to be published on *Human & Experimental Toxicology*).
2. Xu J. and Ray D. E. (1997): Metabolic aspect of age-related susceptibility of the rat to p-bromophenylacetylurea-induced delayed neuropathy, (which was presented at BTS meeting, 24-26 March, 1997, Warwick and to be published on *Human & Experimental Toxicology)*
3. Xu J. Ray D. E. and Lister T. (1996): Metabolism and toxicokinetics of *m*-dinitrobenzene in target tissues in relation to its toxicity in rats. *Hum & Experimental Toxicology*, **15** (8): 671 (This was a oral communication which was given at BTS meeting, 1-3 April, 1996, York.).
4. Xu J. & Ray D. E. (1995): The effect of Phenylmethylfonylfluoride (PMSF) on the metabolism of p-bromophenylacetylurea (BPAU*), Human & Experimental Toxicology*, **14** (4): 376.
5. Nolan C. C., Romero, I. Xu J., Lister T. & Ray D. E. (1995): The role of pharmacokinetic factors in the neurotoxicity of *m*-dinitrobenzene in the rat, *Human & Experimental Toxicology*, **14** (4): 364.
6. Xu J., Ray D.E. & Johnson M.K.(1994): Promotion of *p*-Bromophenylacetylurea Induced Neuropathy by Phenylmethylfonyl fluoride, *Human & Experimental Toxicology* **13** (3): 203.
7. Xu J. (1995): Neurotoxic synergism and metabolic interaction between p-bromophenylacetylurea and phenylmethylsulfonyl flouride. (This was a oral

communication which was given on 18/12/1995, at the Meeting of British Drug Metabolism Group, London.)

8. Johnson M. K., Xu J. & Ray D.E. (1994): Mechanism of augmentation of p-bromophenylacetylurea neuropathy by phenylmethylsulfonylflouride in rats. *Toxicology Letters* Supplement 1/74: 40.

References

Abramovitz M., Homma H., Ishigake S., Tansey F., Cammer W., and Listowsky I. (1988): Characterization and localization of glutathione S-transferase in rat brain and binding of hormones, neurotransmitters and drugs, *J. Neurochem.*, **50**: 50-57.

Aboudonia M. B., Wilmarth K. R., Jensen K. F., Oehme F. W. and Kurt T. L. (1996): Neurotoxicity resulting from coexposure to pyridostigmine bromide, DEET, and permethrin-implications of Gulf-War chemical exposures. J. Toxico. Environ. Health, **48**(1), 35-56.

Alder H. L. and Roessler E. B. (1968): *Introduction to probability and statistics*, 4th Edition W H Freeman and Company, San Fracisco, pp 155-164.

Anadatheerthavarada H. K., Shankar S. K., Bhamre S., Boyd M. R., Song B. J. and Ravindranath V. (1993): Induction of brain cytochrome P450IIE1 by chronic ethanol treatment, *Brain Res.*, **601**: 279-285.

Anadatheerthavarada H. K., Williams J. F., and Wecker L. (1993): The chronic administration of nicotine induces cytochrome P450 in rat brain, *J. Neurochem.*, **60**:1941-1944.

Benet L. Z. (1995): Basic principles of pharmacokinetics, *Toxicol. Pathol.*, **23**(2):115-123.

Beritic T. (1956): Two cases of meta-dinitrobenzene poisoning with uneqaul clinical response, *Br. J. Ind. Med.*, **13**, 114-118.

Bhamre S., Bhagwat S. V., Shankar S. K., Willams D. E., and Ravindranath, V. (1993): Cerebral flavin-containing monooxygenase-mediated metabolism of antidepressants in brain: Immunochemical properties and Immunocytochemical location, *J. Pharmaco. Exp. Ther.*, **267** (1): 555-559.

Bhagwat S. V., Boyd M. R., and Ravindranath V. (1995): Brain mitochondrial cytochromes P450: xenobiotic metabolism, presence of multiple forms and their selective inducibility, *Arch. Biochem. Biophys.*, **320**:73-83.

Bischoff K B and Dedrick (1968): Thiopental pharmacokinetics, *J. Pharm. Sci.*, **57**:1346-1357.

Blakemore W. F. and Cavanagh J. B. (1969): "Neuroaxonal dystrophy" occurring in an experimental "dying back" process in the rat, *Brain*, **92**: 789-804.

Bond J. S. and Buttler P. E. (1987): Intracellularprotease, *Ann. Rev. Biochem.*, **46**: 305-311.

Brimijoin S. and Mintz K.P. (1984): Unimpaired energy metabolism in experimental neuropathy induced by p-bromphenylacetylurea, *Muscle and Nerve*, 7(9): 725-732.

Brown C. D., Forman C. L., McEuen S. F., and Miller M. G. (1994): Metabolism and testicular toxicity of 1.3-dinitrobenzene in rats of different ages, *Fundam. Appl. Toxicol.*, **23**, 439-446.

Cader P. J., Hume R., Fryer A. A., Strange R . C., Lauder J. and Bell J. E. (1990): Glutathione S-transferase in human brain, *Neuropath. Appl. Neurobiol.*, **16**; 293-303.

Caldwell J. (1980): Comparative aspects of detoxication in mammals, In *Enzymatic Basis of Detoxication*, W Jakoby (ed), Academic Press, New York, pp 85-114.

Caldwell J. Gardner I. and Swales N. (1995): An introduction to drug disposition: The basic principles of absorption, distribution, metabolism, and excretion, *Toxicol. Pathol.*, **23**(2): 102-114.

Cammer W., Tansey F., Abramovitz M., Ishigake S. and Listowsky I. (1989): Differencial localization of glutathione S-transferase Y_p and Y_b subunits in oligodendrocytes and astrocytes of rat brain, *J. Neurochem.* **52**; 876-883.

Cavanagh J. B. (1973): Peripheral neuropathy caused by chemical agents, CRC *Crit. Rev.Toxicol.*, 365-417.

Cavanagh J. B., and Chen F. C-K. (1968): The experimental neuropathy in rats caused by p-bromophenylacetylurea, *J. Neurosurg. Psychiatry*, **31**: 471.

Cayen M. N. (1995): Consideration in the design of toxicokinetic programs, *Toxicol. Pathol.*, **23**(2); 148-157.

Chasseaud L. F. (1993): Role of toxicokinetics in toxicity testing, In: *Drug Toxicokinetics*, PG Welling and FA de la Iglesia (eds), Marcel Dekker, New York, pp. 105-142.

Chen F. C-K. and Cavanagh L. B. (1971): Factors affecting neurotoxicity by p-bromophenylacetylurea in rats, *Br. Exp. Pathol.*, **52**: 315.

Clark B., and Smith D. A. (1984): Pharmacokinetics and toxicity testing, CRC *Crit. Rev. Toxicol.*, **12**:343-385.

Comel M. (1931): *Boll. Soc. Ital. Biol. Sper.*, **6**: 225.

Commandeur J. N. M., Stijntjes G. J. and Vermeulen N. P. E. (1995): Enzymes and transport systems involved in the formation and disposition of glutathione S-conjugates: Role in bioactivation and detoxication mechanisms of xenobiotics, *Pharmacol. Rev.*, **47**(2): 271-325.

Cody T. E., Witherup S., Hastings L., Stemmer K. and Christian R. T. (1981): 1.3-Dinitrobenzene. Toxic effects in vivo and in vitro, *J. Toxicol Environ. Health*, **7**: 829-847.

Cossum P. A. and Rickert D. E. (1985): Metabolism of dinitrobenzenes by rat red blood cells, *Pharmacologist*, **27**: 250.

Cossum P. A. and Rickert D. E. (1985): Metabolism of dinitrobenzenes by rat isolated hepatocytes, *Drug Metab. Dispos.*, **13**(6): 664-668.

Cossum P. A., Rickert D. E. and Working P. K. (1986): Comparison of the testicular toxicity of the dinitrobenzenes and their major reduced metabolites in the rat, *The Pharmacologist*, **28**: 178.

Dayan A. D. (1994): What use is toxicokinetics? *Drug inform. J.*, **28**: 143-144.

DeBethizy J. D. and Rickert D. E. (1984): Metabolism of nitrotoluenes by freshly isolated Fischer-344 rat hepatocytes, *Drug. Metab. Dispos.*, **12**: 45-50.

Diezel P. B. and Quadbeck G. (1960): Nervenschadigung durch p-bromphenylacetyl-harnstoff, *Naunyn. Schmiedeberg's Arch. Pharmakol. Exp. Pathol.*, **238**: 534,.

Draft Tripartite Guideline, International Conference on Harmonization (ICH-2) (1993): *Toxicokinetics*: The assessment of systemic exposure in toxicity studies.

Fioroni F., Morretto A. and Lotti M. (1995). Triphenylphosphite Neuropathy in hens, *Archiv. Toxicol*, **69** (10): 705-711.

Forster P. M. D., Lioyd S. C., and Prout M. S. (1987): Nitroreduction of 1,3-dinitrobenzene by rat testicular cell cultures and its relationship to target organ toxicity, *The Toxicologist*, **7**: 143.

Forster P. M. D., Lioyd S. C., and Prout M. S. (1987): Txicity and metabolism of 1,3-dinitrobenzene in rat testicular cell cultures, *Toxical. In Vitro*, **1**: 31-37.

Fossom L. H., Messing R. B. and Sparber S. B. (1985): Long lasting behavioral effects of dimethyl sulfoxide and the "peripheral" toxicant p-bromophenylacetylurea, *NeuroToxicol.*, **6**(1): 17-28.

Ghersi-Egea J. Faulkner., Leninger-Muller B., Suleman G., Siest G., and Minn A. (1994): Localization of drug-metabollizing enzyme activities to blood-brain interfaces and circumventricular organs, *J. Neurochem.* **62**: 1089-1096.

Gibaldi M. & Perrier D. (1982): *Pharmacokinetics*, Marcel Dekker, New York, 2nd edition, pp 433.

Gold M. S. and Ziehler D. M. (1973): Dimethylaniline N-oxidase and aminopyrine N-demethylase activities of human liver tissues, *Xenobiotica*, **3**: 179-189.

Gospe S. M. and Calaban M. J. (1988): Central nervous system distribution of inhaled toluene, *Fundamental and Appl. Toxicol.*, **11**: 540-545.

Guengerich F. P. and Macdonald T. L. (1990): Mechanisms of cytochrome P450 catalysis, *FASEB J.*, **4**: 2453-2459.

Haglung L., Kohler C., Haaparata T., Goldstern M. and Gustafsson J-A. (1984): Presence of NADPH-cytochrome P450 reductase in central catecholaminergic neurones, *Nature*, **307**: 259-262.

Halliwell B. (1989): Current status review: Free radicals, reactive oxygen species and human disease: a critical evaluation with special reference to atherosclerosis, *Br. J. Exp. Path.*, **70**: 737-757.

Halliwell B. (1992): Short review: Reactive oxygen species and the central nervous system, *J. Neurochem.*, **59**(5): 1609-1623.

Hansson T., Tinberg N., Ingelman-Sundberg M., and Kohler C. (1990): Regional distribution of ethanol-inducible cytochromes P450 IIEI in rat central nervous system, *Neurosci.*, **40**: 323-341.

Hartter D. R. (1985): The use and importance of nitroaromatic chemicals in the chemical industry, In "*Toxicity of Nitroaromatic Compounds*" (Rickert, D.E.Ed.) pp 1-13, Hemisphere Publishing Corporation, Washington, DC.

Hu H. L. and Ray D. E. (1995): Metabolism of *m*-dinitrobenzene in brain studied in vitro, *Hum. Exp. Toxicol.*; **14**: 363.

Hu H. L., Bennett N., Lister T., Nolan C. C., Holton J. L., Ray D. E. (1996): Increased susceptibility of brain towards m-dinitrobenzene by glutathione depletion, *Hum. Exp. Toxicol.*, **15**: 145.

Hu H. L., Bennett N., Holton J. L., Nolan C. C., Lister T., Ray D. E. (1996): Regional heterogeneity in turnover and novel functions of glutathione in rat brain, *Hum. Exp. Toxicol*, **15**: 658.

Igarashi T. (1994): The use and abuse of toxicokinetics: What does actual data tell researchers? *Drug Inform. J.*, **28**: 285-293.

Ishihara N., Kanaya A., and Ikeda M. (1976): *m*-Dinitrobenzene intoxication due to skin exposure. *Int. Arch. Occup. Environ. Health*, **36**: 161-168.

Jacobs J. M. and Ford W. C. L. (1981): The neurotoxicity and antifertility properties of 6-chloro-6-deoxyglucose in the mouse, *Neurotoxicol.*, **2**: 405-417.

Jakobsen J., Lambert E. H., Carlson G. and Brimijoin S. (1982): Clinical and electrophysiological characteristics of the experimental neuropathy caused by p-bromophenylacetylurea, *Exp. Neurol.*, **75**:173.

Johnson J. A., Barbary A. E., Kornguth S. E., Brugge J. F. and Siegel F. L. (1993): Glutathione S-transferase isoenzymes in rat brain neurons and glia, *J. Neurosci.*, **13**: 2013-2023.

Johnson M. K. (1969): The delayed neurotoxic effect of some organophosphorus compounds, *Biochem. J.*, **114**: 711.

Johnson M. K. and Lauwerys R. (1969): Protection by some carbomates against the delayed neurotoxic effects of diisopropyl phosphorofluoridate, *Nature,* **222**: 1066-1067.

Johnson M. K. (1974): The primary biochemical lesion leading to the delayed neurotoxic effects of some organophosphorus esters, *J. Neurochem.*, **23**: 785-789.

Johnson M. K. (1982): The target for initiation of delayed neurotoxicity by organophosphorus esters: Biochemical studies and toxicological applications. In

Reviews in Biochemical Toxicology (E. Hodgson, J. R. Bend, and R. M. Philipot, Eds), Vol. 4 pp. 141-212, Elserier, New York.

Johnson M. K. (1987): Receptor or enzyme: the puzzle of NTE and organophosphate-induced delayed polyneuropathy, *Trend. Pharmacol. Sci.*, **8**(5): 174.

Johnson M. K. and Ray D. E. (1992): Evaluation of phenylmethanesulphonyl fluoride as a promoter of peripheral neuropathies in the rat, *Hum. Exp. Toxicol.*, **11**: 421-422.

Johnson M. K. (1992): Inhibition, reactivation and ageing of cholinesterases, *Hum. Exp. Toxicol.*, **11**: 555-557.

Kato R., Case D. E., Hakusui H., Noda K., Sagami F., Horrii I., Mayahara H., Cayen M. N., Marriott M. B. and Igarashi T. (1993): Toxicokinetics: Its significance and practical problems, *J. Toxical. Sci.*, **18**: 211-238.

Keesey J. (1987): Biochemica Information, 1st Edition, pp119-120, Boehringer Mannheim Biochemicals, Indianapolis.

Kemp W. (1987): *Organic spectroscopy*, 2ed, Macmillan Publishers LTD, Hapshire and London, pp 83-157.

Kiese M (1949): Pharmakologischc untersuchungen uber *m*-dinitrobenzol, *Arch. Exp. Path. Pharmak.*, **206**: 361-383.

Kunz G. (1942): Studien uber Methamoglobinbildung, *Arch. Exp. Path. Pharmak.*, **199**: 508-520.

Lazverev N. V. & Levina E. N. (1976): *o*-, *m*-, *p*-DNB In: *Harmful Substances in Industry* II, pp 724-727, Khiimya Press, Leningrad, (Tranlated by Literature Research, Annadale, Va).

Lefauconnier J. M. and Bouchaud C.: (1994): Neurotoxicity in *General & Applied Toxicology*, Edited by Ballantyne B., Marrs T. and Turner P., vol. 1, pp 469-471, Stockton press, U S A.

Lemoine A., Johann M. and Cresteil T. (1990): Evidnce of presence of distinct flavin-containing monooxygenase in human tissues, *Arch. Biochem. Biophys.*, **276**: 336-372.

Levi G. (1969): Chapter 5: Spinal cord, Volume II, In *Handbook of Neurochemistry*, Edited by Lajtha A., Plenum Press, New York, pp 71-101.

Levin A. A. and Dent J. G. (1982): The role of gut microflora in nitrobenzene induced testicular necrosis, *Toxicologist*, **2**: 77.

Linder R. E., Hess R. A. and Strader L. F. (1986): Testicular toxicity and infertility in male rats treated with 1.3-dinitrobenzene, *J. Toxicol. Environ. Health*, **19**: 477-489.

Linder R. E., Strader L.F., Barbee R. R. and Rehnberg G. L. and Perreault S. D. (1990): Reproductive toxicity of a single dose of 1.3-dinitrobenzene in two ages of young adult male rats, *Fundam. Appl. Toxicol.*, **14**: 284-298.

Lipschitz W. L. (1948): *Arch. Wxp. Pathol. Pharmak.*, **205**: 305.

Lotti M. (1987): Organophosphate induced delayed polyneuropathy in man and perspectives for biomonitering, *Trends Pharmacol. Sci.*, **8**: 176-177.

Lotti M., Caroldi S., Capodicasa E. and Moretto A. (1991): Promotion of Organophosphate-induced polyneuropathy by phenylmethanesulfonyl fluoride, *Toxicol. App. Pharmacol.*, **108**: 234.

Lowndes H. E., Beiswanger C. M., Philbert M. A. and Reuhl K. R. (1994): Substrates for neural metabolism of xenobiotics in adult and developing brain, *NeuroToxicol.*, **15**(1): 61-74.

Martin B. K. (1986): Pharmacokinetics, *In Handbook of Clinical Drug Research*, Edited by Glenny H and Nelmes P, pp 59-93, Blackwell Scientific Publications, London.

Mason R. P. and Josephy P. D. (1984): Free radical mechanism of nitroreductase. In: *Toxicity of Nitroaromatic Compounds*, Edited by Rickert D. E. (CIIT), pp 121-140. Hemisphere, Washington DC.

McEuen S. F. and Miller M. G. (1991): Metabolism and pharmacokinetics of *1,3*-dinitrobenzene in the rat and the hamster, *Drug Metabo. and Dispos.*, **19**(3): 661-666.

Mead R. and Curnow R. N. (1987): *Statistical methods in agriculture and Experimental Biology*, pp 142, Chapman and Hall, London.

Monro A (1994): Toxicokinetics: What one can and cannot do with plasma concentrations, *Drug Inform. J.*, **28**: 259-262.

Moretto A., Bertolazzi M., Capodicasa E., Peraica M., Richardson R. J., Scapellato M. L. and Lotti M. (1992): Phenylmethanesulfonyl fluoride elicits and intensifies the clinical expression of neuropathic insults, *Arch Toxicol*, **66**: 67-72.

Nagata H. and Brimijoin S. (1986): Neurotoxicity of halogenated phenylacetylureas is linked to abnormal onset of rapid axonal transport, *Brain Res.*, **385**:136-142.

Nagata H., Brimijoin S., Low P. and Schmelzer J. D. (1987): Slow axonal transport in experimental hypoxia and in neuropathy induced by p-bromophenylacetylurea, *Brain Res.*, **422**:319-326.

Nebert D. W., Nelson D. R., Coon M. J., Estabrook R. W., Feyereisen R., Fujii-Kuriyama Y., Gonzales F. J., Guengerich F. P., Gunsalas I. C., Johnson E. F., Loper J., Sato R., Waterman M. R. and Waxman D. J. (1991): The P450 subfamily-Update on new sequences, gene mapping and recommended nomenclature, *DNA Cell Biol.*, **10**: 1-14.

Nebert D. W., Nelson D. R., Coon M. J., Estabrook R. W., Feyereisen R., Fujii-Kuriyama Y., Gonzales F. J., Guengerich F. P., Gunsalas I. C., Johnson E. F., Loper J., Sato R., Waterman M. R. and Waxman D. J. (1991): Correction, *DNA Cell Biol.*, **10**: 397-398.

Nolan C. C., Romero I., Xu J., Lister T. and Ray D. E. (1995): The role of pharmacokinetic factors in the neurotoxicity of m-dinitrobenzene in the rat, *Hum. Exptl. Toxicol.*, **14** (4): 364.

Nystrom D. D. and Rickert D. E. (1987): Metabolism and excretion of dinitrobenzene by male fischer-344 rats, Drug Metab. Dispos., 15 (6): 821-825.

Obasaju M. F., Katz D. F. and Miller M. G. (1991): Species differences in susceptiblity to 1.3-dinitrobenzene-induced testicular toxicity and methemoglobineamia, *Fundam. Appl. Toxicol.*, **16**, 257-266.

Oka N. and Brimijoin S. (1990): Premature onset of fast axonal transport in bromophenylacetylurea neuropathy: an electrophoretic analysis of proteins exported into motor nerve, *Brain Res.*, **509**:107-110.

Parke D. V. (1961): The metabolism of *m*-dinitro[14C]benzene in the rabbit, *Biochem. J.*, **78**: 262-271.

Parkinson, A.(1996), Biotransformation of xenobiotics, Chapter 6 in: Casarett & Doull's Toxicology — The basic science of poisons, 5th Edition, Edited by C. D. Klaassen, New York, pp113-186.

Philbert M. A., Nolan C. C., Cremer J. E., Tucker D. and Brown A. W. (1987): 1.3-Dinitrobenzene-induced encephalopathy in rats, *Neuropathol. Appl. Neurobiol.*, **13**: 371-389.

Pope C. N. and Padilla S. (1990): Potentiation of organophosphorus-induced delayed neurotoxicity by phenylmethylsulfnyl floride. J. Toxicol. Environ. Health, **31**: 261-273.

Pope C. N., Chapman M. L., Tanaka J. R. and Padilla S. (1992): Phenylmanephonyl fluoride alerts sensitivity to organophosphorus-induced delayed neurotoxicity in developing animals, *NeuroToxicol.*, **13**: 355-364.

Potkonjak D., Stern P. and Tomic S. (1965): An attempt at chemotherapeutic treatment in the anterior horn of the rat spinal cord, *Med. Pharmacol. Exp.*, **12**: 32-36.

Poulsen L. L., Hyslop R. M. and Ziegler D. M. (1974): S-oxidation of thioureylenes catalyzed by a microsomal flavoprotein mixed function oxidase, *Biochem. Pharmacol.*, **23**: 3431-3440.

Poulsen L. L. and Ziegler D. M. (1977): Microsomal mixed function oxidase dependent renaturation of reduced ribonuclease, *Arch. Biochem. Biophys.*, **183**: 565-570.

Ravindranath V., Anandatheerthavarada H. K. and Shivakumar B. R. (1989): Low levels of glutathione in aged rat brain regions, *Neurosci. Lett.*, **101**: 187-190.

Ravindranath V., Bhamre S., Bhagwat S. V., Anandatheerthavarada H. K., Shankar S. K. and Tirumalai (1995): Xenobiotic metabolism in brain, *Toxico. Lett.*, **82/83**: 633-638.

Rechthand E. and Rapoport S. I. (1987): Regulation of the microenvironment of peripheral nerve: role of the blood-nerve barrier. *Pro. Neurobiol.*, **28**: 303-343.

Rickert D. E. (1987): Metabolism of nitroaromatic compounds, *Drug Met. Rev.*, **18** (1): 23-53.

Risau W.. and Wolburg H..(1990): Development of the blood-brain barrier, *TINS*, **13**: 174-178.

Roland M. and Tozer T. N. (1980): *Clinical Pharmacokinetics*: *Concepts and Applications*, pp 9-18, Lea & Febier Philadephia, London.

Romero I., Brown A. W., Cavanagh J. B., Nolan C. C., Ray D. E. and Seville M. P. (1991): Vascular factors in the neurotoxic damage caused by 1.3-dinitrobenzene in the rat, *Neuropathol. Appl. Neurobiol.*, **17**: 495-508.

Roubal J., Tuny K. and Pokorny F.(1946): *Cas. Lek. Ces.*, 85: 1002..

Schwartz W. J. and Sharp F. R. (1978): Autoradiographic maps of regional brain glucose consumption in resting, awake rats using (^{14}C)2-deoxyglucose, *J. Comparative Neurol.*, **177**: 335-360

Sipes I. G. and Gandolfi A. J. (1991): Chapter 4. Biotransformation of toxicants, In *Casarett and Doll's Toxicology- The Basic Science of Poisons*, Edited by Amdur, M. O. et al., 4th edition, McGraw-Hill, Inc., New York, pp 88-105.

Spector W. S. (1956): *Handbook of biological data*, W. B. Saunders Company, Philadephia and Lodon, 70-74.

Strobel H. W., Hidenori Kawshima J. G., Sequeira G. D., Bergh A., Hodgson A. V., Wang H. and Shen S. J. (1995): Expression of multiple forms of brain cytochrome P450, *Toxico. Lett.*, **82/83**: 639-643.

Takacs A. R. (1995): Ancillary approaches to toxicokinetic evaluation, *Toxicol. Pathol.*, **23**(2): 179-186.

Tansey F. A. and Cammer W. (1991): A Pi form of glutathione S-transferase is a myelin- and oligodendrocyte-associated enzyme in mouse brain, *J. neurochem.*, **57**: 95-102.

Testa B. (1983): Non-ezymatic biotransformation. In: *Biological Basis of Detoxication*, Caldwell J. and Jakoby W. B. (eds). Academic Press, London, New York, pp 137-150.

Troncoso J. C., Griffin J. W., Price D. L., and Hess-Kozlow K. M. (1982): Pathology of the peripheral neuropathy induced by *p*-bromophenylacetylurea, *Lab. Invest.*, **46**(2): 215.

Tynes R. E. and Hodgson E. (1985): Catalytic activity and substrate specificity of the microsomal flavin-containing mono-oxygenase: Characterazation of hepatic, pulmonary and renal enzymes in mouse, rabbit and rat, *Arch. Biochem. Biophys*, **240**: 77-93.

Veronesi B. and Padilla S. (1985): Phenylmethylsulfonyl fluoride protects rats from mipafox-induced delayed neuropathy, *Toxicol. Appl. Pharmacol.*, **81**: 258-264.

Vogt C. and Vogt O. (1922): Erkrankungen der grosshirnrinde in lichte der topisik, pathoklise und pathoarchitectonik, *J. Psychatr. Neurol.*, **28**: 1-171.

Volk B., Hettmannsperger U., Papp T., Amelizad Z. Oesch F. and Knoth R. (1991): Mapping of phenytoin-inducible cytochrome P450 immunoreactivity in the mouse central nervous system, *Neurosci.*, **42**: 215-235.

Walther B., Ghersi-Egea J. F., Minn A. and Siest G. (1986): Subcellular distribution of cytochrome P450 in the brain, *Brain Res.*, **75**: 338-344.

Warner M., Kohler C., Hansson T. and Gustafsson J. A. (1988): Regional distribution of cytochrome P450 in the rat brain: spectral quantitation and contribution of P450 b,e and P450 c, d, *J. Neurochem*, **50**: 1057-1065.

Williams D. E., Ziegler D. M., Nordin D. S., Halle S. E. and Masters B. S. S. (1984): rabbit lung flavin-containing monooxygenase is immunochemically and catalytically distinct from the liver enzyme, *Biochem. Biophys. Res. Commun.*, **125**: 116-122.

Xu J. and Ray D. E. (1995): The effect of phenylmethanesulfonylfloride on the metabolism of *p*-bromophenylacetylurea, *Hum. exp. Toxicol.*, **14** (4): 376.

Xu J., Ray D. E. and Johnson M. K. (1994): Promotion of p-bromophenylacetylurea induced neuropathy by phenylmanephonyl fluoride, *Hum. exp. Toxicol.*, **13**(3): 203.

Ziegler D. M. and Poulsen L. L. (1978): Hepatic microsomal mixed function oxidase, In *Methods in Enzymology*, ed. by Fleischer S. and Poulsen L., vol. 52, pp 142-151, Academic press, New York.

Ziegler D. M. (1980): Microsomal flavin-containing monooxygenases: Oxygenation of nucleophilic nitrogen and sulphur compounds. In *Enzymatic Basis of Detoxication*, ed by W.B. Jakoby, vol. I, pp 201-207, Academic Press, New York, *Trends. Pharmacol. Sci.*, 11: 321-324.

Ziegler D. M. (1988): Flavin-containing monooxygenases: Catalytic mechanism and substrate specificities, *Drug Metabo. Rev.*, 19 (1): 1-32.

Ziegler D. M. (1990): Flavin-containing monooxygenases: Enzymes adapted for multisubstrate specificity, *Trends. Pharmacol. Sci.*, 11: 321-324.